A balancing act between stratification and EMT in cultured human thymic epithelial cells

THÈSE N^{O} 6942 (2016)

PRÉSENTÉE LE 26 AVRIL 2016

À LA FACULTÉ DES SCIENCES DE LA VIE
LABORATOIRE DE DYNAMIQUE DES CELLULES SOUCHES
PROGRAMME DOCTORAL EN APPROCHES MOLÉCULAIRES DU VIVANT

ÉCOLE POLYTECHNIQUE FÉDÉRALE DE LAUSANNE

POUR L'OBTENTION DU GRADE DE DOCTEUR ÈS SCIENCES

PAR

Matteo PLUCHINOTTA

acceptée sur proposition du jury:

Prof. D. Constam, président du jury
Prof. Y. Barrandon, directeur de thèse
Prof. G. Anderson, rapporteur
Dr P. Bonfanti, rapporteuse
Prof. F. Radtke, rapporteur

ÉCOLE POLYTECHNIQUE
FÉDÉRALE DE LAUSANNE
Suisse
2016

"You are killing me, fish, the old man thought.
But you have a right to. Never have I seen a greater,
or more beautiful, or a calmer or more noble thing than you,
brother. Come on and kill me. I do not care who kills who.

Now you are getting confused in the head, he thought.
You must keep your head clear. Keep your head clear and
know how to suffer like a man. Or a fish, he thought."

Ernest Hemingway

—The old man and the sea

Acknowledgments

I would like to thank my parents for teaching me that you can achieve anything you believe in, and for making everything possible.

I am very grateful to Prof. Yann Barrandon for giving me the opportunity to work in his laboratory. I learned a lot in the last 4 years, on human TECs, epithelia and myself.

I warmly thank the members of my thesis jury, Prof. Graham Anderson, Dr. Paola Bonfanti, Prof. Freddy Radtke and Prof. Daniel Constam for taking the time to review and discuss my work.

Grazie mille to all the people that contributed to this project. Especially, Melissa Maggioni, who started the project and was always kindly available when I needed help. Roxana Wasnick, for the idea of the EpCAM sort. Tiphaine Arlabosse for the inspiring scientific and cooking discussions. Ariane Rochat, for her help, and for maintaining the quality of our cell culture system. Andrea Zaffalon for his precisous advice on how to present things in a simpler way.

Of course, thank you to all present and past LDCS members. In particular, Christèle for the pichenettes, Pierluigi for the drama, Nathalie Guex for her fundamental work in the administrative part, Pauline for her good work as a master student, Marine for singing with her headphones on and all the other at EPFL and CHUV for their help and support, and for being such good colleagues.

This work would not have been possible without the beautiful work done by the EPFL core facilities. Thus, I am very grateful to Miguel, Loïc, Telma, Letitia, Valérie and André from the FCCF for being competent and fun, to Isabelle, Sandra and Sonia from the TCF for their precious help with the lentiviral vectors, Keith, Léonore, Johann and Floriane at the LGTF (UNIL) for performing the miRNA microarray analysis, and to Jacques and Julien from the BCCF for the statistical analysis of the RT-qPCR validation.

I also thank Prof. Shin-Ichi Nishikawa, Satomi-sensei, Kataoka-sensei, Misato, Martin, Moriwaki-san and all the members of the former LSCB (Riken CDB) for patiently taking me by the hand when I was an undergraduate student.

I would like to express my gratitude to the mountains and lakes that surround us for their eternal presence, to the snow for making life so much better and to snowboarding for providing an insane crew in Villars and for helping me to keep my sanity of mind. Thank you also to the ocean and waves that keep me dreaming.

I thank from the bottom of my heart Léonor, Tadeo & Oskar for raising their glasses to "une amitié qui dure" and for their lifelong friendship and support.

I would also like to thank all my family and friends for trying to convince me of the utility of my research, and Mme Miazza, my high school math teacher, that convinced me to study at EPFL during my maturity's oral exam.

Last but not least, thank you Kat for your love and support. I am grateful to your beautiful mind for your help in the proofreading of this work. You're the best. Love you.

Abstract

The thymus is the primary organ for T cell differentiation and maturation. Its stroma forms a characteristic sponge-like 3D structure mainly composed of thymic epithelial cells. Despite of this unconventional epithelial architecture, TECs express markers associated with epidermal specification and differentiation. We have uncovered that the human thymus contains a population of clonogenic TECs that can be extensively expanded in a culture system originally developed for skin keratinocyte stem cells.

In vitro, human TECs (hTECs) can give rise to four morphologically distinct colony-types and express markers of stratified epithelia's basal layers, such as P63, K5/K14 and CD49f. We were able to demonstrate that cultured hTECs can be split in two distinct subpopulations based on their EpCAM expression level. $EpCAM^+$ hTECs only give rise to stratified colonies that contain squame-like cells and express markers of epidermal differentiation, whereas $EpCAM^-$ hTECs mostly give rise to non-stratifying colonies but have the capacity to generate $EpCAM^+$ hTECs. $EpCAM^-$ hTECs maintain a basal epithelial identity but display hallmarks of EMT, such as the upregulation of ZEB1, the loss of CDH1 and a reduced expression of the miR-200 family members. We were also able to show that miR-200c overexpression is sufficient to convert $EPCAM^-$ hTECs into $EpCAM^+$ ones, implying a crucial role for the ZEB/miR-200 double-negative feedback loop in the control of stratification and EMT in cultured hTECs.

Our work suggests that hTECs possess an intrinsic stratification program of functional importance, not likely to result from promiscuous gene expression. We speculate that the maintenance of the thymic tridimensional epithelial network requires a fine balance between stratification and EMT, which could be regulated by the ZEB/miR-200 double-negative feedback loop. In this context, cultured hTECs represent an insightful system to better understand the mechanisms governing epithelial stratification and plasticity

Key words: thymus, thymic epithelial cells (TECs), stratification, EMT, ZEB, miR-200

Résumé

Le thymus est l'organe responsable de la différenciation et de la maturation des lymphocytes T. Son stroma est principalement composé de cellules épithéliales thymiques (TECs), qui forment une structure tridimensionnelle en filet. Malgré cette architecture particulière pour un épithélium, les TECs expriment des marqueurs généralement associés avec le développement et la différenciation de l'épiderme. Nous avons découvert que le thymus humain contient une population de TECs clonogéniques qui peut être cultivée et multipliée dans un système de culture développé pour les cellules souches de l'épiderme.

In vitro, les TECs humains (hTECs) peuvent générer des colonies possédant quatre morphologies différentes et expriment des marqueurs des couches basales des épithéliums stratifiés, tels que P63, K5/K14 et CD49f. Nous avons démontré que le niveau d'expression d'EpCAM peut être utilisé pour distinguer deux sous-populations d'hTECs en culture. Les hTECs $EpCAM^+$ n'engendrent que des colonies stratifiées pouvant former des squames et chez qui l'ont peut détecter l'expression de marqueurs de différenciation épidermique, alors que les hTECs $EpCAM^-$ engendrent principalement des colonies non stratifiées, tout en ayant la capacité de générer des hTECs $EpCAM^+$. Les hTECs $EpCAM^-$ maintiennent une identité cellulaire similaire à celle des couches basales des épithéliums stratifiés, mais montrent aussi des traits typiques de l'EMT, tels que l'expression accrue de ZEB1, la perte de CDH1 et une expression réduite des membres de la famille des miR-200. Nous avons aussi été capables de montrer que la surexpression de miR-200c est suffisante pour convertir les hTECs $EpCAM^+$ en hTECs $EpCAM^-$, ce qui semble indiquer un rôle crucial pour la boucle de feedback doublement négative ZEB/miR-200 dans le contrôle de la stratification et de l'EMT chez ces cellules.

Ce travail suggère que les hTECs possèdent un programme de stratification intrinsèque d'importance fonctionnelle qui ne semble pas résulter de l'expression génique promiscue. Nous pensons que le maintien du réseau tridimensionnel qui compose l'épithélium thymique nécessite un équilibre entre la stratification et l'EMT, qui pourrait être contrôlé par la boucle de feedback doublement négative ZEB/miR-200. Dans ce contexte, les hTECs en culture représentent un système qui peut être utilisé pour étudier les mécanismes gouvernant la stratification et la plasticité des épithéliums.

Mots clés: thymus, cellules épitheliales thymiques, stratification, EMT, ZEB, miR-200

Table of contents

1. Introduction

1.1 The thymus

Thymic function

The thymus is a bilobed primary lymphoid organ responsible for providing a suitable environment for the differentiation and selection of maturing T cells. It is located in the middle of the thoracic cavity, on top of the heart and behind the sternum. The thymus is divided into two histologically distinct subcompartments: an outer cortex and an inner, less dense, medulla (Fig. 2.1). It is surrounded by a mesenchymal capsula that invaginates, forming interconnected lobules. The thymic stroma is mostly composed of thymic epithelial cells (TECs), along with mesenchymal cells, endothelial cells and dendritic cells. However, although they are not part of the stroma, the majority of the cells that can be found in the thymus are developing thymocytes (Gordon & Manley, 2011).

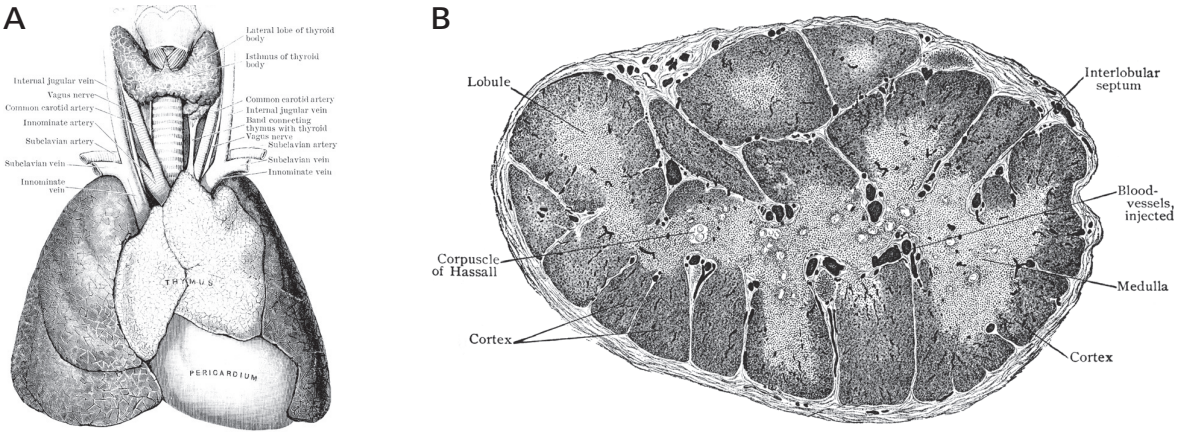

Figure 2.1 | Anatomy and histology of the thymus

A The thymus is located at the center of the thoracic cavity, on top of the heart and behind the sternum. Copied from (Cunningham, 1903). **B** The thymus is composed of an outer cortex and an inner medulla. It forms interconnected lobules and is surrounded by a mesenchymal capsula. Copied from (Piersol, 1908).

The immunological function of the thymus was only unveiled in 1961 thanks to the work of Jacques Miller. Until then, it was widely believed that "As a predominantly epithelial organ, the thymus had become redundant during the course of evolution and was just a graveyard for dying lymphocytes." (Miller, 2002). Miller showed that thymic ablation in newborn mice led to a marked deficiency in T lymphocytes and to a depression in the immune response against infection and foreign skin grafts (Miller, 1961; Miller, 1962a; Miller, 1962b). His work established the thymus as an essential organ for the formation of a functional and self-tolerant T cell repertoire (Miller, 2002). In humans, evidence for this role of the thymus came from the ability of thymic transplantation to rescue T cell deficiency in patients suffering from complete DiGeorge syndrome, a congenital disease characterized by athymia, cardiac malformations and parathyroid hypoplasia (Markert *et al.*, 1999).

T cell precursors enter the thymus through the bloodstream as multipotent lymphoid progenitors after leaving the bone marrow (Heinzel *et al.*, 2007; Serwold *et al.*, 2009). Within the thymus, T cell maturation occurs in distinct phases and places; initial substantial proliferation, progressive commitment to T cell lineage and rearrangement of the T cell receptor (TCR) locus take place in the sub-capsular zone and in the cortex, while the final selections for functionality and self-tolerance are carried out in the cortex and medulla, respectively (Koch & Radtke, 2011; Rothenberg & Yui, 2014).

After entering the thymus through blood vessels at the cortico-medullary junction, $CD4^-$ $CD8^-$ double-negative T cell precursors migrate to the subcapsular zone. There, they commit to the T cell lineage and mature into $CD4^+CD8^+$ double-positive thymocytes, which accumulate in the cortex. Next, these cells are first positively, and then negatively selected for their ability to recognize antigens presented on the surface of TECs, through Major histocompatibility complex (MHC) class I and II molecules (Anderson *et al.*, 2007; Vrisekoop *et al.*, 2014). The positive selection takes place in the cortex and leads to the "death by neglect" of T cells unable to recognize peptide-MHC complexes through their TCR. Conversely, apoptosis is induced at this stage in T cells whose TCR reacts too strongly to peptide-MHC (Klein *et al.*, 2009; Klein *et al.*, 2014). Surviving thymocytes differentiate into $CD4^+$ or $CD8^+$ single-positive T cells and migrate to the medulla, where they are screened for self-reactivity before exiting the thymus as mature T cells (Klein et al, 2014) (Fig. 2.2). This negative selection step is essential for the establishment of T cell self-tolerance and to avoid autoimmunity, as during this process, T cells expressing potentially auto-reactive TCRs are eliminated (Hogquist *et al.*, 2005; Anderson *et al.*, 2007).

Although the maturation of developing T cells is mainly sustained by TECs, other stromal cells are also involved. Neural crest-derived mesenchymal cells and endothelial cells are important for the correct functioning of the thymic microenvironment, while dendritic cells and macrophages participate in the clonal deletion and elimination of apoptotic thymocytes (Anderson *et al.*, 2007).

Mature T cells can be divided into two different lineages depending on the rearrangement of their TCR: a predominant αβ T cell and a minor γδ T cell population. Upon activation by antigen-presenting cells, αβ T cells can be further subdivided in several subsets with diverse functions: helper T cells assist other white blood cells in immunologic processes, cytotoxic T cells destroy cells deemed as infected or malignant, memory T

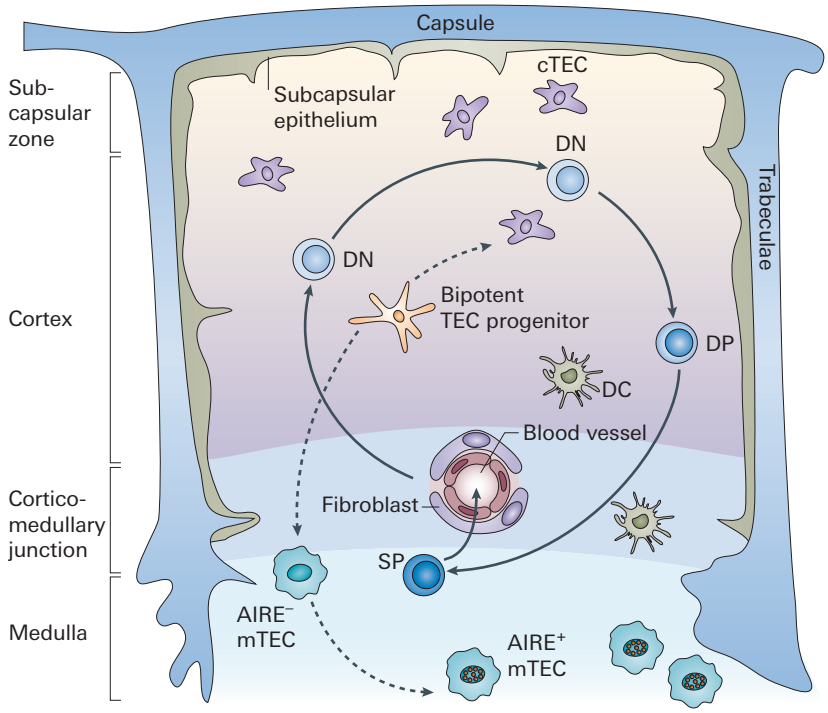

Figure 2.2 | T-cell development within the thymus

In the postnatal thymus, T-cell precursors enter the thymus through the bloodstream at the cortico-medullary junction as $CD4^{-}CD8^{-}$ double-negative (DN) thymocytes and migrate to the subcapsular zone. Following pre-TCR-mediated selection, they mature into $CD4^{+}CD8^{+}$ double-positive (DP) thymocytes that accumulate in the cortex. There, positive selection is mediated by cTECs and surviving thymocytes further differentiate into $CD4^{+}$ and $CD8^{+}$ single-positive (SP) T cells. Those relocate to the thymic medulla, where they are screened for self-reactivity by mTECs before exiting the thymus as mature T cells. Dotted arrows represent suggested TEC developmental stages. Mature cTECs and mTECs are generated from bipotent TEC progenitors that are found in the thymus at least until birth. DC: dendritic cell. Adapted from (Anderson *et al*., 2007)

cells persist long after an infection has resolved, regulatory T cells have a major role in the maintenance of T cell tolerance and natural killer T cells share properties of both naïve and effector T cells. On the other hand, γδ T cells are mostly found in epithelia and represent a bridge between the innate and adaptive immune systems (Dong & Martinez, 2010; Purnama *et al.*, 2013).

Thymic epithelial cells

The thymic stroma forms a characteristic complex 3D meshwork mainly composed of TECs (Fig. 2.3a; van Ewijk *et al.*, 1999). Three distinct TEC subpopulations can be identified on the basis of their keratin expression profile in the adult thymus: cortical TECs (cTECs) mainly express Keratin 8 (K8) and K18, medullary TECs (mTECs) preferentially express K5 and K14, and a few cells typically located at the cortico-medullary junction express both sets of keratins (Fig 2.3b; Klug *et al.*, 1998; Klug *et al.*, 2002). When analyzed by flow cytometry, all mouse TECs express Epithelial cell adhesion molecule (EpCAM) (Nelson *et al.*, 1996). cTECs are characterized by the expression of Ly51 and CD205, while mTECs are $Ly51^{-}CD205^{-}$ and express Ulex europaeus agglutinin 1 (UEA1) (Gray et al, 2002; Anderson & Takahama, 2012). In humans, however, EpCAM only marks mTECs and CD205 is generally used to identify cTECs (de Maagd *et al.*, 1985; Ritter & Palmer, 1999; Farley et al, 2013).

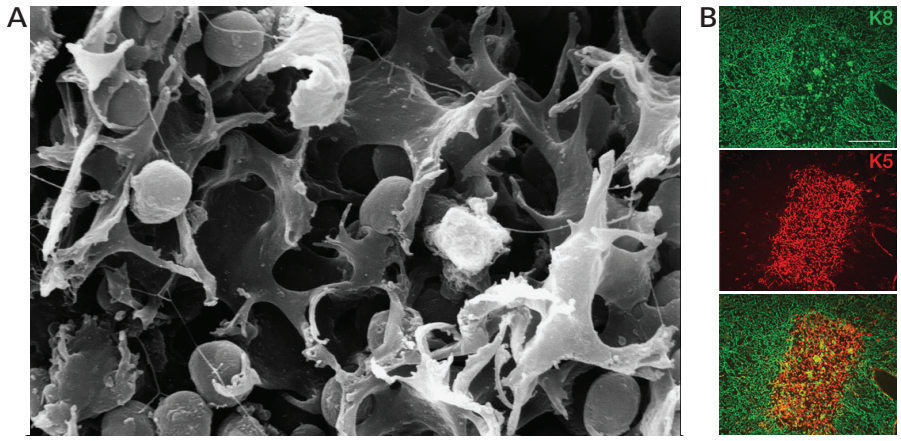

Figure 2.3 | Cellular composition of the thymus

A Scanning electron microscopy micrograph of thymocytes and cortical epithelial cells (3300x). TECs form a characteristic 3D meshwork structure that allows developing T cells to migrate through the thymic stroma. Copied from (van Ewijk *et al*., 1999). **B** Immunofluorescence on frozen sections of adult murine thymus. cTECs preferentially express K8 and mTECs preferentially express K5. A minor population of $K5^{+}K8^{+}$ double-positive cells can be observed, mostly at the cortico-medullary junction. Scale bar = 150µm. Copied from (Su *et al*., 2003).

While both TEC subtypes can express MHC class I and II molecules in order to present antigen peptides to developing thymocytes, their role in the selection process is quite different; cTECs are crucial in the positive selection of developing T cells, whereas mTECs are fundamental for their negative selection. For instance, the proteasome catalytic subunit ß5t is expressed exclusively in cTECs and plays a key role in the selection process through the generation of peptides for MHC class I presentation (Murata *et al.*, 2007; Nitta *et al.*, 2010). On the other hand, failure to develop a normal thymic medullary compartment is often associated with autoimmunity (Hogquist *et al.*, 2005; Anderson *et al.*, 2007). mTECs can further be subdivided into two distinct subsets: Autoimmune regulator $(AIRE)^{-}CD80^{low}$MHC class II^{low} mTEC progenitors and $AIRE^{+}CD80^{high}$MHC class II^{high} mature mTECs (Rodewald *et al.*, 2001; Rossi *et al.*, 2007a; Anderson & Takahama, 2012). The latter have the capacity to express tissue-restricted antigens (TRAs), a phenomenon known as promiscuous gene expression (Derbinski *et al.*, 2001). This process is essential for the negative selection of developing T cells and is highly dependent on AIRE (Blechshmidt *et al.*, 1999; Anderson *et al.*, 2002, Liston *et al.*, 2003).

AIRE is a transcriptional regulator that binds preferentially to unmethylated histone H3 at lysine-4 (H3K4me0), through one of its two PHD zinc finger domains. H3K4me0 usually marks inactive chromatin regions, suggesting a way for AIRE to be recruited on genes that are repressed in mTECs and to induce their expression (Org *et al.*, 2008). In this process, AIRE collaborates with other transcription activators such as CREB-binding protein (CBP) and pTEFIIb (Peterson *et al.*, 2008; Mathis & Benoist, 2009; Ucar & Rattay, 2015). *Aire*-deficient mice display reduced promiscuous gene expression in mTECs and organ-specific autoimmunity (Anderson *et al.*, 2002). In humans, AIRE appears to have a similar function, as its deficiency causes autoimmune polyendocrinopathy-candidiasis-ectodermal dystrophy (APECED), which causes multi-organ lymphocytic infiltration and autoantibody production (Björses *et al.*, 1998; Peterson *et al.*, 2008; Mathis & Benoist, 2009). However, even though AIRE is the main driver of promiscuous gene expression, other mechanisms have been shown to fulfill a similar function (Ucar & Rattay, 2015).

Thymus organogenesis

The embryonic origin of the thymic epithelium was for long debated, as many claimed a dual origin involving both the endoderm and the ectoderm, while others favored an endoderm-centric model (Manley & Blackburn, 2003). Eventually, lineage-tracing experiments published in 2004 by Gordon and colleagues proved that the pharyngeal ectoderm does not contribute to the formation of the thymus. Through transplantation experiments, they also showed that the embryonic day 9 (E9) mouse pharyngeal endoderm is sufficient for the formation of a functional thymic environment containing both medullary and cortical compartments (Gordon *et al.*, 2004). Two years later, Rossi and colleagues showed that cTECs and mTECs share a common origin in $K5^{+}K8^{+}$ double-positive bipotent progenitors (Rossi *et al.*, 2006). This combination of evidence settled once and for all the debate by establishing the strictly endodermal origin of the thymic epithelium.

Although ectodermal cells do not contribute directly to the formation of the thymic epithelium, the ectoderm still plays an essential role in its development; neural crest cells (NCCs) give rise to its pericytes and surrounding mesenchymal capsula (Le Douarin & Jotereau, 1975). This NCC-derived mesenchyme is fundamental to the regulation of TEC proliferation and differentiation as a source of Fibroblast growth factor (Fgf) 7 and Fgf10, which bind Fgf receptor 2 isoform IIIb (Fgfr2-IIIb) on the surface of TECs. Indeed, removal of these soluble growth factors has been shown to prevent the development of a functional thymus (Bockman & Kirby, 1984; Revest *et al.*, 2001; Jenkinson *et al.*, 2003; Itoi *et al.*, 2007; Rossi *et al.*, 2007b) (Fig. 2.4b).

In mouse, the thymus and the parathyroid glands originate from the third pharyngeal pouch, which emerges from the anterior part of the foregut at E9.5. The transcription factor Forkhead/winged-helix-n1 (Foxn1), is expressed on the posteroventral parts of the primordium by E11 and is the first true marker of thymic epithelial identity. At this stage, the anterodorsal parts already express Glial cells missing homologue 2 (Gcm2), which marks the parathyroid fate of these domains (Gordon *et al.*, 2001). At E12.5, the primordia detach from the pharynx and by E13.5, parathyroid- and thymus-specific domains have become separated organs. At birth, both of them have completed their migration to their final positions (Gordon & Manley, 2011) (Fig. 2.4a).

T cell precursors start entering the thymus around E11.5, guided by the controlled expression of specific chemokines by TECs (namely, Ccl21 and Ccl25) (Takahama, 2006; Anderson & Takahama, 2012). The entrance of T cell precursors in the thymus is not a continuous process but occurs in successive, discrete waves. The first one takes place at E11.5 and involves a very small number of cells, which must enter through the mesenchymal capsula as this event occurs prior to the vascularization of the thymic primordium. Starting from E13.5, the thymic function becomes dependent on the "crosstalk" between TECs and the developing thymocytes. This "crosstalk" is not only necessary for the differentiation of the maturing T cells but also for the correct development of the thymic epithelium (Nitta *et al.*, 2011). Indeed, mice with an early and profound arrest in thymocyte differentiation, such as the recombination-activating gene 2/common cytokine receptor γ-chain-deficient (RAG2/γc) and the *Ikaros*-null mice, have strong thymic development defects such as a disorganized cortex and an

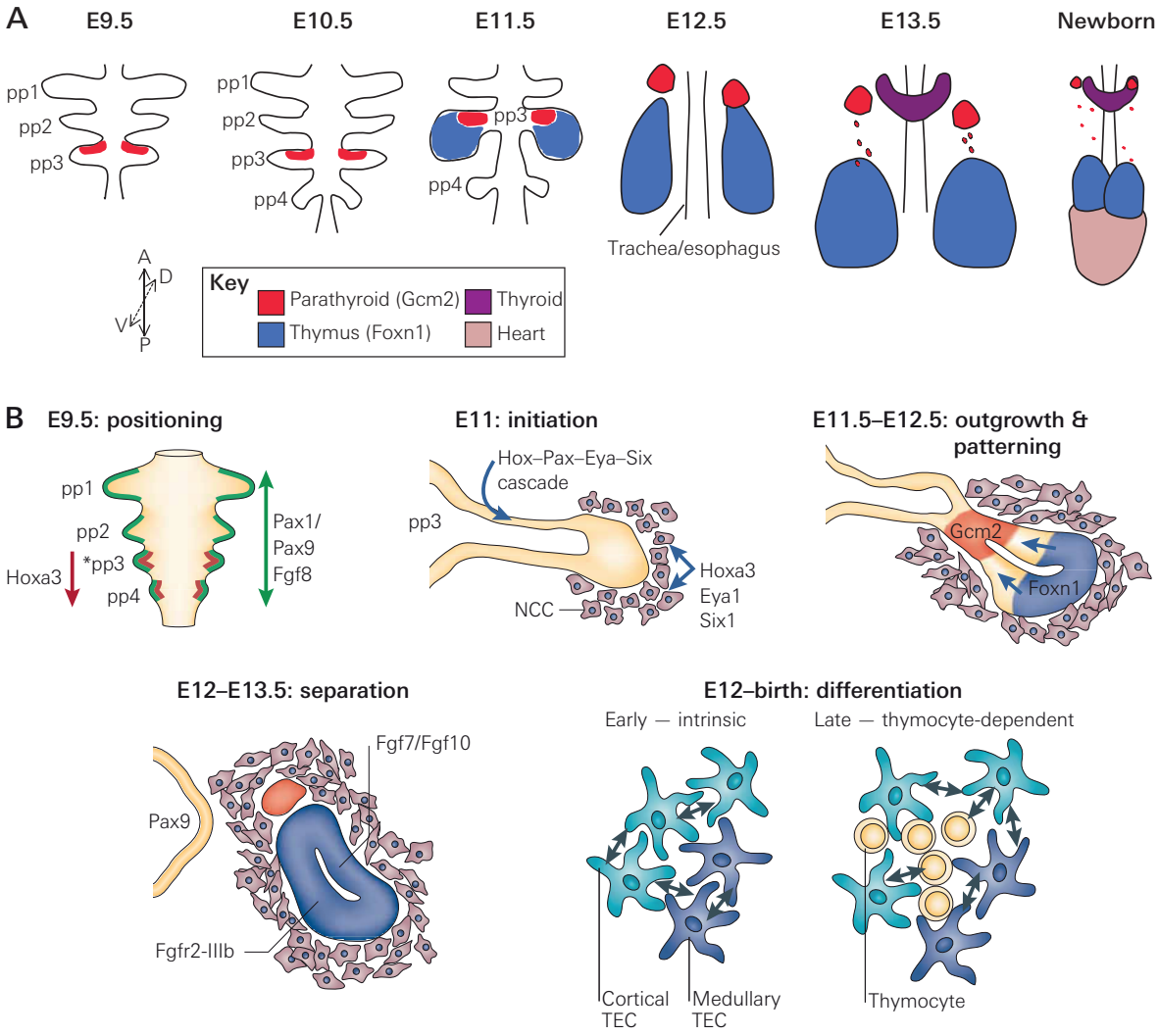

Figure 2.4 | Thymus organogenesis in mouse

A The pharyngeal pouches (pp) emerge laterally from the foregut, with the third pouches (pp3) appearing at E9.5. At this stage Gcm2 expression already marks the parathyroid domain. The fourth pouch (pp4) appears around E10.5. By E11.5, the third pouches have developed into primordia that are patterned into thymus and parathyroid domains, marked by Foxn1 and Gcm2 expression, respectively. At E12.5, the primordia have detached from the pharynx, and the parathyroid glands begin to separate from the thymus lobes. By E13.5, the parathyroid glands have parted from the thymus and remain adjacent to the thyroid. At the newborn stage, the organs are in their final positions. Adapted from (Gordon & Manley, 2011). **B** E9.5: positioning. Pax1, Pax9 and Fgf8 (green) are required for pp formation. Hoxa3 (red) is required for pp3 axial identity. E11: initiation. Rudiment outgrowth begins at this stage. The Hox–Pax–Eya–Six cascade is required in the endoderm (yellow); Hoxa3, Eya1 and Six1 might also be required in NCCs. E11.5–E12.5: outgrowth and patterning of the rudiment. The rudiment is regionalized into thymus- and parathyroid-specific domains. This patterning actually begins at E9.5 with the expression of Gcm2 (red) in the third pouch. Lymphoid progenitors (not shown) also begin to arrive at this time, entering the thymus through the mesenchymal capsule. E12–E13.5: separation from the pharynx and migration of the rudiment. NCCs regulate TEC proliferation and differentiation through the secretion of Fgf7 and Fgf10, which bind Fgfr2-IIIb on the surface of TECs. Pax9 is required for separation from the pharynx. E12–birth: differentiation. Foxn1 is required for the generation of both cTECs and mTECs. Initial differentiation is thymocyte-independent, whereas final differentiation requires thymocyte-derived signals. Adapted from (Blackburn & Manley, 2004).

almost absent medullary epithelium. Studies on these mice also established the fact that T cell progenitors do not appear to be involved during early organogenesis and seem to be essential only starting at E13.5 (Fig. 2.4b) (Van Ewijk *et al.*, 2000; Klug *et al.*, 2002; Nitta *et al.*, 2011).

A number of transcription factors have been shown to have an essential role in the early stages of thymus development, such as Homeobox A3 (Hoxa3; Manley *et al.*, 1995), Eyes absent 1 homologue (Eya1; Xu *et al.*, 2002), Sine oculis-related homeobox 1 homologue (Six1), Six4 (Zou *et al.*, 2006), Paired box gene 1 (Pax1; Wallin *et al.*, 1996), Pax9 (Hetzer-Egger *et al.*, 2002), and T-box transcription factor 1 (Tbx1; Jerome & Papaioannou, 2001; Manley & Condie, 2010; Gordon & Manley, 2011) (Fig. 2.4b & Table 2.1). Indeed, the deletion of a single one of these genes has been shown to lead to either thymic aplasia or hypoplasia, although it remains unclear whether they have a direct impact on TEC development rather than on upstream patterning processes. The early patterning of the thymus has, on the other hand, been shown to involve the Sonic hedgehog (Shh; Moore-Scott & Manley, 2005), Bone morphogenic protein (BMP; Bleul & Boehm, 2005), Wnt (Balciunaite *et al.*, 2002) and FGF signaling pathways (Frank *et al.*, 2002; Gordon & Manley, 2011) (Table 2.1).

Factor	Gene family	Relevant expression pattern	Relevant function
Signaling molecules			
Bmp4 (bone morphogenic protein 4)	Transforming growth factor-beta secreted signal superfamily	Distal-posterior (presumptive thymus) domain of third pouch; prior to Foxn1	Epithelial-mesenchymal interactions involved in morphogenesis
Fgf8 (fibroblast growth factor 8)	Fibroblast growth factor, secreted signal	Distal-posterior (presumptive thymus) domain of third pouch; prior to Foxn1	Early pouch formation, possible role in patterning
Shh (sonic hedgehog)	Hedgehog family, secreted signal	Pharyngeal endoderm, but excluded from third pouch	Initial parathyroid fate
Wnt5b (wingless-int 5b)	Wingless homolog family, secreted signal	Distal-posterior (presumptive thymus) domain of third pouch; prior to Foxn1	No functional evidence to date
Transcription factors			
Eya1 (eyes absent homolog 1)	Eyes absent family of transcriptional co-activators	Pharyngeal endoderm, mesenchyme and ectoderm	Early pouch formation and patterning
Foxn1 (forkhead box protein n1)	Winged-helix transcription factor	Ventral domain of third pouch from E11.25; mature TECs	TEC differentiation
Hoxa3 (homeobox protein a3)	Hox-class homeobox transcription factor	Pharyngeal endoderm and NCC-derived mesenchyme; E10.5	Early pouch patterning and initial organ formation
Pax1 (paired box protein 1)	Pax transcription factor containing a paired domain only	Pharyngeal pouches (endoderm)	Early pouch formation and parathyroid development; minor role in thymus size
Pax9 (paired box protein 9)	Pax transcription factor containing a paired domain only	Pharyngeal pouches (endoderm)	Pouch and initial organ formation; TEC differentiation
Six1/4 (sine oculis homolog 1/4)	Homeobox transcription factor	Pharyngeal endoderm, mesenchyme and ectoderm	Early organ formation and patterning
Tbx1 (T-box 1)	T-box transcription factor family	Dorsal third pouch and mesodermal core of pharyngeal arches	Pouch formation and patterning, might establish parathyroid fate

Table 2.1 | Factors implicated in thymus development (Gordon & Manley, 2011)

The transcription factor Foxn1 is crucial for the development of TECs (Blackburn *et al.*, 1996). Deletion or mutations that lead to Foxn1 loss of function result in the nude mouse phenotype, which is characterized by hairlessness, athymia and severe immunodeficiency (Nehls, 1994). In these mice, TECs undergo maturational arrest and persist

as progenitors after the thymic primordium has formed. As Foxn1 marks all developing TECs, its promoter has been widely used to drive the ectopic expression of genes specifically in the TEC compartment of transgenic mice (Rodewald, 2008).

Although most of the knowledge we have on the genetic mechanisms governing thymus organogenesis is based on mouse work, a recent study demonstrated that these processes may be conserved in humans (Farley *et al.*, 2013).

Thymic involution

Soon after birth, the thymus undergoes a progressive age-induced atrophy that is named thymic involution. In mice, this process is characterized by a significant reduction in the size of the organ, progressive loss of the normal cortical/medullary compartmentalization and disintegration of the cortico-medullary junction, along with a depletion of the TEC pool that is accompanied by accumulation of adipocytes (Lynch *et al.*, 2009). In humans on the other hand, the overall size of the thymus remains relatively unchanged throughout life, although, just as in mice, its main cellular component is gradually shifted from TECs to a vast majority of adipocytes. Despite the fact that thymic function progressively declines with age, a substantial T cell output is maintained into late adulthood both in mice and humans (Lynch *et al.*, 2009).

A number of conditions, including myastena gravis (an autoimmune disease), chemotherapy and HIV infections have been shown to induce premature thymic atrophy (Haynes *et al.*, 2000). Interestingly, androgen blockade, as well as the treatment of HIV or the suspension of chemotherapy, have been shown to revert thymic atrophy and induce thymus regeneration with a consequent increase of thymic functionality (Douek *et al.*, 1998; Sutherland *et al.*, 2005; Lynch *et al.*, 2009).

The exact mechanisms that govern this slow decline in the function of the thymus have not yet been fully elucidated. However, recent evidence suggests that the regulation of Foxn1 is most likely implicated in thymic involution. Indeed, the post-natal downregulation of Foxn1 induces premature thymic atrophy in mice, and its overexpression is sufficient to regenerate a fully involuted thymus and to restore the characteristics of the juvenile organ (Chen *et al.*, 2009; Bredenkamp *et al.*, 2014).

Thymic epithelial stem cells?

Whether or not the adult thymus contains *bona fide* thymic epithelial stem cells remains an unanswered question, as formal proof of their existence is still lacking. However, the fact that thymic involution can be reversed under certain experimental conditions supports the idea that there is a TEC population that maintains the capacity to proliferate and to differentiate upon activation throughout adulthood, the two key characteristics of adult stem cells (Gray *et al.*, 2006; Smith, 2006). Moreover, it has been proven that some postnatal TECs have the capacity to generate thymic tissue with defined cortical and medullary areas (Bleul *et al.*, 2006), and to express the functional markers Aire and MHC class II, even after extensive expansion *in vitro* (Bonfanti *et al.*, 2010).

In early studies, embryonic TECs expressing the surface antigens Mts20 and Mts24 (now known to be Plet-1) were proposed as candidate thymic epithelial progenitors, as they had the capacity to reconstitute a functional thymus when transplanted under the kidney capsula of nude mice (Bennett *et al.*, 2002; Gill *et al.*, 2002). These results were challenged soon afterwards when Mts20^{-}Mts24^{-} embryonic TECs where also shown to have the capacity to generate a functional thymus in a similar experiment, if enriched for epithelial cells (Rossi *et al.*, 2007c).

During development, all TECs arise from a common K5^{+}K8^{+} double-positive bipotent progenitor population (Rossi *et al.*, 2006). Although some K5^{+}K8^{+} double-positive cells can still be found in the postnatal thymus, whether or not they represent a population of thymic epithelial stem or progenitor cells in the adult remains to be proven. However, several lines of evidence seem to support their existence; an increased proportion of K5^{+}K8^{+} double-positive TECs can be observed after transient thymic involution achieved by steroid treatment or irradiation, and these cells appear to be marked by the proliferation marker Ki67 (Popa *et al.*, 2007). This data suggests that the postnatal thymus contains a population of TECs that can be induced to proliferate in order to regenerate the thymus in specific circumstances (Rode & Boehm, 2012).

The considerable turnover of MHC class II^{+} TEC subpopulations, and the clustered organization of the differentiated cells upon thymic regeneration observed in the adult thymus, raise the possibility that the maintenance of its epithelial-cell environments may also involve the expansion of lineage-restricted progenitors in the medullary and cortical compartments (Rodewald *et al.*, 2001; Gray *et al.*, 2006; Bleul *et al.*, 2006; Shakib *et al.*, 2009). The existence of these committed TEC progenitors is supported by the presence of a population of AIRE^{-}CD80^{low} mTEC progenitors able to yield AIRE^{+}CD80^{high} mature mTECs (Rodewald *et al.*, 2001; Rossi *et al.*, 2007a). In addition, there is a population of embryonic Claudin-3^{high}Claudin-4^{high} TECs that exclusively generates mTECs and that can contributes to the lifelong maintenance of mTEC regeneration and central T cell tolerance (Hamazaki *et al.*, 2007; Sekai *et al.*, 2014). On the other hand, cTEC-restricted progenitors have proven to be more difficult to identify. Perhaps, this struggle in their identification can be explained by the fact that, during development, immature TECs expressing the common cortical marker CD205 have been shown to have the capacity to generate both cortical and medullary TECs (Baik *et al.*, 2013). Moreover, lineage-tracing experiments demonstrated that the majority of postnatal TECs originate from precursors expressing the ß5t proteasome subunit, the other usual marker of cortical identity (Ohigashi *et al.*, 2013).

Recently, it was proven that the adult thymus contains a population of MHCII^{low} UEA-1^{-}Ly51^{low}CD49f^{high}Sca-1^{high} TECs that displays substantial self-renewal capacity and multilineage differentiation potential. Most of these cells were label-retaining and were found at the cortico-medullary junction. Importantly, they had the capacity to differentiate into cortical and medullary TEC lineages, including tolerogenic Aire^{+} mTECs, when challenged in an *in vivo* thymus reconstitution assay, even after growing in a 3D culture system for a week (Wong *et al.*, 2014). These results support the existence of an adult population of thymic epithelial stem/progenitor cells, characterized by *in vivo* quiescence, self-renewal and the capacity to generate cTEC and mTEC lineages.

Clinical relevance of the identification of thymic epithelial stem cells

HIV infection and the cytotoxic treatments that often accompany hematopoietic stem cell transplants used to cure malignant diseases, such as chemotherapy and radiotherapy, have been shown to induce a severe thymic function reduction (Haynes *et al.*, 2000; Chidgey *et al.*, 2007). The age-correlated inability of adults to restore immune function after these events is linked to thymic involution and leads to increased morbidity and often mortality in the aged. Thus, the rapid restoration of a functional thymus is crucial to these patients as it would boost their recovery. More generally, age-dependent thymic involution *per se* has been shown to reduce the efficacy of the immune system and is linked to an increase in the occurrence of opportunistic infections, autoimmunity and the in the incidence of cancer (Lynch *et al.*, 2009).

In the context of an aging society, it is of paramount importance to develop strategies to restore thymic function. Proof of principle for the transplantation of thymic tissue as a means to rescue immunodeficiency comes from children affected by complete DiGeorge syndrome. It has been demonstrated that ectopic transplantation of neonatal human thymic tissue can provide these patients with an adequate environment for the development of a functional adaptive immune system (Markert *et al.*, 1999). This data establishes ectopic thymic tissue transplantation and its subsequent thymic function enhancement as a potential method to reconstitute a mal- or non-functioning immune system.

In order to make up for the lack of compatible donors, we need to identify thymic epithelial stem cells and understand the mechanisms that govern their behavior. Indeed, this knowledge could pave the way for the development of treatments leading to thymus regeneration or to the generation of transplantable thymic tissue (Blackburn *et al.*, 2002). Such treatments would augment thymopoiesis and promote output of naïve T cells, which could greatly benefit patients that suffer from a reduced or absent thymic function.

1.2 Similarities between the thymic epithelium and the epidermis

The skin

The skin protects the organism from dehydration and from the environment through its vital barrier function. It also has a central role in the collection of sensory information. Mammalian skin is composed of three distinct layers: the epidermis, the dermis and the hypodermis. The outermost layer, the epidermis, is a self-renewing squamous stratified epithelium mostly composed of keratinocytes. Its basal layer rests on a basement membrane, which separates it from the dermis, a thick layer of connective tissue populated by fibroblasts. The extracellular matrix of the dermis confers the skin its mechanical strength and is composed of collagen, proteoglycans and elastic fibers. The hair follicles, sebaceous glands and sweat glands are skin appendages that are

embedded in the dermis, although they form a continuum with the epidermis. Finally, the hypodermis is the innermost layer of the skin. It is mainly populated by adipocytes, is responsible for fat accumulation and plays an important role in thermoregulation and energy storage (Fig 2.5).

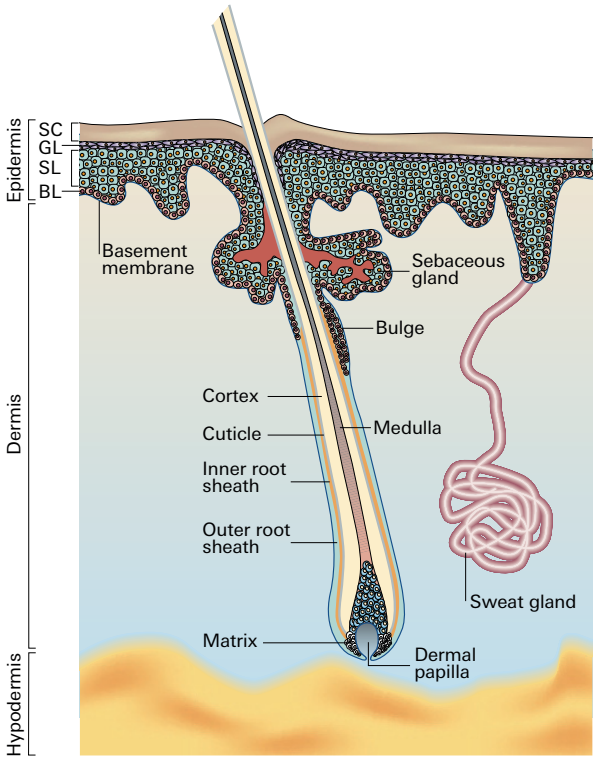

Figure 2.5 | Mammalian skin structures
The mammalian skin is composed of three distinct layers: the epidermis, the dermis and the hypodermis. The basal layer (BL) of the epidermis rests on a basement membrane that separates it from the dermis. It contains the mitotically active cells of the epidermis. As they differentiate and stratify, they form the outer layers of the epidermis: the spinous layer (SL), granular layer (GL) and the stratum corneum (SC). The hair follicle, depicted here in cross-section, forms a continuum with the epidermis. The hair bulb is found at the bottom of the follicle and is made of proliferating matrix cells that differentiate into the various structures of the hair follicle. The dermal papilla is formed of specialized mesenchymal cells and is surrounded by the hair matrix cell. In rats, multipotent hair follicle keratinocyte stem cells concentrate within the bulge region. In humans, most of these clonogenic cells are found right underneath the bulge. Copied from (Fuchs & Raghavan, 2002).

Epidermal and hair follicle stem cells

The capacity of the epidermis to perpetually self-renew and of the hair follicle to continuously undergo cycles of growth and degeneration are known to rely on a dedicated population of stem cells. These two tissues thus quickly became excellent model systems to explore the mechanisms that govern the development, homeostasis and regeneration of stratified epithelia.

The mitotically active cells of the epidermis are restricted to its basal layer. As they progressively differentiate, they withdraw from the cell cycle and migrate outward to the suprabasal layers. By the time they reach the epidermal surface, they have become terminally differentiated, anucleated, dead, flattened cells, called squames. Those are then shed from the skin surface and are continuously replaced by inner cells moving outward (Fuchs, 2008). Epidermal stem cells are known to reside within the basal layer of the epidermis. However, a precise molecular marker combination to identify them unambiguously is still lacking (Barrandon *et al.*, 2012; Mascré *et al.*, 2012).

In 1975, Rheinwald and Green were the first to successfully grow human epidermal keratinocytes (hEKs) *in vitro*. To do so, they cultured them on an irradiated 3T3-J2 mouse embryonic fibroblast feeder layer (Rheinwald & Green, 1975). In these conditions, some cells isolated from the interfollicular epidermis progressively grew as stratified colonies and were shown to have a high clonogenic potential (Rheinwald & Green, 1975;

Barrandon & Green, 1985). A few years later, Barrandon and Green demonstrated that clonogenic hEKs can be classified in three classes according to their growth potential, termed holoclones, meroclones and paraclones. Holoclones display the highest clonogenic potential, generate very few aborted colonies and are likely to represent epidermal stem cells *in vitro*. Meroclones form both large progressively growing and aborted colonies. Finally, paraclones only generate aborted colonies (Fig. 2.6).

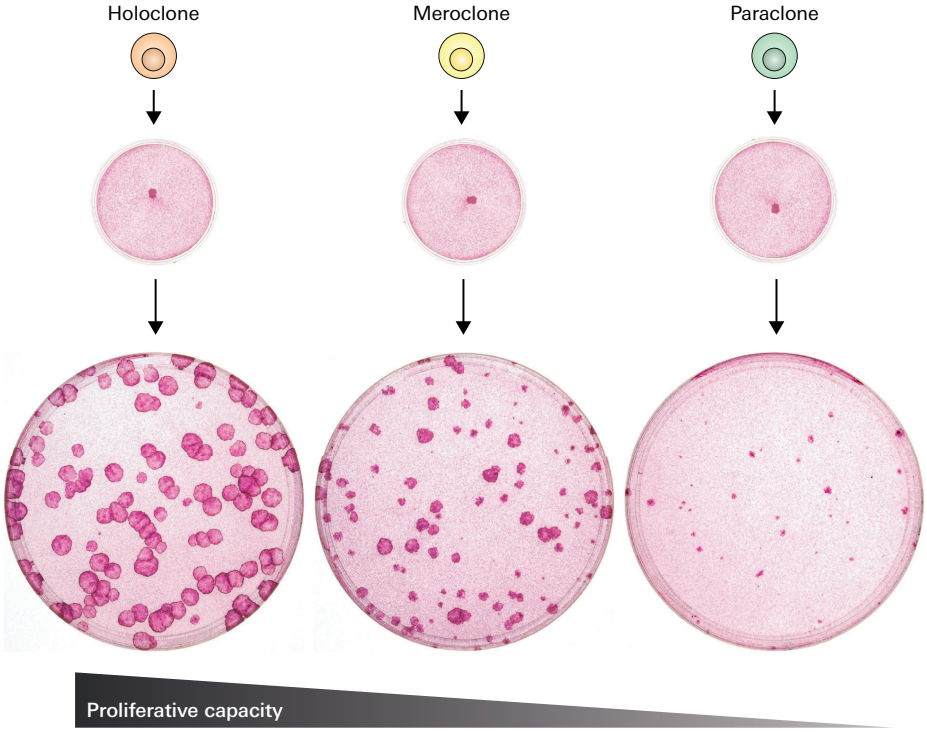

Figure 2.6 | Clonogenic epidermal keratinocytes have different proliferation potentials *in vitro*
Holoclones have the highest clonogenic potential and generate less than 5% of aborted colonies. Meroclones form both large progressively growing and aborted colonies. Finally, paraclones only generate aborted colonies. Adapted from (Barrandon *et al*., 2012).

Definitive proof that some of these cultured cells are *bona fide* adult keratinocyte stem cells comes from the fact that they can be transplanted back on patients and regenerate a functional epidermis that will persist for more than 20 years. Transplantation of these cultured epithelium autografts is a life-saving technology that is used in the clinic to treat extensive third degree burns (O'Connor *et al.*, 1981; Gallico *et al.*, 1984; Green *et al.*, 2008). However, these grafts only form scar tissue and no skin appendages are regenerated. This represents a lower quality of life for the patients, both physically and socially. Despite this obvious need for progress, skin culture and grafting techniques have proven to be difficult to significantly improve in the past 30 years (Rochat *et al.*, 2013).

In contrast to clonogenic hEKs, which are unipotent stem cells that can only regenerate the multiple layers of the epidermis, rat and mouse clonogenic hair follicle cells are multipotent stem cells. Indeed, they have the capacity to give rise to hair follicles, sebaceous glands and interfollicular epidermis (Blanpain *et al.*, 2004; Claudinot *et al.*, 2005). Clonogenic keratinocytes can also be isolated from human hair follicles, although their multipotency hasn't been formally demonstrated due to the lack of a proper assay

(Rochat *et al.*, 1994). In rat hair follicles, clonogenic keratinocytes concentrate within a region known as the bulge area, located at the insertion site of the arrector pili muscle (Fig. 2.5) (Kobayashi *et al.*, 1993). In humans, most of the colony-forming cells are found below the bulge area, in a region containing the peripheral columnar cells of the outer epithelial sheath (Rochat *et al.*, 1994).

Similarities between TECs and skin keratinocytes

Despite of its unconventional epithelial architecture, the thymus shares striking similarities with the epidermis (Lobach & Haynes, 1987; Patel *et al.*, 1995; Roberts & Horsley, 2014). Indeed, an intriguing resemblance can be observed between the keratin expression patterns of the two mature TEC subsets and those of epidermal keratinocytes. cTECs are marked by the expression of K8 and K18, which are also expressed by the surface ectoderm and the periderm, two embryonic epidermal sheets that precede stratification (Byrne *et al.*, 1994). On the other hand, mTECs express K5 and K14, whose expression marks the basal layer of the epidermis (Fuchs & Green, 1980). Finally, stratified squamous epithelial structures called Hassall bodies can be found in the thymic medulla, especially in humans. These structures are thought to be composed of terminally differentiated mTECs and express markers usually associated with terminal epidermal differentiation such as K1, Filaggrin (FLG) and Involucrin (IVL) (Langbein *et al.*, 2003; Hale & Markert, 2004; Yanos *et al.*, 2008; Wang *et al.*, 2012) (Fig 2.7).

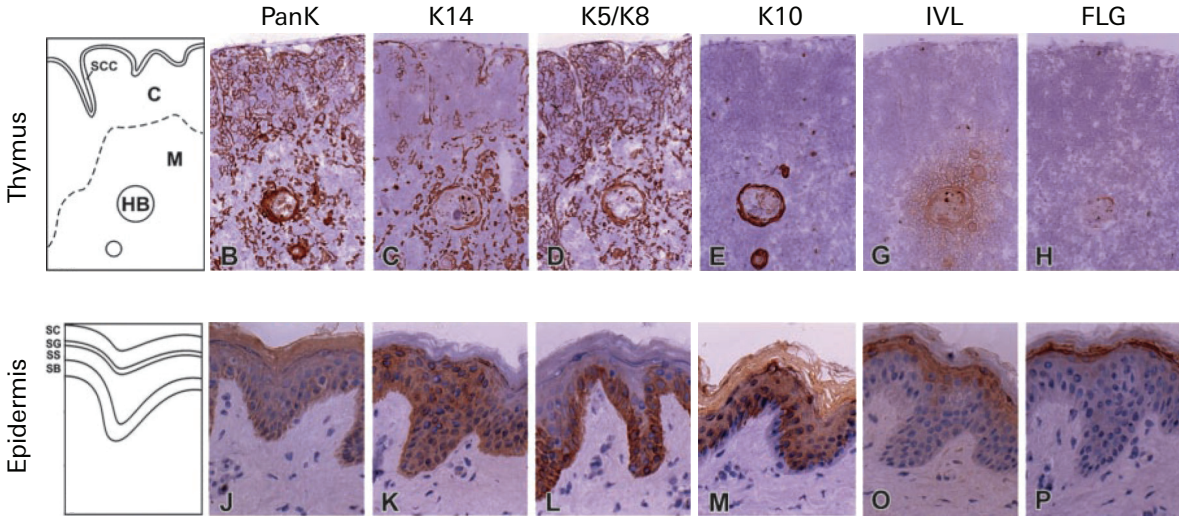

Figure 2.7 | Similarities between TECs and epidermal keratinocytes

TECs appear to reproduce part of the program that marks epidermal development. cTECs express K8 and K18, which are expressed by the surface ectoderm and the periderm, whereas mTECs express K5 and K14, which mark the basal layers of the epidermis. Moreover, as mTECs differentiate towards Hassall corpuscles, they start to express K10, IVL and FLG, three markers of epidermal differentiation that are expressed by the upper layers of the epidermis. Adapted from (Hale & Markert, 2004).

The thymic epithelium also expresses the transcription factor p63, a master regulator of stratified epithelia's development and maintenance. p63-knockout mice have been shown to present severe developmental defects in all stratified epithelia, truncated or absent limbs and craniofacial abnormalities. These animals die of dehydration several hours after birth due to the permeability of their skin. p63 specifically marks the basal

layers of stratified epithelia and two hypotheses have been proposed for its function; it is believed to act either on the differentiation capacity of these epithelia, or on the maintenance of their stem cell population (Mills *et al.*, 1999; Yang *et al.*, 1999; Pellegrini *et al.*, 2001; Candi *et al.*, 2015).

In 2007, Senoo and colleagues demonstrated that p63 knockout mice also suffer from thymic hypoplasia, caused by a reduced TEC proliferation rate and enhanced TEC apoptosis. Nevertheless, the thymus of these mice is still functional as cTEC and mTEC development and thymocyte differentiation occur normally. This data suggests that p63 is necessary for TEC proliferation and survival but that it is not required for their initial commitment and differentiation. In the same study, Senoo and colleagues showed that the rat thymus contains a population of clonogenic epithelial cells that can be isolated and extensively cultured using the 3T3-J2 culture system. In these conditions, cultured rat TECs (rTECs) grow as stratified colonies and are morphologically very similar to cultured epidermal keratinocytes. The authors were also able to show that most rTECs express p63 *in vitro* and that its down-regulation leads to a reduced proliferation rate, just as it does in epidermal keratinocytes (Senoo *et al.*, 2007).

1.3 *In vitro* cultured TECs

Cultured rat TECs

Research performed in our lab by Bonfanti and colleagues has demonstrated that cultured rTECs express genes related to thymic identity (*Pax1/9, Eya1, Six1, Foxn1,* and *Hoxa3*), as well as epidermal differentiation markers such as IVL and LEKTI. Moreover, these cells maintain the capacity to integrate a thymic epithelial network and to express MHC-II and Aire, two thymic functional markers, in a whole-organ re-aggregation assay (Bonfanti *et al.*, 2010).

Surprisingly, rTECs are also able to regenerate a fully functional epidermis and its appendages when challenged in an *in vivo* long-term skin reconstitution assay. They even surpass the regeneration capacity of *bona fide* hair follicle stem cells as the latter are unable to durably regenerate an epidermis in the same assay (Claudinot *et al.*, 2005). This study proved that a skin inductive microenvironment is sufficient to reprogram rTECs into hair follicle multipotent stem cells, in a process that involves crossing germ layer boundaries (Bonfanti *et al.*, 2010).

Cultured human TECs

In unpublished work from our laboratory, the human thymus has also been shown to contain a population of clonogenic epithelial cells that can be extensively cultured *in vitro* using the 3T3-J2 culture system. Like their rat counterpart, they express genes related to thymic identity (*PAX1/9, HOXA3, TBX1, EYA1* and *SIX1*), and *p63* (Bonfanti *et al.*, 2010; Maggioni, 2012).

However, unlike rTECs, human TECs (hTECs) form four morphologically distinct colony-types in culture, which we named simple, refringent, stratified and aborted. Colonies classified as simple have an appearance similar to simple epithelial cells growing in culture, with only little contact between cells. Colonies classified as stratified are composed of densely packed cells and some of them even form squame-like cells. This morphology is similar to the one displayed by hEKs in the same culture conditions. Aborted colonies have a morphology that closely resembles the aborted colonies formed by hEKs. Finally, refringent colonies are compact, but do not stratify (Maggioni, 2012) (Fig. 2.8).

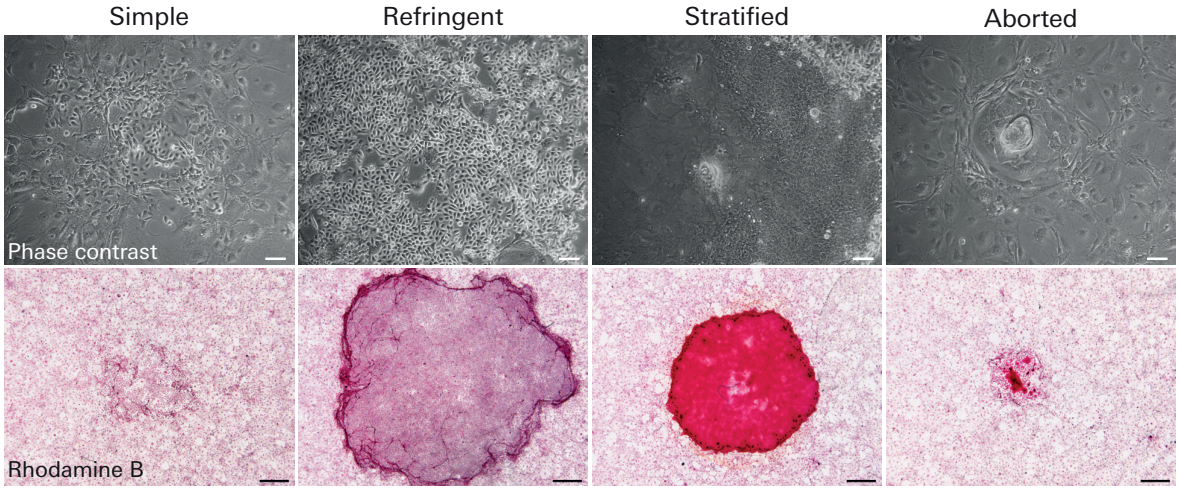

Figure 2.8 | Four morphologically distinct hTEC colony types
Cultured hTECs can from four morphologically distinct colony types: simple, refringent, stratified and aborted. Up: phase contrast imaging, scale bar = 100µm. Down: Rhodamine B staining, scale bar = 1mm. Phase contrast images are courtesy of M. Maggioni.

All four colony types express K5 and K14, but the expression of K8 and K18 at the protein level is observed only during the first week in culture in a minor fraction of the cells, similarly to what can be observed in rTECs. Integrinβ4 and Integrinα6 (CD49f), two markers of the basal layer of the epidermis used in attempts to isolate epidermal stem cells, are expressed in all colony morphologies. Further on, this expression of markers of the basal layer of the epidermis will be referred to as a "basal epithelial phenotype" to simplify the writing. On the other hand, markers of epidermal differentiation (K1, CLDN1/7, IVL, LEKTI) are expressed only in the stratified and aborted colonies (Maggioni, 2012).

By analyzing the progeny of single-cell-derived hTEC clones, Melissa Maggioni was able to establish a hierarchical organization between the colony types. Cells from refringent clones can give rise to colonies of all four hTEC colony types, whereas cells from stratified clones yield stratified and aborted colonies. Finally, cells from simple and aborted clones appear to have very limited clonogenic potentials in our culture system (Maggioni 2012) (Fig 2.9). Surprisingly, when analyzed by microarray, stratified clones cluster closer to hEKs than to other hTEC colony types, clones with simple morphology are the furthest away from keratinocytes and refringent clones are found in-between (Maggioni, 2012).

So far, we have been unsuccessful in identifying conditions that allow cultured hTECs to participate in the formation of a thymic epithelial network in a whole-organ re-aggregation assay. These cells are also incapable of forming epidermal tissue in an epidermis regeneration assay, whereas hEKs are able to do so under the same conditions (Maggioni, 2012; Droz-Georget Lathion *et al.*, 2015).

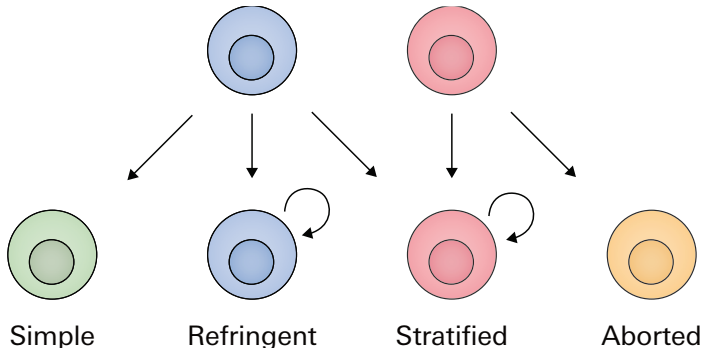

Figure 2.9 | Hierarchical organization of hTEC colony types
hTEC clones were serially amplified and the morphology of their progeny analyzed. Cells from refringent colonies can give rise to colonies of all four hTEC colony types. Cells from stratified colonies only yield stratified and aborted colonies. Finally, cells from simple and aborted colonies have very limited clonogenic potentials in our culture system. Adapted from (Maggioni, 2012).

1.4 microRNAs

microRNA biogenesis

MicroRNAs (miRNAs) are a class of endogenous, small (18-25nt), non-coding, single-stranded RNA molecules (Lee *et al.*, 1993; Wightman *et al.*, 1993; Bartel *et al.*, 2004). They silence complementary target mRNAs by driving their decay or translational repression. Because single miRNAs commonly have the ability to regulate the expression of numerous genes, they have an effect on a large variety of cellular processes. In addition, they can act either as switches or fine-tuners of translation, giving them a predominant role as regulators of development, homeostasis and disease (Mukherji *et al.*, 2011; Sayed & Abdellatif, 2011; Ebert & Sharp, 2012; Gurtan & Sharp, 2013).

miRNA biogenesis is a multistep process that starts with the transcription of a miRNA primary transcript (pri-miRNA), which contains at least one hairpin-like miRNA precursor. These genes are generally transcribed by a type II RNA polymerase (RNA pol II) and are often polycistronic (Lee *et al.*, 2002; Cai *et al.*, 2004; Lee *et al.*, 2004). Next, the Microprocessor protein complex cleaves the pri-miRNA into ~65nt hairpin precursor miRNAs (pre-miRNAs). This protein complex contains DiGeorge Syndrome Critical Region 8 (DGCR8), a dsDNA-binding protein, and Drosha, an RNase III-type protein that specifically cuts out the pre-miRNAs (Kim *et al.*, 2009; Krol *et al.*, 2010, Ha & Kim, 2014). The cut made by Drosha already defines the 5' end of the mature miRNA. Some short spliced-out introns are an exception, as they represent a Drosha/DGCR8-independent source of pre-miRNAs (Kim *et al.*, 2009). Then, Exportin 5 and its cofactor RanGTP actively transport all pre-miRNAs to the cytoplasm. There, Dicer, another type III RNase, removes the loop region of pre-miRNAs, generating miRNA/miRNA* duplexes. For this purpose, Dicer interacts with TAR RNA-binding protein (TRBP), whose role

has not been clearly defined yet. Finally, the mature single-stranded miRNA is incorporated in a ribonucleoprotein complex called RNA-induced silencing complex (RISC), which it guides to complementary mRNA targets (Kim *et al.*, 2009; Krol *et al.*, 2010; Ha & Kim, 2014) (Fig. 2.10).

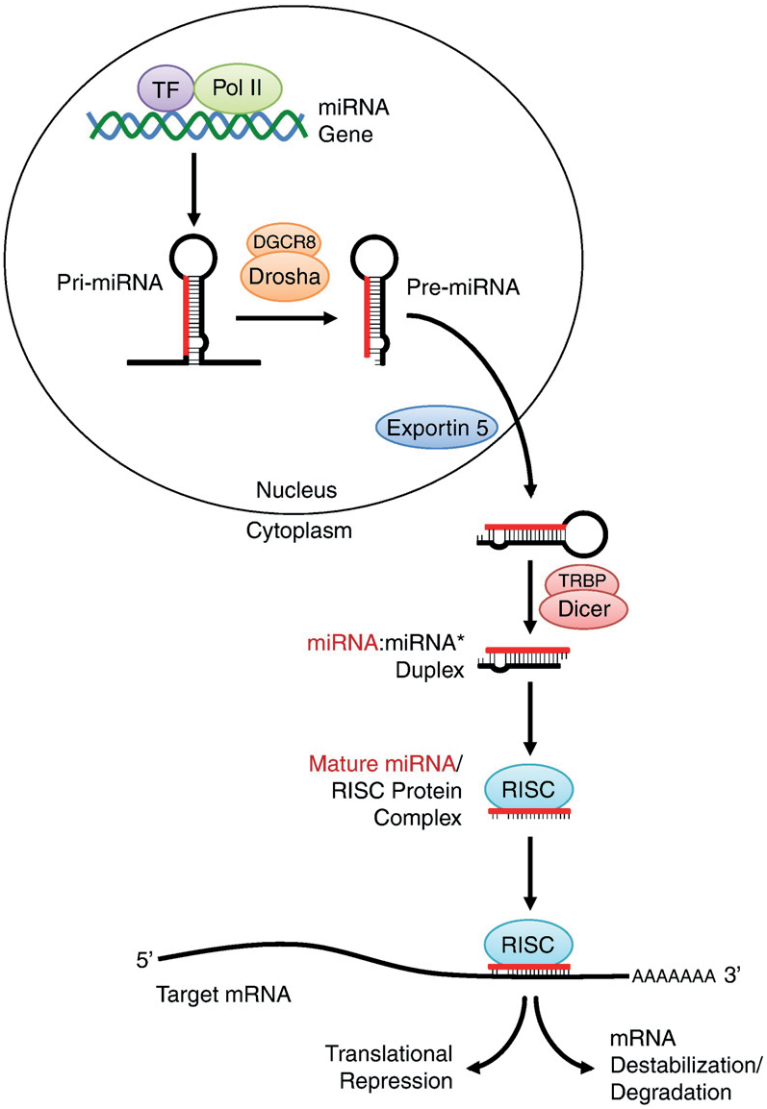

Figure 2.10 | miRNA biogenesis
In the canonical pathway, miRNA biogenesis starts with the transcription of a pri-miRNA gene by a type II RNA polymerase. The pri-miRNA is then processed in two steps, catalyzed by two type III RNases: Drosha and Dicer. The first step is performed in the nucleus, where Drosha and DGCR8 process it into a 60-70nt pre-miRNA. Exportin 5 and its cofactor, Ran-GTP, then export it to the cytoplasm. There, cleavage of the pre-miRNA by Dicer, assisted by TRBP, yields a ~20-bp miRNA/miRNA* duplex. Following this step, one strand of the duplex is loaded on an Ago protein (the miRNA* is generally discarded). Together with GW182, they form RISC, a ribonucleoprotein complex that silences target mRNAs through translational repression or mRNA decay. Copied from (Gurtan & Sharp, 2013).

miRNA activity

In animals, the vast majority of miRNAs are only partially complementary to their targets. Target recognition is driven by the 5' nucleotides 2-7 of the miRNA, a region called the "seed". In most cases the sequences recognized by miRNAs can be found on the 3'UTR of the target mRNA (Bartel *et al.*, 2009; Huntzinger & Izaurralde, 2011) (Fig. 2.11). In the rare cases of complete matching between the miRNA and its target, the mRNA is degraded. However, imperfect pairing between the seed region and its target is generally sufficient to repress gene expression (Pasquinelli, 2012). This flexibility in the requirements for miRNA-targeting explains the capacity of a single miRNA to regulate the expression of up to hundreds of genes.

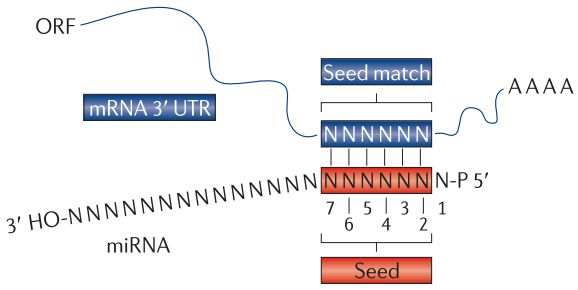

Figure 2.11 | miRNA targeting & the seed region
miRNAs recognize partially complementary binding sequences on target mRNAs. Complementarity to the seed region, defined as nucleotides 2–7 at the 5′ end of the miRNA, is a major determinant in target recognition; for most miRNA-binding sites, pairing is limited to this sequence. In some cases, complementarity to the rest of the miRNA can compensate for a weak seed match. In general, miRNA nucleotides 9–12 bulge out to prevent endonucleolytic cleavage by Ago family proteins. Copied from (Huntzinger & Izaurralde, 2011).

The silencing effect of miRNAs is performed by RISC. The minimal version of this ribonucleoprotein complex contains an argonaute protein (Ago), which directly interacts with the miRNA, and a glycine-tryptophan protein of 182 kDa (GW182), a downstream effector in the repression. The Ago protein interacts with the translation machinery and mRNA decay factors, while the miRNA serves as a guide for target recognition (Krol *et al.*, 2010; Ha & Kim, 2014; Jonas & Izaurralde, 2015). Upon binding to complementary mRNAs, RISC mediates their silencing either through translation inhibition, mRNA destabilization, co-translational protein degradation or mRNA degradation (Filipowicz *et al.*, 2008; Carthew & Sontheimer, 2009; Huntzinger & Izaurralde, 2011; Pasquinelli, 2012).

The role of miRNAs in thymus and skin development and function

miRNAs have an essential role in skin development and homeostasis. Indeed, ablating Dicer, Drosha or DGCR8 (and therefore, all mature miRNAs) from the epidermal compartment using conditional KO systems, leads to neonatal death due to dehydration. Developing hair follicles fail to invaginate and distort the epidermal morphology, thus compromising its barrier function (Yi *et al.*, 2006; Yi *et al.*, 2009; Teta *et al.*, 2012). This led Yi and colleagues to suggest that miRNAs could have a critical role in regulating epithelial-mesenchymal interactions essential for the morphogenesis of epithelial appendages (Yi *et al.*, 2006).

Among the miRNAs expressed in the epidermis, miR-203 seems to have a predominant role. Within the epidermis, it is detectable exclusively in the suprabasal layers and in the differentiated sheets of the hair follicle, where it represses p63 expression through two target sites within the 3′UTR of p63. Thus, miR-203 and p63 expression are inversely correlated in epidermal keratinocytes. This ensures the proper identity of the epidermal cell layers by defining a molecular boundary between proliferative basal progenitors and differentiated suprabasal cells (Lena *et al.*, 2008; Yi *et al.*, 2008; Candi *et al.*, 2015).

miRNAs have also been shown to be indispensable for thymic maintenance and functionality. TEC-specific Dicer or DGCR8 ablation using a *Foxn1*-Cre conditional knockout system progressively drives the degeneration of the thymic architecture, leading to involution, lower T cell output and increased autoimmune susceptibility. Interestingly, the proportion of $K5^{+}K8^{+}$ double-positive and $p63^{+}$ immature TECs appears to be increased in these altered thymi. This data suggests an important role for miRNAs

in the TEC differentiation program and could provide an explanation for the dramatic reduction of both Aire-dependent and -independent promiscuous gene expression in mTECs in the absence Dicer (Papadopoulou *et al.*, 2011; Zuklys *et al.*, 2012; Ucar *et al.*, 2013; Khan *et al.*, 2014).

This premature thymic atrophy phenotype is recapitulated in *miR-29a*-knockout mice. However, these mutants do not display the defects in epithelial organization that result from the loss of all miRNAs (Papdopoulou *et al.*, 2011; Ucar *et al.*, 2013). In addition, the absence of miR-29a only affected the expression of Aire-dependent TRAs, suggesting a role for other miRNAs in the maintenance, differentiation and function of TECs (Ucar *et al.*, 2013).

1.5 The epithelial-mesenchymal transition

The epithelial–mesenchymal transition and its role in development and disease

Epithelial cells show apico-basal polarity and are in close contact with their neighbors through the sequential arrangement of adherens junctions, desmosomes, and tight junctions. In addition, cells in epithelial layers are connected to each other through gap junctions and a basement membrane separates them from adjacent tissues. This allows epithelia to function as permeability barriers that form the boundaries of organs and tissues. In opposition, mesenchymal cells are loosely organized in a three-dimensional extracellular matrix (ECM) and generally form the connective tissues that are adjacent to epithelia.

The epithelial-mesenchymal transition (EMT) is defined as the process through which epithelial cells acquire a mesenchymal phenotype, at the expense of their epithelial identity. This phenomenon is evolutionarily conserved and involves major phenotypic changes that include the loss of cell-cell adhesion and apico-basal polarity, the disruption of the basement membrane, a profound reorganization of the cytoskeleton and the acquisition of a migratory and invasive phenotype (Fig. 2.12). In 1968, Elizabeth Hay was the first to establish the fundamental role of EMT for cell movements in the embryo and gave the process its name (although she used the term "transformation", that was replaced later by "transition") (Hay, 1968). Importantly, the underlying processes of EMT are later reactivated in wound healing, fibrosis and cancer progression (Thiery *et al.*, 2009).

While full epithelial and mesenchymal cellular identities represent both ends of EMT, a whole spectrum of intermediate states exists between them. These intermediate phenotypes are termed "partial EMT" (or "metastable" phenotype) and allow cells to gain mobility while keeping some epithelial features, such as the capacity to maintain loose contacts with neighboring cells. Interestingly, EMT is often reversible by a process called mesenchymal-epithelial transition (MET). Moreover, it is common for cells to cycle between epithelial and mesenchymal states. This ability of epithelial cells to reversibly undergo EMT, either partially or fully, is a strong example of the inherent plasticity of the epithelial phenotype (Lamouille & Derynck, 2014).

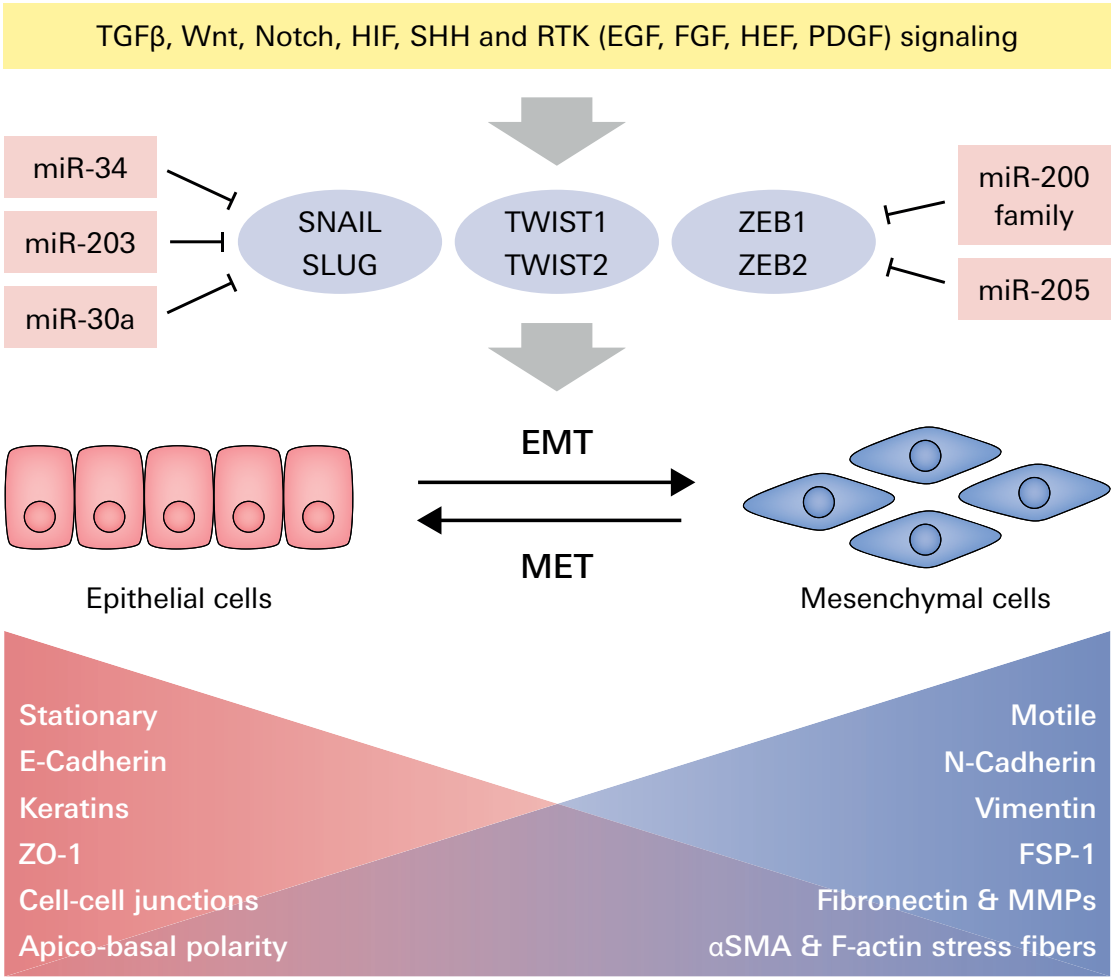

Figure 2.12 | The epithelial-mesenchymal transition (EMT)

EMT is the process through which epithelial cells become mesenchymal. Pro-EMT signaling activates the transcription factors Snail, Twist and ZEB and increase their expression. miRNAs have an important role in the repression of these factors and favor the reverse process of EMT, MET. Although full epithelial and mesenchymal cellular identities represent both extremes of EMT, a variety of intermediate states exist between them.

Depending on the physiological or pathological context in which EMT occurs, the phenotype of the output cells can be quite different. This has led to the definition of three distinct types of EMT, named type 1, 2 and 3 (Kalluri & Weinberg, 2009 ; Zeisberg & Neilson, 2009). Type 1 EMTs are generally associated with embryonic development. They most often generate mesenchymal cells that subsequently undergo MET to generate secondary epithelia. For example, during gastrulation, EMT is necessary for the ingression of epiblast cells into the primitive streak as they give rise to mesoderm and definitive endoderm (Thiery *et al.*, 2009; Nieto, 2011; Lim & Thiery, 2012). Then, the condensation, aggregation and epithelial conversion of presumptive kidney mesenchymal cells to generate a simple tubule represents a classical example of MET (Stark et *al.*,1994).

Type 2 EMTs refer to secondary epithelial cells transitioning to fibroblasts in response to inflammation. This is the case in wound healing, where keratinocytes located at the border of the injury undergo EMT. This confers them enhanced mobility and accelerates the healing process. Generally, these EMTs cease once inflammation is attenuated. However, persistent inflammation can lead to fibrosis (Kalluri & Weinberg, 2009; Zeisberg & Neilson, 2009; Nieto, 2011).

Type 3 EMTs occur during cancer progression, as part of the metastatic process, earning the EMT phenomenon to become the subject of particular attention in cancer research (Peinado *et al.*, 2007; Puisieux *et al.*, 2014). Indeed, type 3 EMTs are believed to be critical for the process leading to metastatic dissemination, which represents a major part of the morbidity and mortality associated with cancer. While EMT seems to be essential for the first steps of the process that eventually leads to the appearance of metastases, MET appears to be required for their establishment at distant sites. On top of contributing to poorer prognosis through the induction of metastases, EMT inducers have been shown to protect tumor cells from senescence, apoptosis and conventional chemotherapy (Vega *et al.*, 2004; Ansieau *et al.*, 2008). They also appear to confer stem cell properties and immunosuppressive capabilities to these cells (Mani *et al.*, 2008; Kudo-Saito *et al.*, 2009; Thiery *et al.*, 2009; Zheng & Kang, 2014). In recent years, much hope has been put into therapeutics aimed at the main actors of EMT because of its correlation with the most aggressive cancer types and poor clinical outcome (Nieto & Cano, 2012).

Molecular mechanisms of EMT

EMT is a very complex process that involves an enormous number of factors. Furthermore, as mentioned above, cells undergoing full or partial EMT can display a vast array of distinct phenotypes. Because of this complexity and the fact that discussing the details of the mechanics of EMT goes beyond the scope of this work, only a few selected key players and markers will be described here, a summary of which is presented in Fig. 2.12.

Although transforming growth factor-beta (TGFβ) is probably the best-characterized EMT-inducing signaling pathways, numerous other signaling pathways cooperate in the initiation and progression of EMT; Wnt, Notch, Hypoxia-inducible factor (HIF), SHH and various receptor tyrosine kinases (RTKs) that are activated by growth factors such as Epidermal growth factor (EGF), FGF, Hepatocyte growth factor (HGF) and Platelet-derived growth factor (PDGF) have all been shown to promote EMT (Gonzalez & Medici, 2014; Lamouille & Derynck, 2014).

Most of the pro-EMT signaling converges to a central core of transcription factors that includes Snail family proteins (SNAI1 and SNAI2, also named Snail and Slug, respectively), zinc finger E-box–binding homeobox 1 (ZEB1, also known as δEF1), ZEB2 (also called SIP1) and basic helix-loop-helix (bHLH) factors (TWIST1, TWIST2 and E47). These transcription factors have all been identified as master regulators promoting EMT. They direct the repression of epithelium-specific genes and the activation of those that participate in the acquisition of a mesenchymal cellular identity (Peinado *et al.*, 2007; Lamouille & Derynck, 2014; Zheng & Kang, 2014).

Snail, ZEB and Twist family members are direct repressors of E-cadherin (also named CDH1), a central component of the adherens junction complex. E-cadherin has a crucial role in the maintenance of the epithelial cytoskeletal organization through its links to the actin cytoskeleton via β-catenin. Its loss is considered the prototypical hallmark of EMT. Along with E-Cadherin, the Snail, ZEB and Twist families of transcription factors repress numerous additional epithelial markers, such as desmosomal proteins

(plakoglobin, desmogleins, desmoplakins) and tight junction proteins (claudins, occuldins and zona occludens 1; ZO-1), leading to the dissolution of junctional complexes and loosening of cell-cell contacts (Peinado *et al.*, 2007; Moreno-Bueno *et al.*, 2009; Zeisberg & Neilson, 2009).

In order to promote mesenchymal adhesion, cadherin expression switches from E-cadherin to N-cadherin during EMT. Concomitantly, the intermediate filament composition changes with the repression of keratins and the activation of Vimentin (VIM) expression. Cells undergoing EMT also start to express Fibroblast-specific protein 1 (FSP-1), Fibronectin (FN1) and matrix metalloproteinases (MMPs), allowing them to remodel the ECM. Finally, alpha smooth muscle actin (α-SMA) is upregulated and F-actin stress fibers are formed as cells reorganize their cytoskeleton into one that enables dynamic cell elongation and enhanced motility (Moreno-Bueno *et al.*, 2009; Zeisberg & Neilson, 2009).

miRNAs also play a crucial role in EMT. For example, miR-200 family members and miR-205 act synergistically to suppress ZEB family members and promote MET (Gregory *et al.*, 2008a). miR-30a, miR-34 and miR-203 all negatively regulate Snail. In addition, all five of these miRNAs are negatively correlated with invasive phenotypes in clinical samples. Interestingly, some of these miRNAs form double-negative feedback loops with their target. Snail can bind to the promoters of miR-34 and miR-203 to repress their transcription and ZEB factors can do the same with members of the miR-200 family. A recent study on these feedback loops suggests that they could function as a robust switch controlling EMT and epithelial plasticity (Bullock *et al.*, 2012; Moes *et al.*, 2012; Zaravinos, 2015).

The ZEB/miR-200 double-negative feedback loop

ZEB factors are crucial during development. For instance, *Zeb1*-null mice have craniofacial and skeletal abnormalities due to the diminished proliferation of mesenchymal progenitors and die perinatally (Takagi *et al.*, 1998; Liu *et al.*, 2008). Surprisingly, these mice also suffer from a severe thymocyte deficiency and have poorly developed thymi with no distinction between cortex and medulla (Higashi *et al.*, 1997; Takagi *et al.*, 1998). On the other hand, the neural tube of *Zeb2*-knockout mice fails to close and they die by E9.5. The essential role of Zeb2 and EMT in the migration of NCCs is highlighted by the fact that NCCs form but fail to delaminate in these mice (Van de Putte *et al.*, 2003). Finally, compound *Zeb1/Zeb2* double-knockout embryos develop similarly to *Zeb2*-mutant ones but display a wider opening of the neural tube (Miyoshi *et al.*, 2006). In humans, *ZEB2* mutations cause Mowat-Wilson Syndrome, characterized by severe mental retardation and variable malformations. The distinctive facial appearance of these patients suggests that the role of ZEB2 in the migratory behavior of NCCs is conserved in humans (Vanderwalle *et al.*, 2009).

The miR-200 family of miRNAs consist of five members and are found in two separate genomic clusters: miR-200a/200b and miR-429 on chromosome 1, miR-141 and miR-200c on chromosome 12. miR-200b/200c/429 share the same seed sequence, whereas miR-141/200a share another one. The seed sequence of these two groups only differs

by one nucleotide (AAUACUG and AACACUG, respectively) and all of them target both ZEB1 and ZEB2 via multiple sites on their 3'UTR. This makes the miR-200 family a powerful inducer of epithelial differentiation. Conversely, ZEB1 and ZEB2 can bind highly conserved sequences in the promoter region of both miR-200 clusters and repress their transcription (Brabletz & Brabletz, 2010) (Fig. 2.13). Thus, ZEB factors and miR-200 family members not only have opposite functions, but also reciprocally control the expression of each other (Bracken *et al.*, 2008 ; Burk et al, 2008; Gregory *et al*., 2008b).

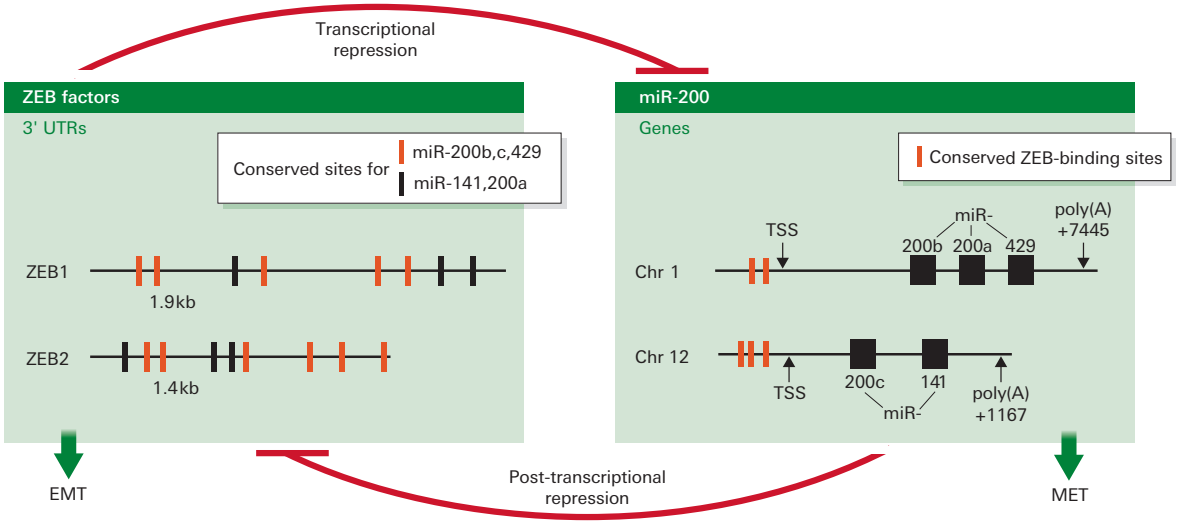

Figure 2.13 | The ZEB/miR-200 double-negative feedback loop

The genes of the miR-200 family members are separated in two polycistronic genomic clusters. ZEB factors transcriptionally repress them by binding to highly conserved recognition sequences in their promoters. Conversely, miR-200 family members silence the ZEB factors at the post-transcriptional level by binding to highly conserved target sites in their 3' UTRs. Copied from (Brabletz & Brabletz, 2010).

While the transcription of ZEB factors is activated by the various EMT-inducing signaling pathways described above, the ubiquitous activating transcription factor Specificity protein 1 (Sp1) and the p53 family proteins p53, p63 and p73 positively regulate miR-200 family members (Kim et al, 2011; Chang *et al.*, 2011; Knouf *et al.*, 2012; Kolesnikoff *et al.*, 2014). What is more, ZEB1 has been shown to repress the transcription of the whole p53 family, adding a supplemental layer of regulation to this double-negative feedback loop (Fontemaggi *et al.*, 2001; Fontemaggi *et al.*, 2005).

The link between p63 and the miR-200 family reinforces the idea that these miRNAs act as gatekeepers of the epithelial phenotype. Furthermore, they are involved in the establishment of epithelial cell lineages during development. All miR-200 family members are highly expressed in the epidermis during skin morphogenesis (Yi *et al.*, 2006) and in the chick embryo, their expression is restricted to the endoderm and ectoderm, as ZEB factors predominate in the mesoderm (Gregory *et al.*, 2008b). Interestingly, recent studies indicate that in mouse and human, miR-200 family members are upregulated in mTECs compared to cTECs and thymocytes (Ucar *et al.*, 2013; Khan *et al.*, 2015).

In vitro, TGFβ is used as a strong activator of EMT. However, overexpression of ZEB1 or ZEB2 can induce EMT in epithelial cells independently of TGFβ addition. Moreover, the downregulation of ZEB factors in mesenchymal cells triggers MET, highlighting their

fundamental role for the stability of the mesenchymal phenotype (Gregory *et al.*, 2011). On the other hand, overexpression of miR-200 family members prevents TGFβ-induced EMT in epithelial cells, leads to the upregulation of E-cadherin and induces MET through the downregulation of ZEB factors in mesenchymal cells. Conversely, miR-200 downregulation is sufficient to induce EMT (Hurteau *et al.*, 2007; Gregory *et al.*, 2008a; Korpal *et al.*, 2008). Finally, the fact that miR-200 family members directly target TGFβ transcripts indicates that the ZEB/miR-200 double-negative feedback loop not only is TGFβ-responsive, but also has the ability to control autocrine TGFβ signaling. Thus, this double-negative feedback loop provides a likely explanation for the stable, but reversible nature of EMT (Gregory *et al*, 2008b; Brabletz & Brabletz, 2010; Gregory *et al.*, 2011).

2. Aim of the thesis

The thymus involutes with age and its function can be compromised by cytoablative treatments or viral infection. Therefore, in the context of an aging society, it is of paramount importance to develop therapeutic strategies to restore thymic function. Identifying thymic epithelial stem cells and understanding the mechanisms regulating thymus development, structure and function are thus essential research topics. Indeed, they could pave the way for the development of therapies aimed at regenerating thymic tissue to boost the output of naïve T cells and greatly benefit patients with reduced or absent thymic function.

The thymic epithelium is unique in that it forms a characteristic, sponge-like 3D meshwork structure, which is crucial to its role in the selection of developing T cells. However, the reasons why TECs need a stratification program highly similar to the one used by epidermal keratinocytes remain enigmatic. This work is aimed at providing elements to answer this question, through the study of the mechanisms that govern the stratification of human TECs (hTECs).

In vitro, hTECs form four morphologically distinct colony-types, two of which form stratified structures, while the remaining two do not. Thus, these cells represent an insightful system to better understand the mechanisms governing epithelial stratification. First, we analyzed the progeny of FACS-isolated $EpCAM^-$ and $EpCAM^+$ hTEC subpopulations and identified EpCAM as marker of stratifying hTECs in culture. Then, we analyzed the miRNA transcriptional landscape in these two subpopulations and compared it to the one observed in human epidermal keratinocytes. Finally, we investigated the role of the ZEB/miR-200 double-negative feedback loop in the control of hTEC stratification *in vitro*.

3. Material & Methods

3.1 Cell culture

Whole-thymus dissociation

Thymic lobes were obtained from young patients (under 20 years old) who underwent cardiac surgery and had their thymus removed during the procedure. They were collected in cold Dulbecco-Vogt modification of Eagle's Medium (DMEM, Gibco) supplemented with 8% bovine serum (BS) (Thermoscientific). Thymic lobes were then cut in small pieces and gently pipetted up and down in Hank's Balanced Salt Solution (HBSS, Gibco) supplemented with 2% Fetal Bovine Serum (FBS, Gibco) and 20mM HEPES Buffer Solution (Gibco-Invitrogen). This procedure was repeated 4 or 5 times. Every time, the supernatant was removed and discarded after the thymic pieces had settled down. Thymic pieces were then resuspended in HBSS, 2% FBS, 20mM HEPES containing 0,2mg/ml Collagenase D (Roche) for 20min at room temperature (RT) with gentle stirring. They were allowed to settle and supernatant was removed. Thymic pieces were then resuspended in HBSS, 2% FCS, 20mM HEPES containing 0,4mg/ml Collagenase/Dispase (Roche) and 50µg/ml DNAse I (Roche) for 30 min at 37° C with gentle stirring. Depending on the size of the tissue, this step was repeated 4 to 7 times. After each round of enzymatic digestion, the supernatant was collected after the thymic pieces had settled down. The cells from the supernatant were isolated by centrifugation and resuspended before being seeded as described below.

hTEC culture

Epithelial cells were cultivated on a feeder layer of lethally irradiated mouse embryonic fibroblast (3T3-J2), as described by Rheinwald and Green (Rheinwald & Green, 1975). 3T3-J2 cells were maintained in DMEM (Gibco) supplemented with 8% BS (Thermo sci-

entific), fed every 3-4 days and passed every 7 days, for up to 12 weeks. For epithelial cells cultivation, 3T3-J2 cells were irradiated with a 60Gy dose of radiation and seeded at 2.5 x 10^4 cells/cm^2 overnight.

Epithelial cells were cultivated on the prepared 3T3-J2 feeder layers, in cFAD medium, which consists in a 3:1 mixture of DMEM and Ham's F12 medium (Gibco), supplemented with 10% FBS (Gibco), 0.4 µg/ml hydrocortisone (Calbiochem, VWR), 10^{-6} M cholera toxin (Sigma), 5µg/ml insulin (Sigma) and 2x 10^{-9} 3,3',5-Triiodo-L-Thyronin (T3, Sigma). Starting 3 days after cell seeding, 10ng/ml Human recombinant epidermal growth factor (EGF) (QED) was added to the culture medium. All cultures were incubated at 37°C in a 10% CO_2 atmosphere and fed every 3-4 days. Cell cultures were serially amplified once a week by dissociating adherent growing cells in 0.05% trypsin / 0.1% EDTA and replating them at the appropriate density onto dishes containing a freshly prepared irradiated 3T3-J2 feeder cell layer.

Colony-forming efficiency assay

400 cells were plated onto a 100mm Petri dish containing lethally irradiated 3T3 cells and cultured for 11-13 days as described before. They were fixed >10min in 3.7% formol and stained >10min in 1% rhodamine-B. Then, colonies of each type were counted separately under a dissecting microscope.

Flow cytometry and cell sorting

Cultivated cells were trypsinized as described above and re-suspended in FACS buffer (HBSS 1x, 3% FBS) at a concentration of 10^7 cells/ml. They were then incubated 15min at RT with a mouse anti-human EpCAM eFluor 660 (1:100, 1B7, eBioscience) and a mouse anti-human CD49f AF488 (1:100, GoH3, BioLegend) conjugated antibodies. Cells were then washed and re-suspended in FACS buffer. Cell sorting was performed by the Flow cytometry core facility (FCCF) using a FACS Aria II (BD Biosciences) with a 100µM nozzle at 20psi. Primary gates based on physical parameters (forward and side light scatter) were set to exclude debris and doublets. Dead cells were excluded using DAPI. Clean separation between $EpCAM^-$ and $EpCAM^+$ cell fractions, and the purity of the isolated $tRFP^+$ cell population, were confirmed by second flow-cytometric analysis. Analysis-only experiments were performed on a LSR II (BD Biosciences) using the same gating strategy. Data was analyzed using the FlowJo software (Tree Star).

3.2 Gene expression analysis

RT-qPCR

After the tRFP sort, hTECs were grown for 7 days in a 12-well plate. Total RNA was extracted from these cells using the mirVana miRNA Isolation Kit (Ambion), following manufacturer's instructions. Lysis was performed directly in the wells. RNA concentra-

tion was quantified using a spectrophotometer with absorbance at 260 nm. For mRNAs, cDNA was synthesized using the SuperScript III Reverse Transcriptase (Life Technologies), following the manufacturer's instructions, with 500ng RNA and random primers (Invitrogen). miRNA reverse transcription was performed using the Taqman MicroRNA Reverse Transcription Kit (Applied Biosystems) and a custom RT primer pool prepared from Taqman MicroRNA Assay 5x RT primers (Applied Biosystems) with 300ng RNA. Each cDNA generated was amplified by qPCR using Taqman Universal Master Mix II, no UNG (Applied Biosystems) and individual 20x TaqMan Gene Expression Assays or 20x Taqman MicroRNA assays (Applied Biosystems) on a QuantStudio 6 Flex Real-Time PCR System (Applied Biosystems). Data analysis was performed using the ExpressionSuite sofware (Applied Biosystems). Expression levels of individual transcripts were normalized to the geometric mean of eEF1A1, TBP and TUBB (mRNAs) or hsa-let-7i, hsa-miR-19b and hsa-miR-92a (miRNAs).

miRNA microarray and RT–qPCR validation

For the miRNA microarray analysis, hEKs and hTECs were cultured at low density (5'000 cells / 100mm dish) on dTomato-expressing 3T3-J2 cells. hEKS, EpCAM$^-$ and EpCAM$^+$ hTECs pure cell populations were isolated by FACS at d10. dTomato$^+$ 3T3 cells were excluded during the sort to limit the amount of contaminating mouse RNA. Total RNA was extracted from 50'000 cells aliquots using the Phenol-Free Total RNA Purification Kit (Amresco), according to the manufacturer's instructions. RNA re-concentration, labeling and hybridization, and statistical analysis of the data were performed at the Lausanne Genomics Technologies Facility (LGTF, UNIL). Briefly, total RNA samples were EtOH precipitated and re-concentrated. RNA quality was assessed using a Bioanalyzer (Agilent). RNA samples were then labeled and hybridized on a Human miRNA v16.0 Array (Agilent). Data was normalized using quantile normalization, control probe sets and probe sets not called "present" in any sample were left out of analysis. Statistical analysis was performed using moderated t-tests, adjusting the p-values through the Benjamini-Hochberg method, in order to control the false discovery rate (FDR).

For RT-qPCR validation, EpCAM$^-$, EpCAM$^+$ hTECs and hEKs grown in regular culture conditions and harvested after 7 days in culture. Total RNA was extracted from these cells using the mirVana miRNA Isolation Kit (Ambion), following the manufacturer's instructions. Total RNA concentration was quantified using a spectrophotometer with absorbance at 260nm. miRNAs were reverse-transcribed using the Taqman MicroRNA Reverse Transcription Kit (Applied Biosystems) with ~30-200ng total RNA and a custom RT primer pool prepared from Taqman MicroRNA Assay 5x RT primers (Applied Biosystems). cDNA was then pre-amplified for 16 cycles using the Taqman PreAmp Master Mix (Applied Biosystems) and a custom PreAmp primer pool prepared from individual 20x Taqman MicroRNA assays (Applied Biosystems). Samples were then run in technical sixplicates on a 96.96 Dynamic Array (Fluidigm), using individual 20x Taqman MicroRNA assays (Applied Biosystems) and Taqman Universal Master Mix II, no UNG (Applied Biosystems) on a Biomark HD system (Fluidigm), following the manufacturer's instructions.

Analysis was performed with the help of the Bioinformatics and biostatistics core facility (BBCF) using the DeltaCt method. First, the data was controlled for quality and curated manually. Then, expression levels of individual miRNAs were normalized to the geometric mean of hsa-let-7i, has-miR-19b, hsa-miR-23a and hsa-miR-92a. Statistical analysis consisted in performing first an F-Test for each target gene. If the Bonferroni-corrected p-value of this test was below 0.05, then we proceeded to a pairwise comparison using t-tests. Differences were considered significant if their associated Bonferroni-corrected p-value was below 0.05 and the fold change above 2x.

Immunofluorescence imaging

Cells were cultivated as described above on glass coverslips (covered with irradiated 3T3-J2) in 12-well plates and fixed after 7 to 10 days in 4% PFA. Non-specific sites were blocked for 60 min at RT with 5% bovine serum albumin (BSA)/ PBS solution with 0.4% Triton X-100 (blocking buffer). Then, cells were incubated overnight with primary antibodies diluted in 50% blocking buffer (diluted 1:1 in PBS 1x) at 4°C. A list of the primary antibodies that were used is presented in Table 4.1. After washing with PBS, they were incubated for 60 min at RT with goat AF488-, AF555- or AF647-conjugated secondary antibodies (Life Technologies) diluted 1:500 in PBS 1x. Nuclear counterstaining was performed with DAPI. For the visualization of the F-Actin cytoskeleton, cells were counterstained with Phalloidin-ActiStain488 (Cytoskeleton) at 100nm for 30min. Finally, the coverslips were mounted on microscope slides in Dako fluorescence mounting medium. Images were acquired using a LSM 700 Invert confocal microscope (Zeiss). Brightness and contrast were adjusted using the Fiji software (Schindelin *et al.*, 2012).

Antibody	Clone	Dilution	Manufacturer
Mouse α-Human EpCAM	1B7	1/100	eBioscience
Rabbit α-ZEB1 (H-102)	Polyclonal	1/100	Santacruz
Mouse α-Involucrin	SY8	1/200	Abcam
mRabbit α-Vimentin	D21H3	1/200	Cell Signaling
Rabbit α-HOPX	FL-73	1/500	Santacruz
mRabbit α-ZO-1	D7D12	1/100	Cell Signaling
Rabbit α-Cytokeratin 1	Polyclonal	1/400	Covance
Rabbit α-E-Cadherin	24E10	1/100	Cell Signaling
Mouse α-Vimentin	V9	1/200	eBioscience
Mouse α-p63	4A4	1/100	DakoCytomation
mRabbit α-SLUG	C19G7	1/200	Cell Signaling
Rat α-hCD49f	GoH3	1/1000	BD pharmingen
Rabbit α-PanK	Polyclonal	1/50	Invitrogen

Table 4.1 | Primary antibodies used for immunofluorescence imaging

3.3 Epidermis regeneration assay

Animals

Fox Chase SCID mice were purchased from Charles River Breeding Laboratories (France). All animals were maintained in a 12 hours light cycle and provided with food and water *ad libitium*. Mice were killed by cervical dislocation and all experiments were carried out under anesthesia and in accordance with the European Community Council Directive (86/609/EEC) for the care and use of laboratory animals.

Human fibroblast culture

$2x10^5$ AFF11 human fibroblasts were seeded in T75 flasks and cultured for 5 days DMEM 10% FBS at 37°C in a 10% CO_2 atmosphere.

Fibrin gel preparation

Fibrinogen was extracted by centrifugation of human plasma from blood donors (Centre for transfusion, CHUV, Lausanne) at 3300rcf for 30min at 4°C and resuspended in DPBS (Gibco). In order to make fibrin gels, a saline solution containing human thrombin 3U/ml from Tissucol kits (Baxter) was added to the fibrinogen solution supplemented with human fibroblasts. 2ml of the obtained fibrin matrix were then plated into each well of a 12 well plate and left at RT for 30min to solidify. Finally, the gels were covered with 1.5ml DMEM 10% FBS and incubated overnight at 37°C in a 10% CO_2 atmosphere.

Epidermis regeneration assay

hEKs, $EpCAM^-$, $EpCAM^+$ and unsorted hTECs were seeded on top of the fibrin gels in cFAD medium supplemented with 10ng/ml human recombinant EGF and were grown for 6-8 days at 37°C in a 10% CO_2 atmosphere. Medium was changed every other day. Grafts were then transplanted on the back of 12 weeks-old Fox Chase SCID female mice using a skin flap procedure. Briefly, a flap was opened on the dorsal middle region of the mice and 100µl of 1/1 mix of Fibrinogen/Thrombin solution from a biocolle kit (Artiss, Baxter) was applied on the muscle fascia. The grafts were placed on in the flaps with the fibrin side facing the muscle fascia. They were then covered with a sheet of Urgotul (Urgo laboratories) and one of silicone (Dow crowing). The mouse skin flaps were closed and stitched to cover the grafts and to prevent their dehydration. 21 days post-transplantation, they were opened and both the Urgotul and the silicone sheets were removed in order to expose the graft to the air. All of these procedures were actually performed by Melissa Maggioni and Tiphaine Arlabosse.

Immunological analysis of biopsies

Three months after transplantation, biopsies were collected from the center of the transplanted area to assess the contribution of the transplanted human cells to the newly formed epidermis. These biopsies were fixed in PFA 4% for 2 hours at 4°C and rinsed in PBS. They were then incubated in sucrose 30% overnight at 4°C, embedded in OCT and frozen at -80°C. 6µm cryosections of the biopsies were made using a cryostat (Leica) and put on suprefrost microscope slides. They were washed in PBS and non-specific sites were blocked for 60 min at RT with a 5% BSA solution containing 0.5% Triton X-100 (blocking buffer). The cryosections were then incubated overnight with an anti-HLA-1 (1:1500, YTH862.2, Acris) antibody diluted in blocking buffer at 4°C. After washing with PBS, they were incubated for 60 min at RT with a donkey AF488-conjugated anti-rat secondary antibody (Life Technologies) diluted 1:500 in PBS 1x. Nuclear counterstaining was performed with DAPI. Slides were mounted in Dako fluorescence mounting medium and images were taken with a fluorescence microscope (Zeiss).

3.4 Lentiviral vectors

Vector construction

The microRNA-adapted non-targeting shRNA sequence from a pGIPZ negative shRNA control (Dharmacon) and the precursors of hsa-miR-141 and hsa-miR-200c (100bp on each side of the mature miRNA sequence) were cloned into the lentiviral miRNA expression plasmid kindly provided by L. Naldini, with the tRFP in replacement of the orange fluorophore (Barde *et al.*, 2013) (pCCL-SFFV-Intron-miR-141-tRFP, pCCL-SFFV-Intron-miR-200c-tRFP and pCCL-SFFV-Intron-miR-Neg-tRFP). Briefly, the desired miRNA precursors were inserted into the expression vector instead of the mmu-miR-351 precursor fragment using the restriction enzymes SphI and MluI.

Lentivirus production

Viral particles containing miRNA expression plasmids were generated in 293T as described previously (Barde *et al.*, 2010). 293T were cultured in DMEM 10% FCS and were split 1/10 twice a week. For each production, 7x15cm 80% confluent dishes were transfected in 22.5mL DMEM with 157.5µg expression vector plasmid, 55.3µg envelope plasmid pMDG (encoding for the VSV G envelope protein) and 102.2µg of pCMVR8.74 (encoding HIV-1 Gag, Pol, Tat and Rev proteins), using the commercial kit CalPhos Mammalian Transfection (Clonetch). All plasmids were kindly provided by I. Barde. Medium was changed 16h after transfection, was harvested 8 and 24 hours later and was kept at 4°C. It was then centrifuged and the supernatant was passed through a 0.22µm filter to remove cell debris before being ultracentrifuged 2h at 19'500rpm at 16°C. The supernatant was discarded and the pellets were re-suspended in 100µl of PBS 1x, centrifuged at maximum speed and stored at –80°C in 5-10µl aliquots. The viral particles were then titrated by flow cytometry in HCT116 cells.

hTEC transduction

EpCAM$^-$ and EpCAM$^+$ hTECs were sorted by FACS and cultured for 3 days in 6-well plates before being transduced at an MOI of 6, in 1ml cFAD. 8 hours later, the medium was changed. Infected cells were isolated 4 days later by FACS and re-cultured in the appropriate vessels: 12-well plates for flow cytometry and RT-qPCR, on coverslips in 12-well plates for immunostainings, 6cm dishes for expansion and 10cm dishes for plating efficiency assays.

3.5 Statistics

Correlation analysis and linear model

The correlation between the proportion of EpCAM$^+$ cells seeded and the amount of stratification was calculated based on Pearson's product moment correlation coefficient using the "cor.test" function of the "stats" package in R (R Core Team, 2015). The linear model predicting the amount of stratification on the basis of the proportion of EpCAM$^+$ cells seeded was calculated using the "lm" function of the "stats" package in R (R Core Team, 2015).

RT–qPCR

The measure of the statistical significance of the difference in gene expression levels between different populations was performed as follows: after normalization, an F-Test was performed for each target gene. If the Benjamini-Hochberg-corrected p-value of this test was below 0.01 (to control the FDR), then we proceeded to a pairwise comparison using paired t-tests. Differences were considered significant if their associated Bonferroni-corrected p-value was below 0.05 and the fold change above 2x. All calculations were performed using the "stats" package in R (R Core Team, 2015).

Stratification and EpCAM, CD49f and tRFP expression after infection

The statistical significance of the increase in the amount of stratification and in EpCAM, CD49f and tRFP expression after lentiviral expression was assessed by first performing an F-test. If the p-value was below 0.05, then we proceeded to a pairwise comparison using paired t-tests. Differences were considered significant if their associated Bonferroni-corrected p-value was below 0.05. All calculations were performed using the "stats" package in R (R Core Team, 2015).

Graphical output

All graphs were produced using the "ggplot2" package in R (Whickam, 2009) and figures were constructed using the Adobe Creative Suite (Adobe).

4. Results

4.1 EpCAM expression marks stratifying hTECs

hTECs form four morphologically distinct colony types when grown in the 3T3-J2 culture system (Maggioni, 2012). However, as mentioned in the introduction, simple and aborted colonies are non-proliferative under these conditions. Therefore, we will mostly make the distinction between stratified and non-stratified colonies from here on. The first group includes stratified and aborted colonies, while refringent and simple colonies belong to the second one.

In previous work from our laboratory, microarray analysis showed that *EpCAM* is upregulated 75x in stratified clones compared to refringent ones. This data was confirmed by RT-qPCR and immunostaining (Maggioni, 2012). We thus decided to investigate whether EpCAM expression could identify cells destined to stratify. In order to do so, hTECs from four different young patients (under twenty years old) were serially passaged (once a week) for 4 weeks before being dissociated to a single-cell suspension. Suspended cells were then fluorescently labeled with antibodies against EpCAM and CD49f (Integrin α6) and sorted by FACS. CD49f was used to exclude the feeder cells as it is expressed in all cultured hTECs but not in 3T3s. Two clear hTEC subpopulations could be distinguished on the basis of their EpCAM expression level (Fig. 4.1a), even though their respective proportions varied widely between independent experiments (75.1% of $EpCAM^+$ cells on average) (Fig. 4.1c).

After the sort, the purity of the isolated $CD49^+EpCAM^-$ (named $EpCAM^-$ hereafter) and $CD49f^+EpCAM^+$ (named $EpCAM^+$ hereafter) subpopulations were always above 90%, except for one, at 86.25% (Fig. 4.1a & c). These cells were then cultured separately and serially passaged for 3 weeks. At each passage, their EpCAM expression level was assessed by flow cytometry. In parallel, colony-forming efficiency assays were performed to determine the proportion of stratified colonies. As expected, $EpCAM^+$ hTECs only gave rise to stratified colonies (99.3% on average), whereas $EpCAM^-$ hTECs mostly

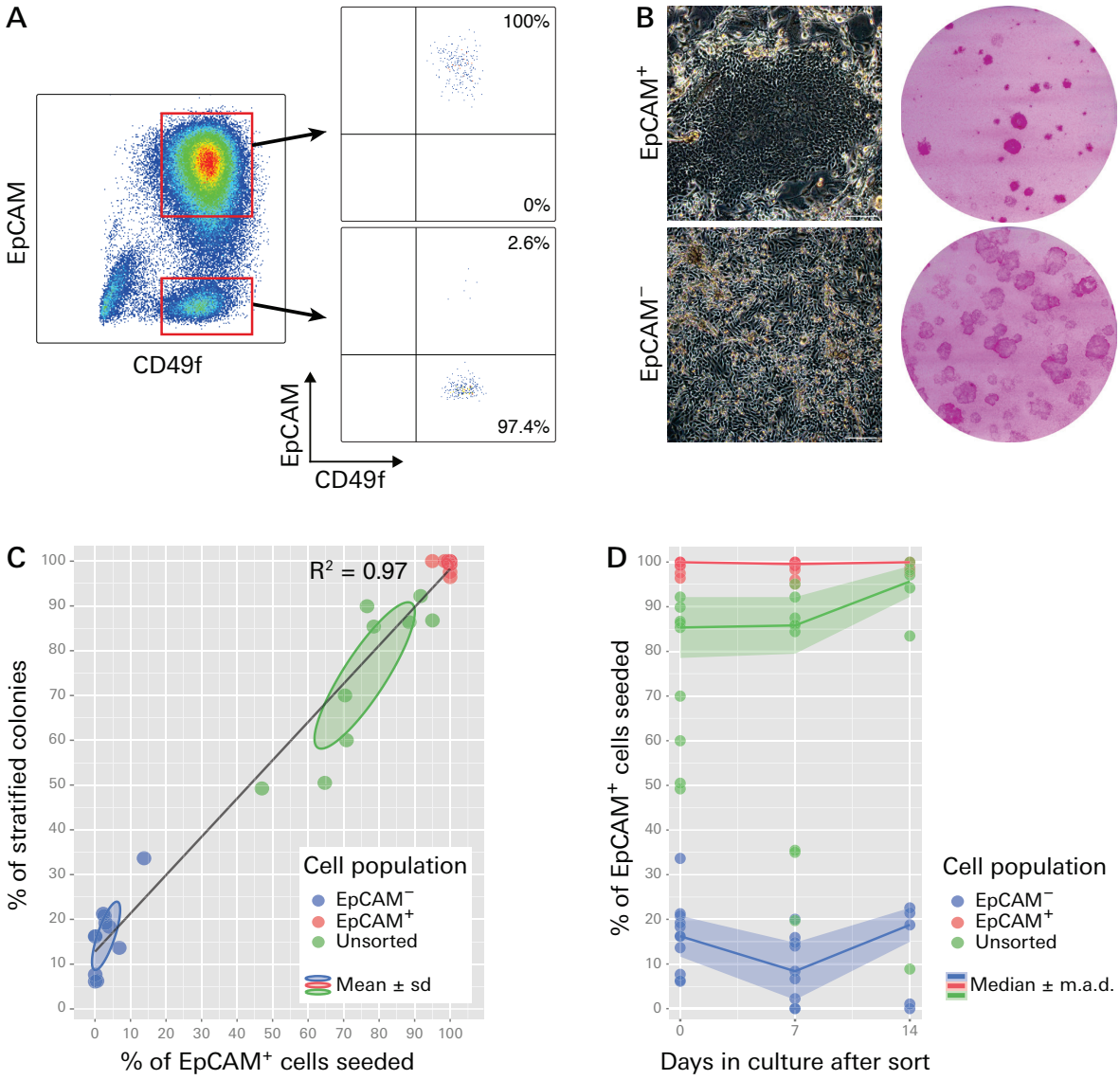

Figure 4.1 | EpCAM expression identifies stratifying hTECs

A EpCAM⁻ and EpCAM⁺ hTECs were isolated by FACS using the gates depicted in red. After each sort, the purity of the isolated subpopulations was systematically over 90%. **B** Cultured EpCAM⁺ hTECs cells gave only rise to stratified colonies, whereas EpCAM⁻ ones yielded mostly non-stratified colonies. Left: phase contrast images of EpCAM⁻ and EpCAM⁺ hTECs after 7 days in culture. Scale bar = 100µm. Right: Rhodamine B staining of colony-forming efficiency assay dishes 13 days after the sort. **C** The proportion of EpCAM⁺ cells that are seeded and the amount of stratification that occurs are almost perfectly positively correlated. The proportion of EpCAM⁺ cells was measured right after the sort by flow cytometry. After 13 days, the proportion of stratified colonies was measured by counting the colonies in the colony-forming efficiency assays. Colony-forming efficiency assays were always made in duplicate; each dot represents the average of the two dishes. Black line: fitted values of the linear model. R^2: adjusted R^2. Sd: standard deviation. **D** The phenotypes displayed by the EpCAM⁻ and EpCAM⁺ subpopulations remained relatively stable for at least two weeks.

yielded non-stratified colonies (14.5% of stratified colonies on average). On the other hand, the unsorted control population generated an intermediate proportion of stratified colonies (74.4%) (Fig. 4.1a,b & c). Importantly, we were able to show that there is an almost perfect positive correlation between the proportion of EpCAM⁺ cells that were seeded and the amount of stratification that occurred (adjusted R^2=0.97) (Fig.4.1c). This data suggests that EpCAM could be used to identify stratifying hTECs.

The phenotypes displayed by the EpCAM⁻ and EpCAM⁺ subpopulations remained relatively stable over 3 passages after sorting; EpCAM⁺ cells continued to only give rise to stratified colonies (although with ever lowering colony-forming efficiency, probably because of terminal differentiation) and cells from the EpCAM⁻ subpopulation still mostly yielded non-stratifying colonies (Fig. 4.1d). The presence of some stratified colonies in dishes seeded with EpCAM⁻ cells was most likely due to their capacity to generate EpCAM⁺ hTECs, which is implied by the previously described hierarchical organization between the colony types (Maggioni, 2012).

EpCAM expression also remained relatively steady over 3 passages after sort (Fig. 4.2a). However, upon closer analysis, it appeared as if the proportion of EpCAM⁺ cells slightly decreased with time in dishes originating from EpCAM⁺ cells; this decrease is actually more representative of a shift towards an EpCAM^{low} expression profile in this subpopulation, similar to the one observed in hEKs (Fig. 4.2b).

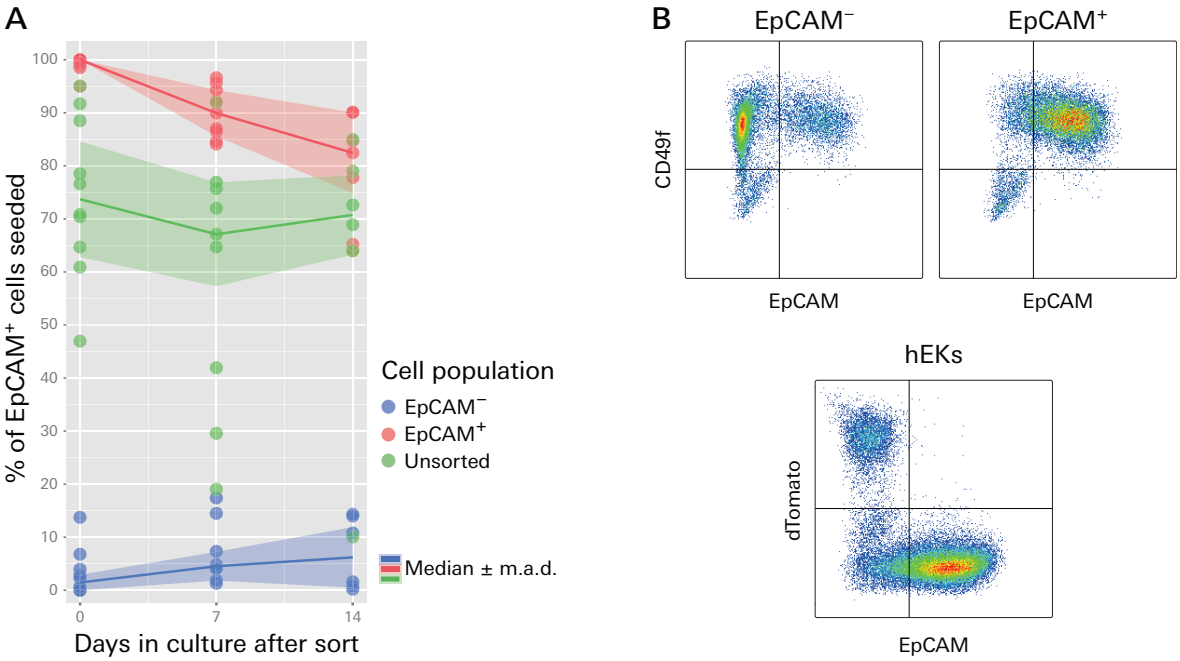

Figure 4.2 | EpCAM expression remains relatively stable over time

A The proportion of EpCAM⁺ cells was measured by flow cytometry analysis every passage after sort. It remained relatively stable for at least 2 weeks. m.a.d.: mean absolute deviation **B** Flow cytometry analysis of hEKs, EpCAM⁻ and EpCAM⁺ hTECs after 7 days in culture. hTECs usually display two cell populations that can be distinguished on the basis of their EpCAM expression level, whereas hEKs form only one population that contains more EpCAM^{low} cells. The flow cytometry analysis was performed at different times for hTECs and hEKS, with the latter being grown on dTomato-expressing 3T3s.

After one week in culture, EpCAM⁺ cells expressed not only EpCAM, but also the epidermal differentiation markers K1 and IVL at much higher levels compared to EpCAM⁻ cells, as measured by RT-qPCR (43.1x, 67.1x and 52.8x, respectively) and immunostaining (Fig. 4.3a & b). In this respect, EpCAM⁺ cells are very similar to cultured hEKs (Fig. 4.3a). Furthermore, Homeodomain only protein X (HOPX), a protein that is upregulated during hEK differentiation (Yang *et al.*, 2010), was also expressed at a significantly lower level in the EpCAM⁻ subpopulation compared to EpCAM⁺ cells (or hEKs), both at the RNA (25.7x less) and protein levels (Fig. 4.3a & b). Taken together, these results demonstrate that EpCAM expression identifies stratifying cultured hTECs.

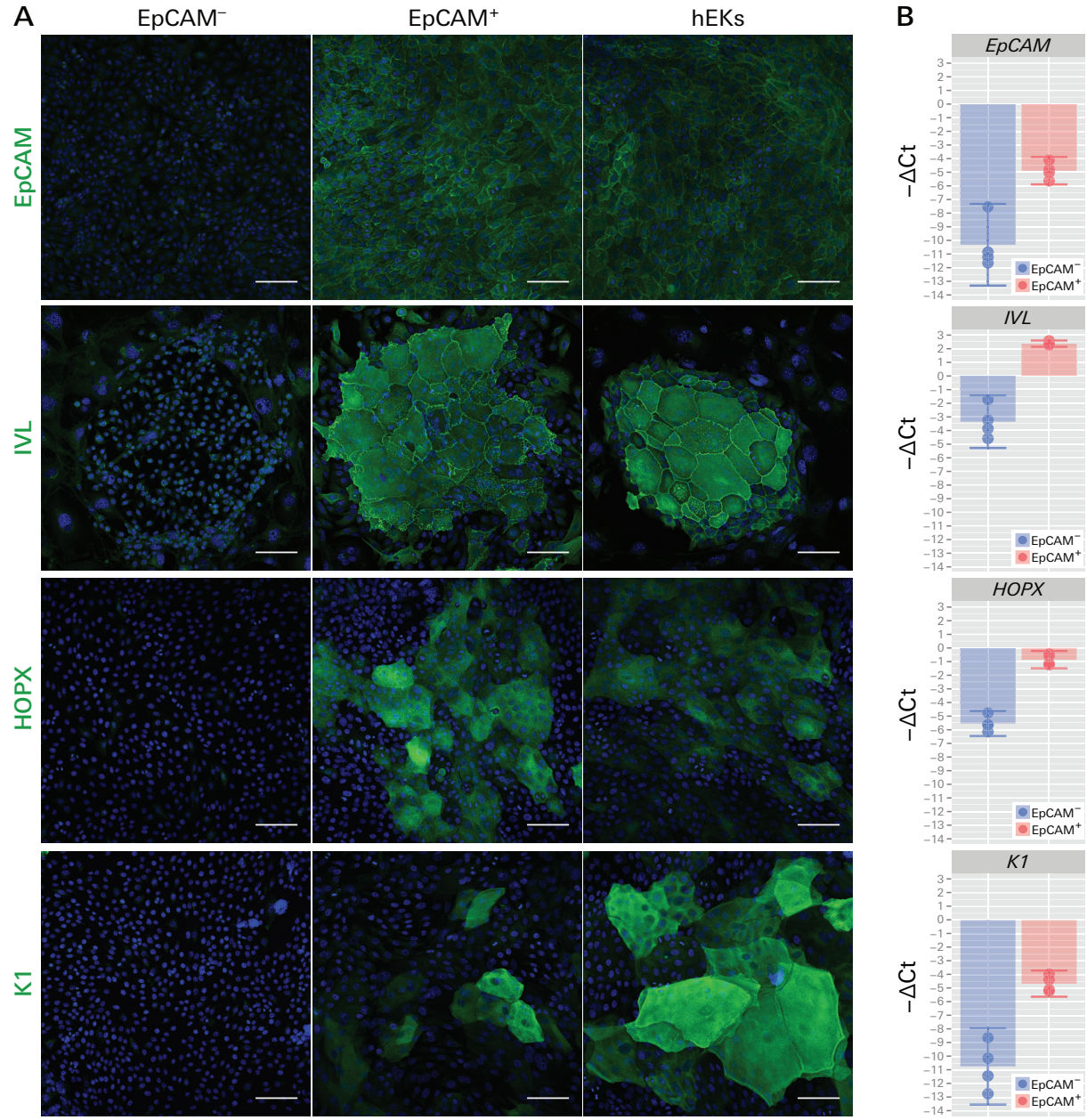

Figure 4.3 | Cultured EpCAM⁺ hTECs express markers of epidermal differentiation

A Immunostainings against EpCAM, IVL, HOPX and K1 on EpCAM⁻, EpCAM⁺ hTECs and hEKs. All of these epidermal differentiation markers are only expressed by the EpCAM⁺ hTEC subpopulation and hEKs. Confocal images were acquired as z-stacks and maximum intensity projections from one representative experiment are presented for each panel. Scale bar = 100µm. **B** RT-qPCR gene expression analysis (n=4). -ΔCt: $\log_2$(relative quantity compared to reference genes). Error bars: 95% Student t-test confidence interval.

4.2 Opposite ZEB/miR-200 double-negative feedback loop activity in EpCAM⁻ and EpCAM⁺ hTECs

Both EpCAM⁻ and EpCAM⁺ subpopulations maintain a basal epithelial phenotype

Although the EpCAM⁻ and EpCAM⁺ subpopulations displayed obvious differences in morphology and gene expression patterns, both of them maintained a basal epithelial phenotype. Like cultured hEKs, both subpopulations expressed keratins and similar levels of CD49f and TP63, two markers of the basal layers of the epidermis (Fig. 4.4a & b).

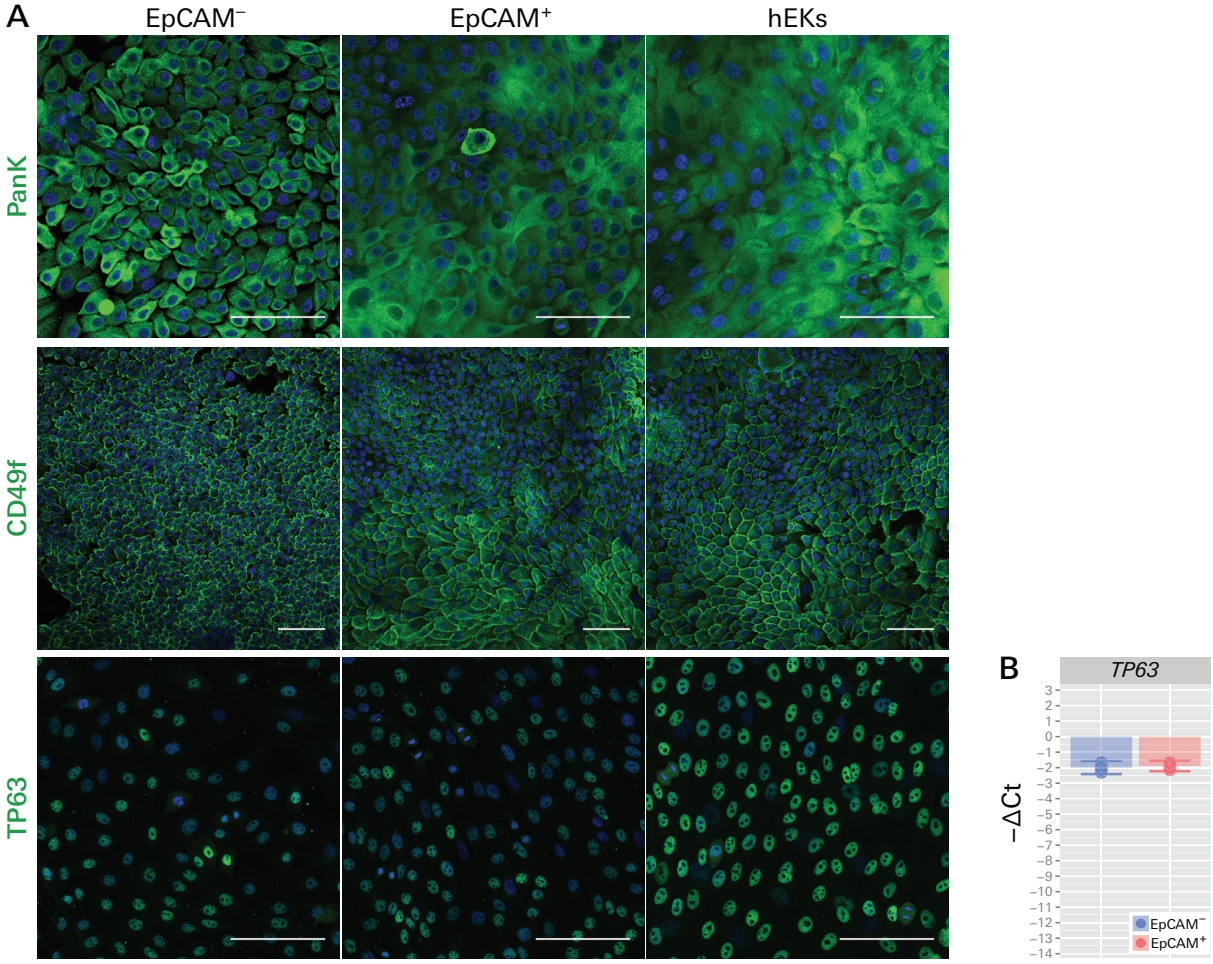

Figure 4.4 | Both cultured hTEC subpopulations maintain a basal epithelial identity

A Immunostainings against Keratins (PanK), CD49f and TP63 on EpCAM⁻, EpCAM⁺ hTECs and hEKs. In all three cell populations, Keratins were located in the cytoplasm, CD49f on the plasma membrane and P63 in the nucleus, as expected. Confocal images were acquired from one representative experiment for each panel. CD49f images were acquired as z-stacks and maximum intensity projections are presented. Scale bar = 100µm. PanK: pan-keratin. **B** RT-qPCR gene expression analysis (n=4). -ΔCt: $\log_2$(relative quantity compared to reference genes). Error bars: 95% Student t-test confidence interval.

EpCAM⁻ hTECs display hallmarks of EMT

To our surprise, microarray analysis showed that *CDH1* (*E-Cadherin*) is downregulated 12.6x in refringent clones compared to stratified ones. In the same experiment, gene ontology analysis revealed that a number of genes that were differentially expressed between these two clone types are involved in EMT. Thus, we investigated whether this difference could also be observed between the EpCAM⁻ and EpCAM⁺ hTEC subpopulations. This was indeed the case; RT-qPCR analysis showed that *CDH1* was downregulated 13x in EpCAM⁻ cells (Fig. 4.5b). Moreover, while CDH1 was clearly detectable on the plasma membrane of EpCAM⁺ cell, just as for hEKs, it appeared to be absent from EpCAM⁻ ones (Fig. 4.5a). EpCAM⁻ cells also appeared to express ZO-1 at a lower level, indicating that they form fewer tight junctions (Fig. 4.5a).

On the other hand, VIM was upregulated in the EpCAM⁻ subpopulation both at the RNA (5.3x) and protein levels (Fig. 4.5a & b). *ZEB1* was also upregulated in this subpopulation (5.7x at the RNA level) (Fig. 4.5b). What is more, ZEB1 was localized into the nucleus only in these cells (Fig. 4.5a). Surprisingly, other EMT master regulators, such as *ZEB2, SNAIL* and *SLUG,* and the EMT marker *FN1,* were not differentially expressed between the EpCAM⁻ and EpCAM⁺ subpopulations (Fig. 4.5a,b & c). Perhaps, this can be partially explained by the basal epithelial identity of both these subpopulations. Indeed, the basal layer of the epidermis has been shown to express specific EMT-inducing genes such as *SLUG* (Turner *et al*., 2006; Shirley *et al*., 2010). At the protein level, the expression pattern for CDH1, VIM, ZEB1 and SLUG were very similar between EpCAM⁺ cells and HEKs (Fig. 4.5a).

As the formation of F-actin stress fibers has been described as another feature of EMT, we stained cultured EpCAM⁻ and EpCAM⁺ cells with fluorescently-labeled Phalloidin. No striking difference was observed between the actin cytoskeleton of these two subpopulations: even though EpCAM⁻ cells appeared to form longer stress fibers and more filipodia than EpCAM⁺ ones, both subpopulations maintained a strong cortical actin signal, which is typical of epithelial cells (Fig. 4.6).

In summary, EpCAM⁻ hTECs display a partial EMT phenotype that is characterized by the absence of CDH1 and the expression of VIM and ZEB1, while they keep expressing basal epithelial markers such as CD49f, TP63 and SLUG. Furthermore, the data presented here suggests a central role for ZEB1 in this process, given that the other tested EMT-inducing transcription factors were expressed at similar levels in both the EpCAM⁻ and EpCAM⁺ hTEC subpopulations.

Figure 4.5 | EpCAM⁻ hTECs display hallmarks of EMT

A Immunostainings against CDH1, ZO-1, VIM, ZEB1 and SLUG on EpCAM⁻, EpCAM⁺ hTECs and hEKs. Epithelial identity marker CDH1 and tight junction protein ZO-1 were only observed in the EpCAM⁺ hTEC subpopulation and hEKs, whereas VIM signal was stronger in the EpCAM⁻ hTEC. ZEB1 was upregulated and nuclear only in the EpCAM⁻ subpopulation. On the other hand, SLUG was present in the nuclei of all cells in the three cell populations. Confocal images were acquired as z-stacks and maximum intensity projections from one representative experiment are presented for each panel. Scale bar = 100µm. **B & C** RT-qPCR gene expression analysis (n=4). -ΔCt: $\log_2$(relative quantity compared to reference genes). Error bars: 95% Student t-test confidence interval.

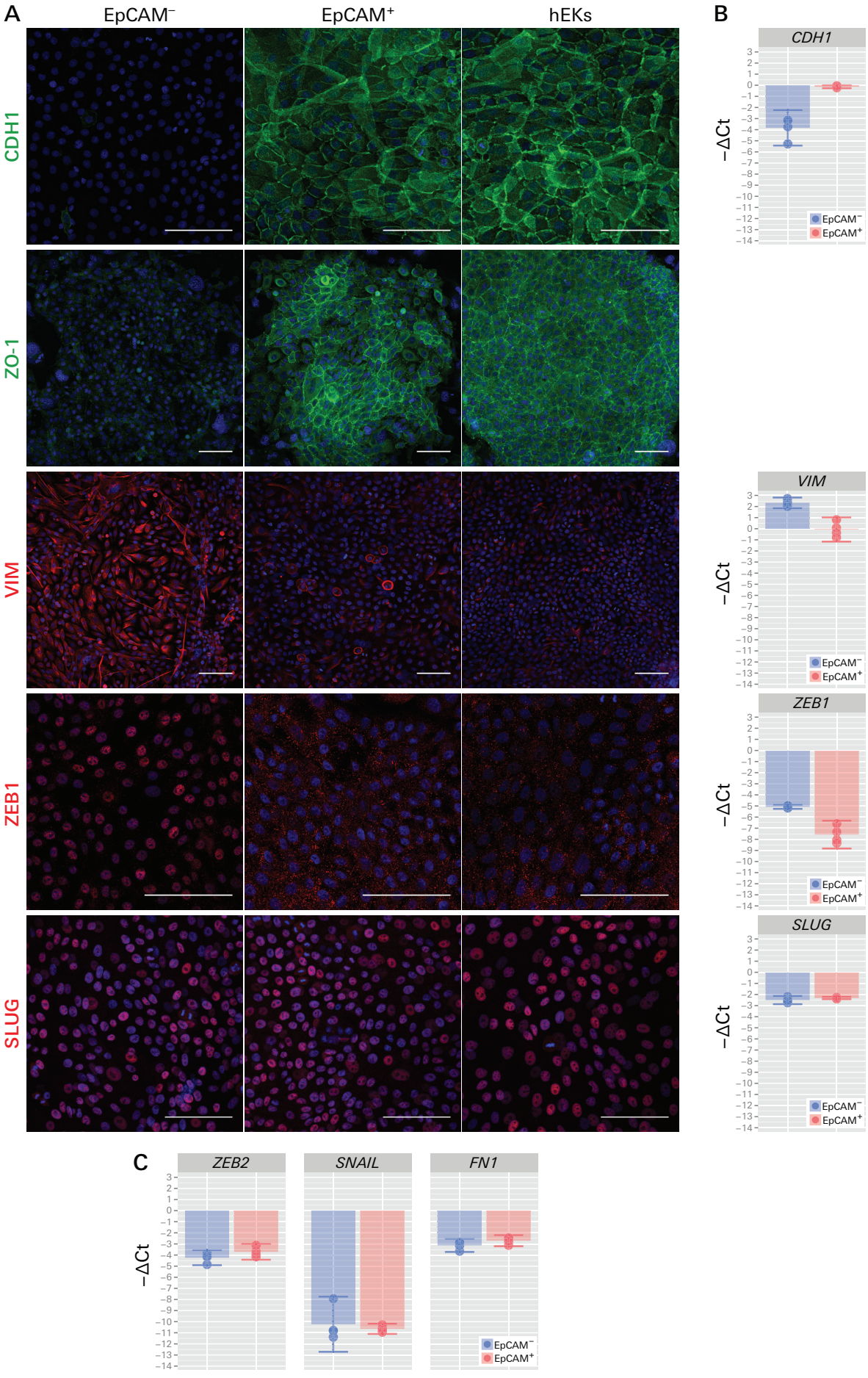
A
EpCAM⁻
EpCAM⁺
hEKs
CDH1
ZO-1
VIM
ZEB1
SLUG
B
CDH1
VIM
ZEB1
SLUG
−ΔCt
EpCAM⁻
EpCAM⁺
C
ZEB2
SNAIL
FN1

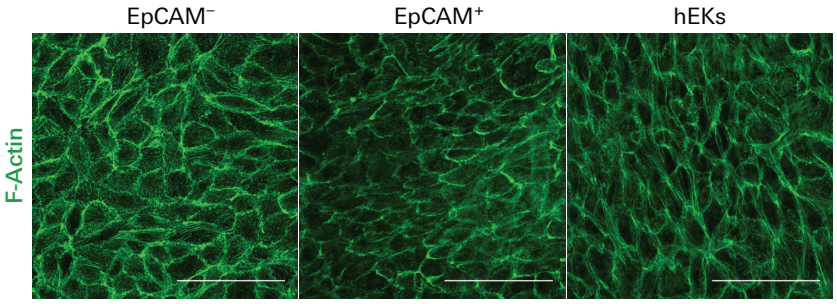

Figure 4.6 | Actin cytoskeleton morphology
F-actin was stained with Phalloidin-ActiStain488. No striking differences were observed between the actin cytoskeleton of the three subpopulations. Confocal images from one representative experiment are presented. Scale bar = 100µm.

Expression profile of essential thymic genes in the EpCAM⁻ subpopulation

Microarray analysis had previously shown that *EYA1* and *SIX1*, two genes essential for the development of the thymic epithelium, are slightly downregulated in stratified clones compared to refringent ones (1.6x and 1.9x, respectively) (Maggioni, 2012). By RT-qPCR, we were able to show that this difference in expression pattern appears to be maintained between the EpCAM⁻ and EpCAM⁺ subpopulations. *EYA1* was upregulated 5.6x in the EpCAM⁻ subpopulation (Fig. 4.7) and *SIX1* also showed a tendency to be more expressed (2.1x), although this difference was not statistically significant in the case of *SIX1* (Fig. 4.7). Conversely, the master regulator of thymic development *FOXN1* was downregulated 16.4x in the EpCAM⁻ subpopulation compared to the EpCAM⁺ one. This was not completely unexpected given the important role of FOXN1 in the differentiation of epidermal keratinocytes (Janes *et al.*, 2004). Thus, its upregulation in the EpCAM⁺ subpopulation most likely reflects a similar function for this gene product in our culture system. Taken together, these results suggest that the EpCAM⁻ subpopulation might have a more preserved thymic identity than its EpCAM⁺ counterpart.

Figure 4.7 | Differential expression of genes essential for thymic development
RT-qPCR gene expression analysis (n=4). -ΔCt: $\log_2$(relative quantity compared to reference genes). Error bars: 95% Student t-test confidence interval.

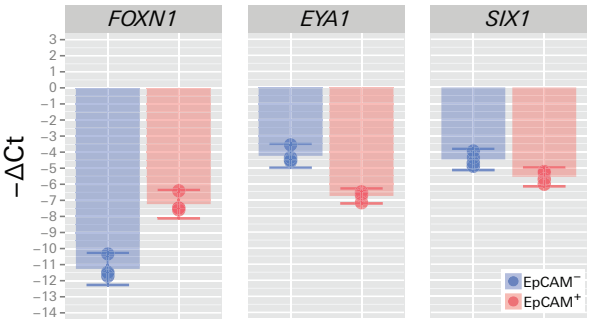

Cultured hTECs are unable to integrate a regenerating epidermis

Since hTECs and hEKs share striking similarities both *in vitro* and *in vivo*, Melissa Maggioni challenged these cells in an epidermis regeneration assay. However, her attempts with hTECs were unsuccessful (Maggioni, 2012). We suspected that the incapacity of cultured hTECs to functionally integrate a regenerating epidermis could be due to the presence of EpCAM⁻ cells in the unsorted cell population that was used in the first trials. We imagined that the partial EMT phenotype of these cells and their seemingly more preserved thymic identity could hinder the capacity of the transplanted hTEC population to form a stratified epithelium. On the other hand, as EpCAM⁺ hTECs were shown to be closer to hEKs, we hypothesized that they might have a similar capacity to contribute to the regeneration of an epidermis.

In order to test this hypothesis, EpCAM$^-$ and EpCAM$^+$ were challenged separately in the same epidermis regeneration assay (Lathion *et al.*, 2015) (Fig 4.8a). Briefly, EpCAM$^-$ and EpCAM$^+$ cells were sorted, cultured for a week, and then seeded on top of fibrin gels containing human fibroblasts. Unsorted hTECs and hEKs were used as negative and positive controls, respectively. When the epithelial cells reached confluence, they were transplanted under a skin flap opened on the back of SCID mice. 21 days later, the skin flaps were opened to expose the grafts to the air. Three months later, small biopsies were taken at the center of the transplanted area to check for the presence of human cells within the regenerated epidermis. Whereas cells positive for Human leukocyte antigen 1 (HLA-1) were detected in 4 out of 5 mice transplanted with hEK-derived positive control grafts, none of the mice transplanted with grafts generated from either of the three hTEC populations showed any sign of HLA-1$^+$ cells in their epidermis (n=5) (Fig. 4.8b). Thus, we concluded that cultured hTECs are unable to functionally integrate a regenerating epidermis, at least under these experimental conditions.

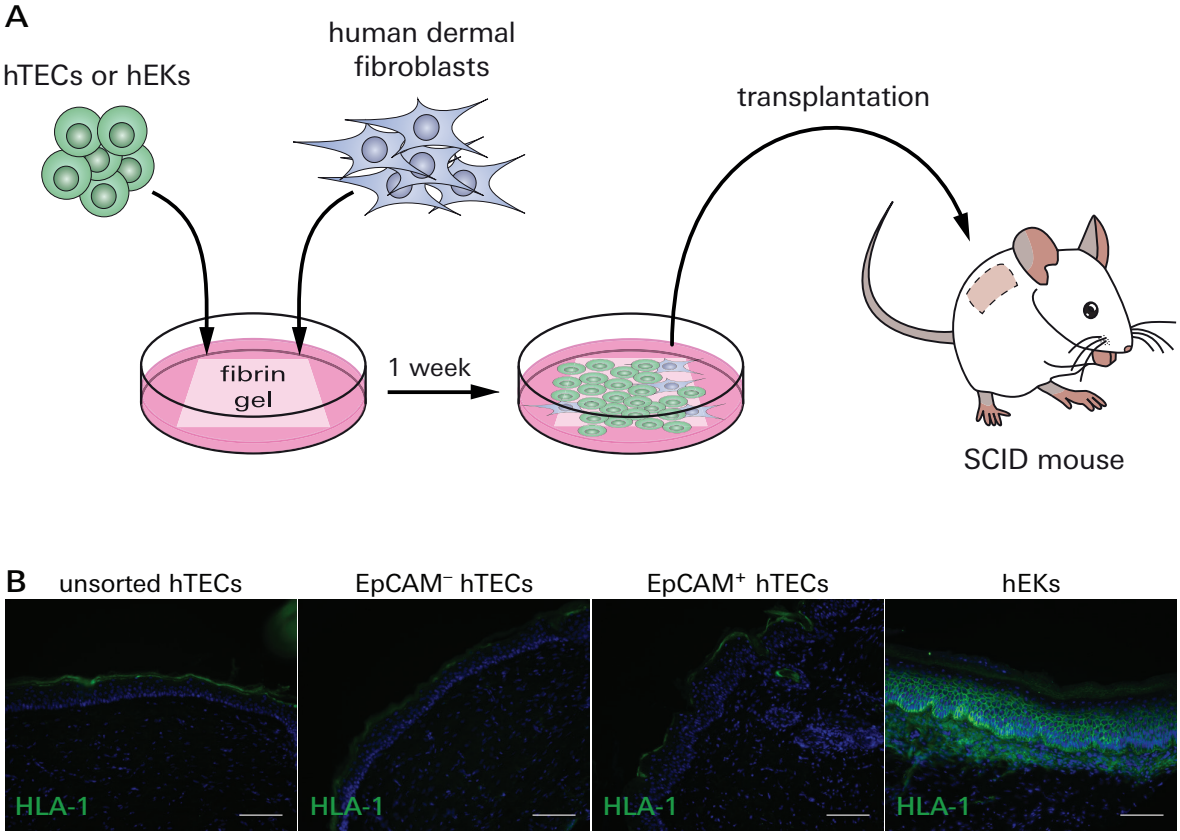

Figure 4.8 | Cultured hTECs are unable to integrate a regenerating epidermis

A Schematic representation of the culture system used to prepare the hTEC-derived grafts. The cells were grown for a week on top of fibrin gels containing human dermal fibroblast before being transplanted in a skin flap opened on the back of SCID mice. hEKs were used as a positive control and unsorted hTECs as a negative control. **B** 3 months after transplantation, small biopsies were taken at the center of the transplanted area to check for the presence of human cells in the regenerated epidermis. Human cells were detected by immunostaining for HLA-1. While human cells were detected in 4 out of 5 mice transplanted with hEKs, no HLA-1$^+$ cells were detected in the epidermis of the mice transplanted with hTECs of either subpopulation (n=5). Scale bar = 100µm.

EpCAM⁻ and EpCAM⁺ hTECs have different miRNA expression profiles

As cultured hTECs were unable to form epidermal tissue, we decided to focus on deciphering the mechanisms governing epithelial stratification. Indeed, hTECs represent an insightful system to better understand this process, since a single starting population of hTECs can give rise to both stratified and non-stratified colonies. miRNAs represented an appealing class of candidates to control stratification, because of their role as molecular switches in a number of cellular processes, including, for instance, EMT (Brabletz & Brabletz, 2010; Mukherji *et al.*, 2011; Ebert & Sharp, 2012).

As there was very little previous knowledge on the miRNA transcriptional landscape of hTECs, we started by performing a miRNA microarray analysis. We decided to use conditions close to the ones used for the mRNA microarray, which was done on single clones. Therefore, unsorted hTECs and hEKs were cultured at low density for 10 days. hTECs were then isolated by FACS on the basis of their EpCAM expression level. Both hTECs and hEKs cells were grown on top of dTomato-expressing feeder cells so as to exclude them from the sort, thus limiting the amount of contaminating mouse RNA in the samples. The purity of the isolated cell populations was assessed after each sort and was systematically over 95% (data not shown). Total RNA was extracted from 50'000 cells aliquots of hEKS, EpCAM⁻ and EpCAM⁺ hTECs isolated directly from the sort. Then, the RNA was labeled and hybridized to the array. Finally, analysis was performed between 3 hEK and EpCAM⁺ hTEC samples, and 2 EpCAM⁻ hTEC samples that were isolated in three distinct culture batches (Fig. 4. 9a).

Upon analysis, out of the 1368 miRNAs measured by the array, 217 were detected in one or more sample. Unfortunately, a date effect was observable for one hEK and one EpCAM⁺ hTEC samples that were obtained from the same batch. However, this could be corrected for in the subsequent pairwise comparisons. Clustering analysis on all the expressed miRNAs revealed a pattern similar to the one observed in the mRNA microarray; EpCAM⁺ hTECs clustered closer to hEKs than to EpCAM⁻ hTECs (Fig. 4.9b & c). Among the detected miRNAs, 34 were differentially expressed between at least two of the three cell populations. A list of these candidate hits is presented in Fig. 4.9c, completed with a few other ones selected from the literature.

RT-qPCR validation of these results was performed on different samples obtained from hEKS, EpCAM⁻ and EpCAM⁺ hTECs cultured for 7 days. The idea behind the use of a different sample isolation method being that, if a miRNA has a role in the stratification process, it should be differentially expressed regardless of the culture and RNA isolation conditions. Out of the 34 candidate miRNAs, 16 were confirmed as validated hits (Fig. 4.10). Among those, the most preeminent hits were the miR-200 family members, as the whole family was downregulated in the EpCAM⁻ subpopulation compared to hEKs and the EpCAM⁺ subpopulation (Fig. 4.11). This is in agreement with the fact that members of the miR-200 family are downregulated in cells that undergo EMT and highly expressed in epithelial cells (Brabletz & Brabletz, 2010). In addition, miR-203 was downregulated in the EpCAM⁻ subpopulation compared to the other two. This was expected considering its high expression in the suprabasal layers of the epidermis (Lena *et al.*, 2008; Yi *et al.*, 2008). On the other hand, miR-196a and miR-196b were virtually only expressed in hEKs, again in agreement with previous results; miR-196a/b are nested

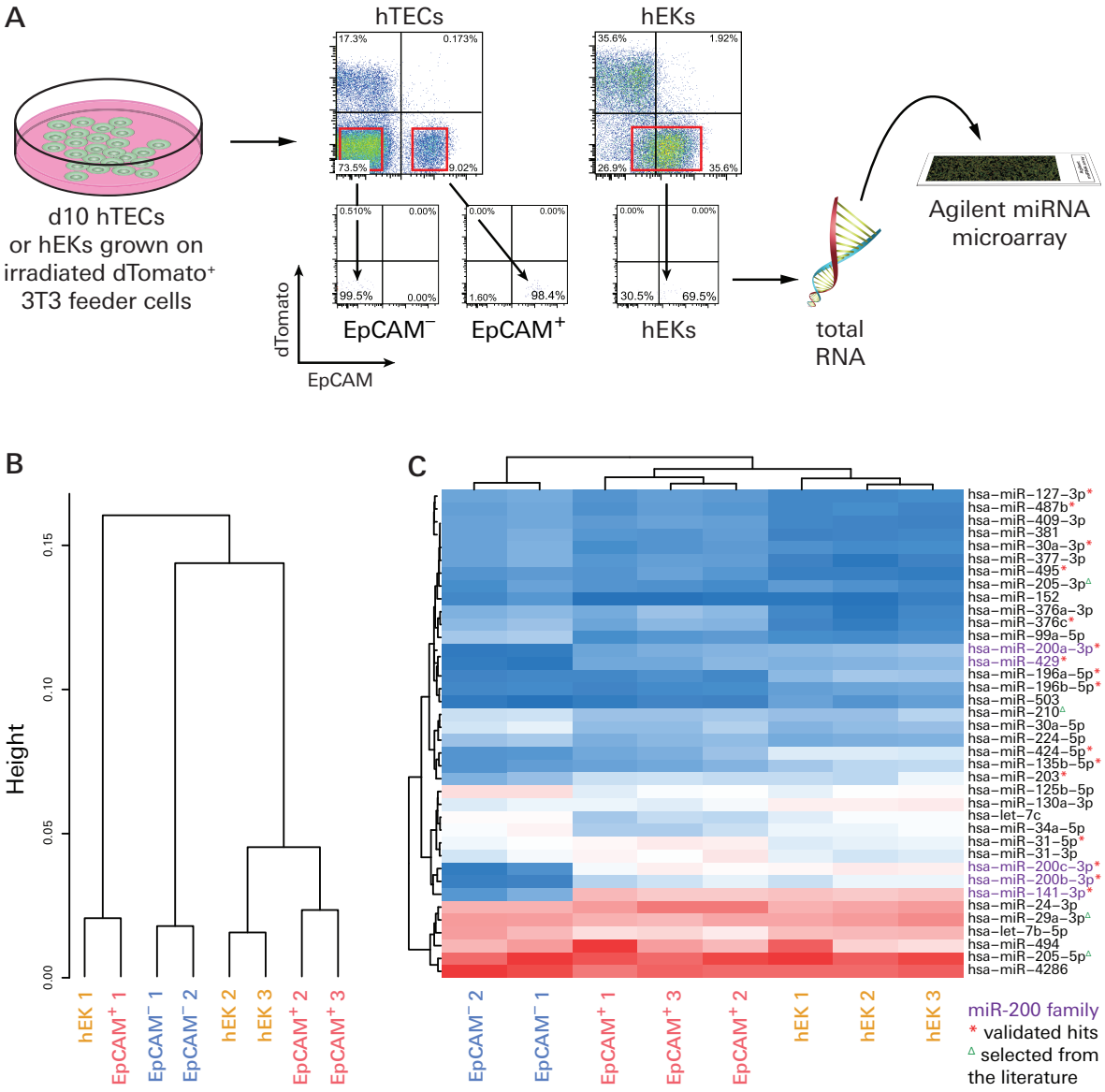

Figure 4.9 | EpCAM⁻ and EpCAM⁺ hTECs have different miRNA expression profiles

A Schematic representation of the miRNA microarray analysis. Cells were grown for 10 days on an irradiated layer of dTomato⁺ 3T3 feeder cells. EpCAM⁻, EpCAM⁺ hTECs and hEKS were isolated by FACS using the gates depicted in red. Feeder cells were excluded during the sort to limit the amount of contaminating mouse RNA. Total RNA was extracted from 50'000 cells aliquots of these subpopulations, labeled and hybridized on the array. **B** Clustering analysis based on the 217 miRNAs that were expressed in one or more samples. Overall, EpCAM⁺ hTECs clustered closer to hEKs than to EpCAM⁻ hTECs. A date effect was observed for two samples (hEK 1 and EpCAM⁺ 1) but could be corrected for in subsequent analysis. **C** Heatmap representation of the relative expression levels for the candidate hits and a few other miRNAs selected from the literature. Red: high expression level. Blue: low expression level. Purple: miR-200 family members. *: hits validated by subsequent RT-qPCR gene expression analysis. Δ: miRNAs selected from the literature.

within the same chromosomal regions than *Homeobox A9 (HOXA9), HOXA10, HOXC9* and *HOXC10* (Chen *et al.*, 2011), which were shown to follow a similar expression pattern in our previous microarray analysis. Surprisingly, miR-29a and miR-205 were found not to be differentially expressed between the three cell populations. This was unexpected given the role of miR-29a in the maintenance and function of the thymic epithelium (Papadopoulou *et al.*, 2011) and the one played by miR-205 in the repression of EMT (Gregory *et al.*, 2008a).

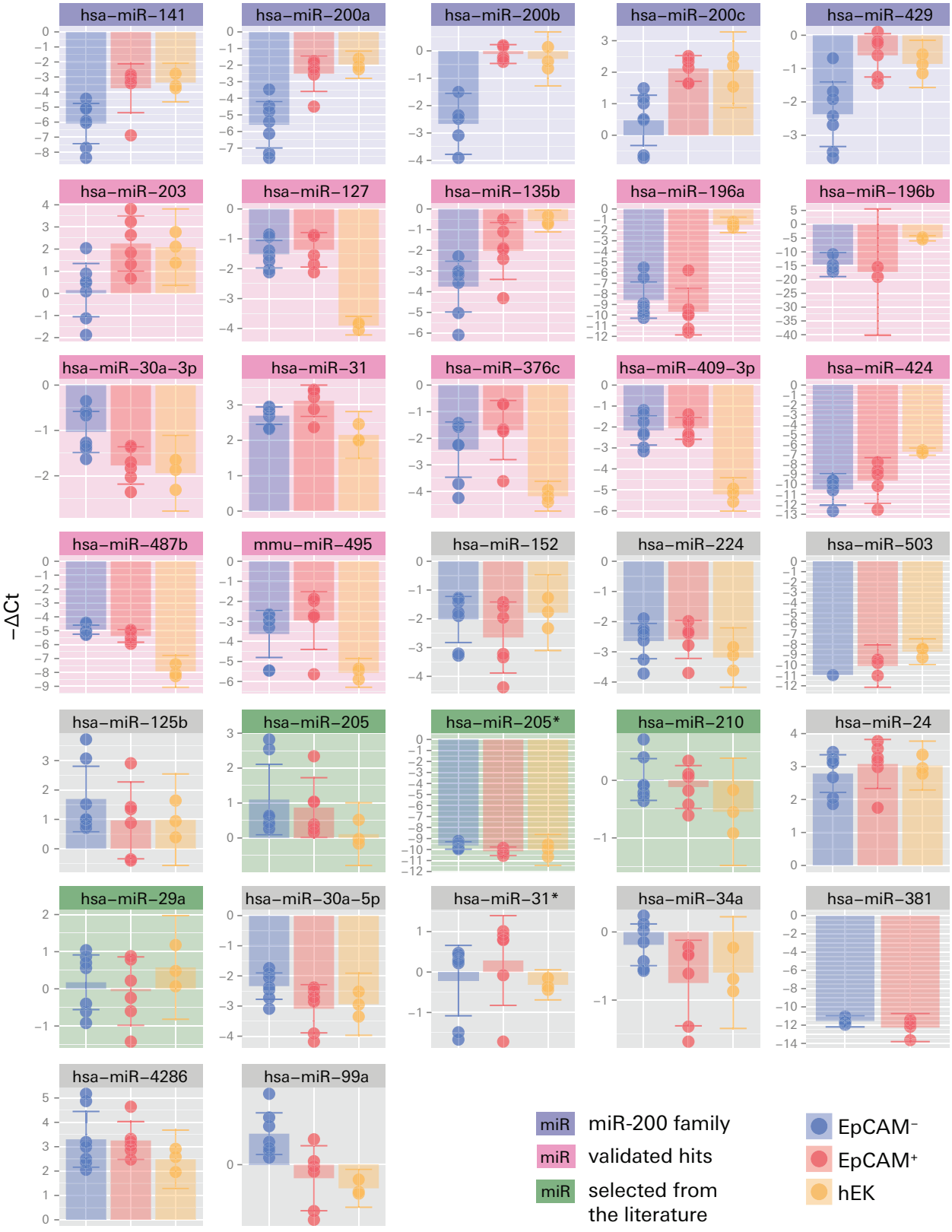

Figure 4.10 | RT-qPCR validation of miRNA microarray candidate hits

Candidate hits from obtained from miRNA microarray were validated by RT-qPCR gene expression analysis. Total RNA was extracted from EpCAM$^-$, EpCAM$^+$ hTECs and hEKs grown for 7 days in regular culture conditions. -ΔCt: $\log_2$(relative quantity compared to reference genes). Error bars: 95% Student t-test confidence interval.

Remarkably, the expression of all miR-200 family members was inversely correlated to that of their main target ZEB1. This is indicative of an opposite ZEB/miR-200 double-negative feedback loop activity in the EpCAM⁻ and EpCAM⁺ subpopulations. Thus, given the role of this feedback loop in the maintenance of the epithelial cell identity, we hypothesized that it might play a role in the control of the stratification process in cultured hTECs.

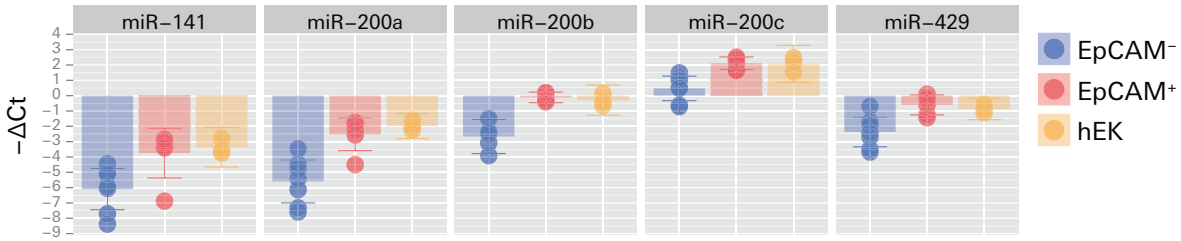

Figure 4.11 | miR-200 family members are down-regulated in the EpCAM⁻ subpopulation
Zoom on the data presented in Fig. 4.10 for the miRNAs belonging to the miR-200 family. RT-qPCR gene expression analysis. -ΔCt: $\log_2$(relative quantity compared to reference genes). Error bars: 95% Student t-test confidence interval.

4.3 miR-200c overexpression converts hTECs from an EpCAM⁻ to an EpCAM⁺ phenotype

miR-200c overexpression induces stratification in EpCAM⁻ hTECs

In order to test whether the ZEB/miR-200 double-negative feedback loop could act as a molecular switch in the control of stratification in cultured hTECs, we decided to overexpress miR-200 family members in these cells. At first, we tried to transfect mature miRNAs because it would have made testing multiple miRNAs easier. However, this technology proved to be rather difficult to adapt to our culture system, probably because of the presence of feeder cells (data not shown). Thus, we switched towards the use of miRNA overexpression lentiviral vectors. Although all the following experiments were performed with miR-141 and miR-200c contemporarily, the results obtained with miR-141 were far from being as convincing as the ones obtained with miR-200c. Hence, they will be presented in the appendix for reasons of clarity.

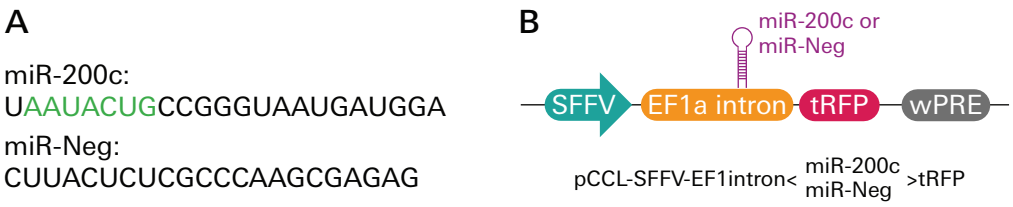

Figure 4.12 | Lentiviral miRNA overexpression vectors
A Mature miR-200c and miR-Neg (non-targeting negative control) sequences. In green, the seed region of miR-200c. **B** Schematic representation of the lentiviral miRNA overexpression vectors that were used. The pre-miRNA sequence was inserted in the 1st intron of EF1a, under the control of the SFFV promoter and followed by tRFP.

To produce the lentiviral vectors, the pri-miR-200c sequence (100bp on each side of the mature sequence) or a miRNA-adapted non-targeting shRNA sequence (called miR-Neg hereafter) was inserted into a lentiviral miRNA overexpression plasmid (pCCL). The insert was placed within the first intron of *EF1a*, under the control of the SFFV promoter and followed by tRFP (Fig 4.12). The lentiviral particles were then produced in 293T cells.

The effects of miR-200c overexpression were tested on EpCAM$^-$ and EpCAM$^+$ cells separately. hTECs were first isolated by FACS on the basis of their EpCAM expression level as previously described, and then recultured. After 3 days in culture, they were transduced with either the miR-200c overexpression vector or the miR-Neg negative control

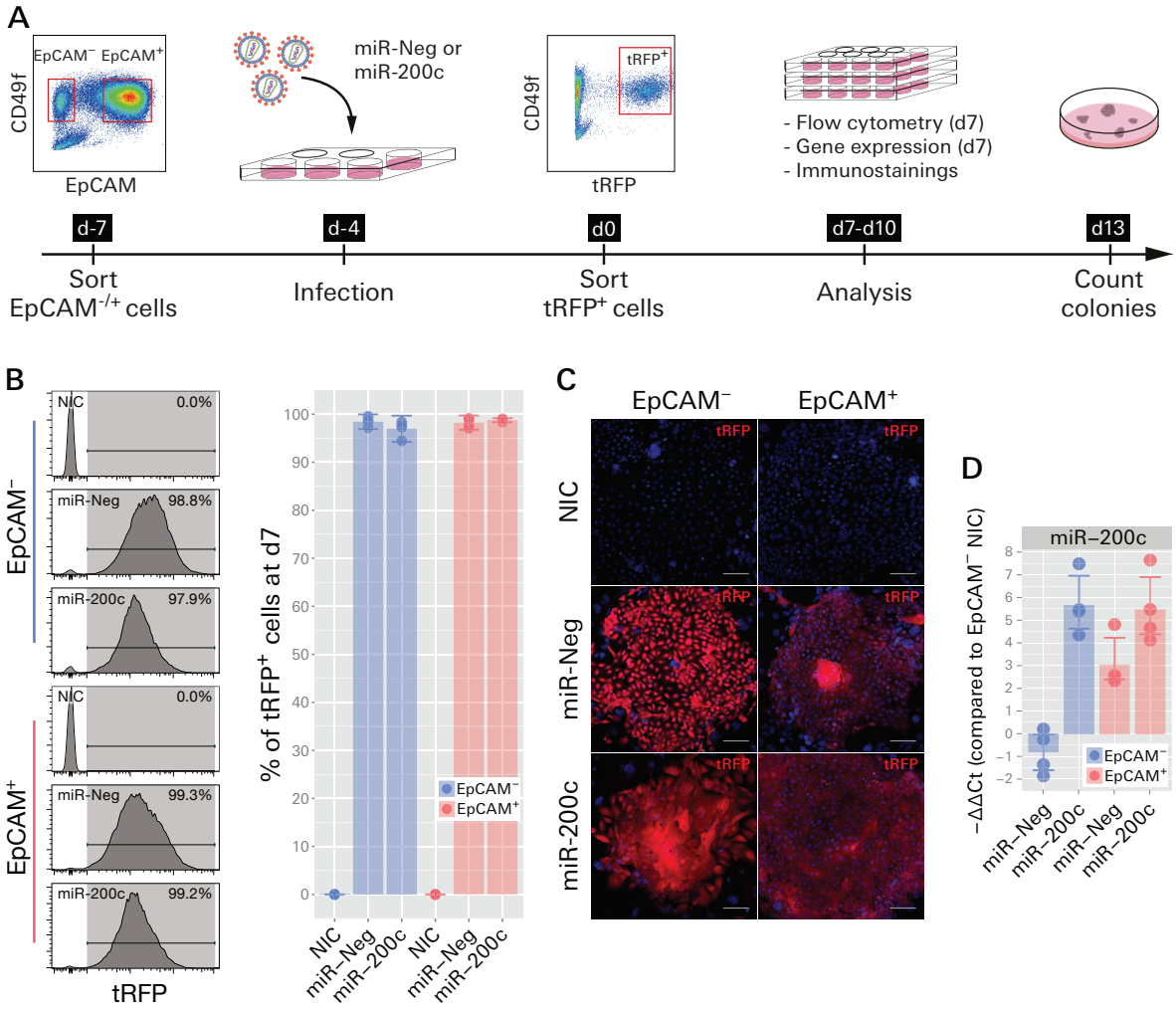

Figure 4.13 | miR-200c overexpression in the EpCAM$^-$ and EpCAM$^+$ hTEC subpopulations

A Schematic representation of the experimental design used to analyze the effects of miR-200c overexpression in the EpCAM$^-$ and EpCAM$^+$ hTEC subpopulations. EpCAM$^-$ and EpCAM$^+$ hTECs were isolated by FACS. 3 days later, they were transduced with miR-200c or miR-Neg lentiviral overexpression vectors. tRFP$^+$ infected cells were isolated by FACS 4 days after infection using the gate depicted in red and re-cultured in the appropriate vessels for subsequent analyses. **B** The proportion of tRFP$^+$ infected cells within the CD49f$^+$ population was measured one week after the sort by flow cytometry (n=4). Error bars: 95% Student t-test confidence interval. Left: proportion of tRFP$^+$ cells for one representative experiment. **C** Confocal fluorescence images of tRFP expression obtained from one representative experiment. Images were acquired as z-stacks and maximum intensity projections from one representative experiment are presented. Scale bar = 100µm. **D** RT-qPCR gene expression analysis of miR-200c (n=4). -ΔΔCt: $\log_2$(relative quantity compared to EpCAM$^-$ NIC). Error bars: 95% Student t-test confidence interval. NIC: non-infected control.

vector. Non-infected cells from both the EpCAM$^-$ and the EpCAM$^+$ subpopulations were also maintained as negative controls for all subsequent analyses. 4 days later, infected CD49f$^+$tRFP$^+$ cells were isolated by FACS and cultured for 7 to 13 days, depending on the assay (Fig. 4.13a). The purity of each isolated population was assessed by flow cytometry at the end of every sort and was systematically above 90% (data not shown). This experiment was repeated with hTECs isolated from 4 different patients.

After one week in culture, the infected cell populations were still more than 95% pure, as marked by the expression of tRFP, whereas no tRFP signal could be detected in the non-infected controls (NICs) (Fig. 4.13b & c). Moreover, only the cells infected with the miR-200c lentiviral vector overexpressed miR-200c (89.7x for EpCAM$^-$ and 5.4x for EpCAM$^+$, compared to their respective miR-Neg controls) (Fig. 4.13d). Importantly, no noticeable difference was observed between the non-infected and miR-Neg controls in any of the following experiments. This indicates that the infection by a lentiviral overexpression vector did not elicit off-target effects.

After 13 days, the colonies in the colony-forming efficiency assay dishes from all tested conditions were counted. Strikingly, miR-200c overexpression induced a drastic increase in the proportion of stratified colonies present in the EpCAM$^-$ dishes (from 7.8% to 95% on average), while the non-targeting control did not (Fig. 4.14a & b). On the other hand, the EpCAM$^+$ cells remained relatively unaffected by miR-200c overexpression (Fig. 4.14a & b), although miR-200c overexpression seemed to slightly lower their average colony size and to increase their proportion of aborted colonies over passages (data not shown). Thus, it is likely that on top of inducing stratification, miR-200c also pushes hTECs towards terminal differentiation.

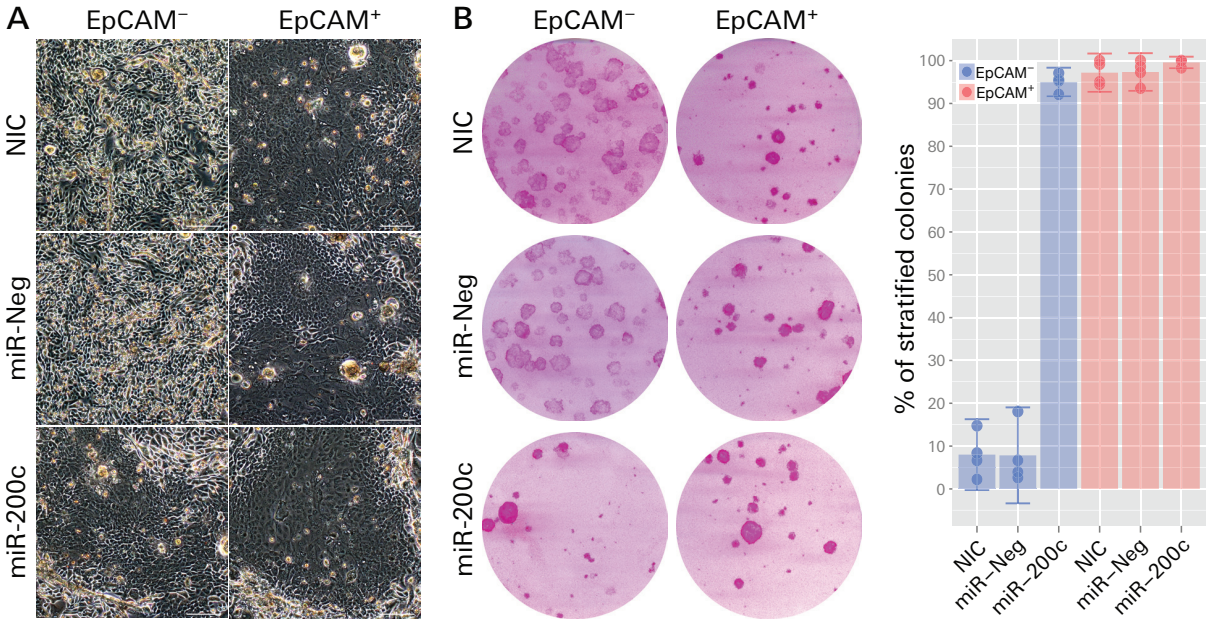

Figure 4.14 | miR-200c overexpression induces stratification in EpCAM$^-$ hTECs

A Phase contrast images from one representative experiment. Scale bar = 100µm. **B** The proportion of stratified colonies was measured by counting the colonies in the colony-forming efficiency assays. miR-200c, but not miR-Neg, induced stratification in the EpCAM$^-$ hTEC subpopulation (n=4). Left: colony-forming efficiency assay dishes stained with Rhodamine B from one representative experiment. Right: Colony-forming efficiency assays were always made in duplicate; each dot represents the average of the two dishes. Error bars: 95% Student t-test confidence interval.

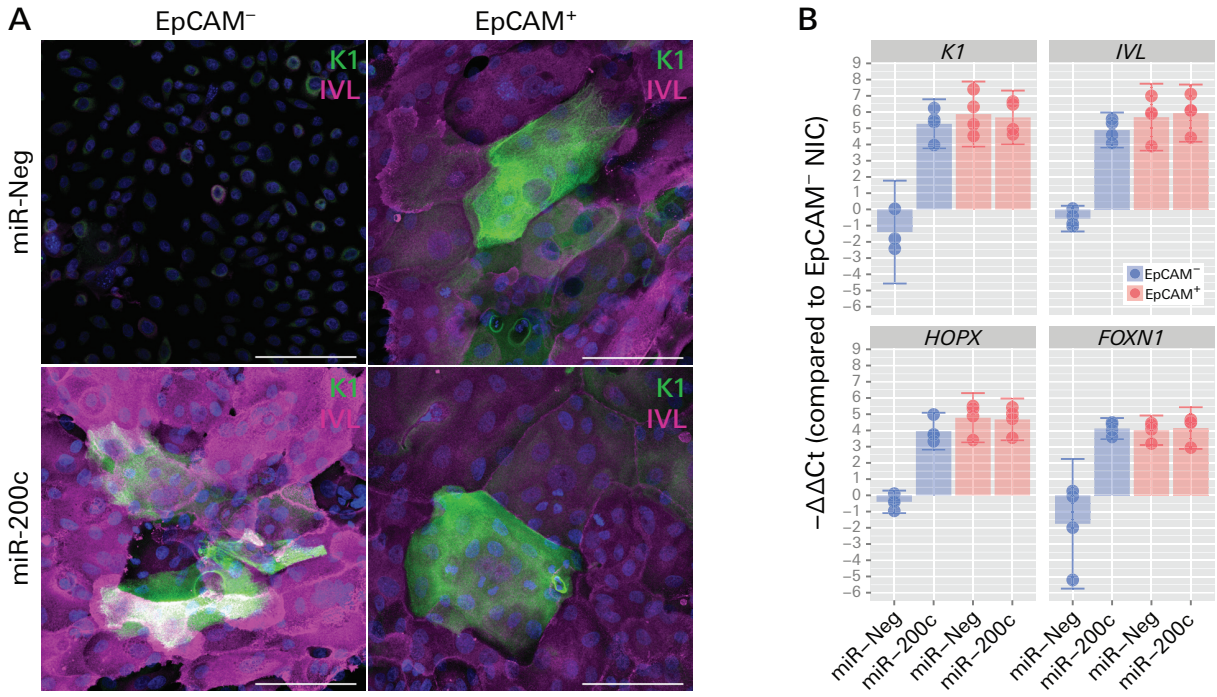

Figure 4.15 | Epidermal differentiation markers are expressed by the EpCAM⁻ hTEC subpopulation upon miR-200c overexpression

A Immunostaining for K1 and IVL. The stratification triggered by miR-200c overexpression in the EpCAM⁻ subpopulation was characterized by the upregulation of epidermal differentiation markers and the appearance of squame-like cells. Confocal images were acquired as z-stacks and maximum intensity projections from one representative experiment are presented. Scale bar = 100µm. **B** RT-qPCR gene expression analysis (n=4). -ΔΔCt: $\log_2$(relative quantity compared to EpCAM⁻ NIC). Error bars: 95% Student t-test confidence interval. NIC: non-infected control.

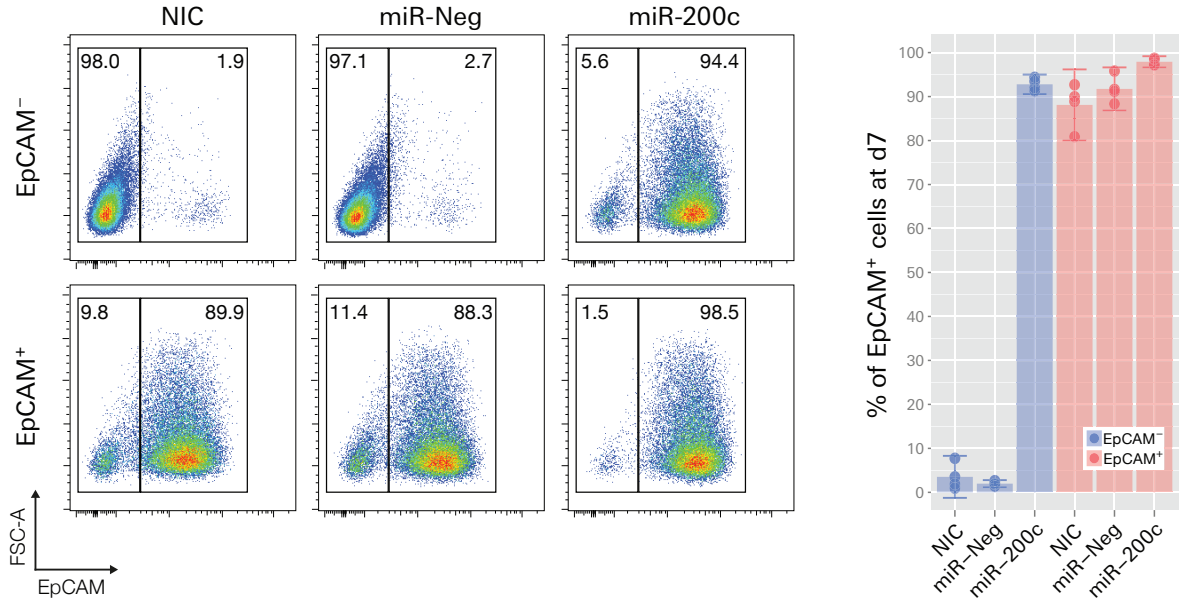

Figure 4.16 | miR-200c overexpression induces EpCAM expression

The proportion of EpCAM⁺ infected cells in the CD49f⁺ population was measured by flow cytometry (n=4). Left: flow cytometry plots and gates from one representative experiment. Error bars: 95% Student t-test confidence interval.

The stratification that occurred in the EpCAM⁻ subpopulation after miR-200c overexpression was characterized by the appearance of squame-like cells that expressed K1 and IVL, similarly to what was observed in the EpCAM⁺ subpopulation (Fig. 4.15a). At the RNA level, miR-200c overexpression led to the upregulation of *K1, IVL, HOPX* and *FOXN1* in the EpCAM⁻ cells, bringing their expression to levels comparable to those found in the EpCAM⁺ subpopulations (Fig. 4.15b). Here again, the expression level of these genes was not affected by miR-Neg (Fig. 4.15a & b).

Remarkably, miR-200c overexpression in the EpCAM⁻ subpopulation also significantly increased the proportion of EpCAM⁺ cells from 2% to 92.8% (Fig. 4.16; Fig. 4.18a). In the EpCAM⁻ subpopulation, *EpCAM* also appeared to be upregulated by miR-200c overexpression at the RNA level (Fig. 4.18c). On the other hand, the basal epithelial identity of both cultured hTECs subpopulations was not affected by the overexpression of miR-Neg or miR-200c; the proportion of CD49f appeared unchanged in infected cells (Fig. 4.17a) and the expression level of *P63* remained stable across all samples (Fig. 4.17b). These results suggest that miR-200c overexpression might be sufficient to convert EpCAM⁻ hTECs into stratifying EpCAM⁺ ones.

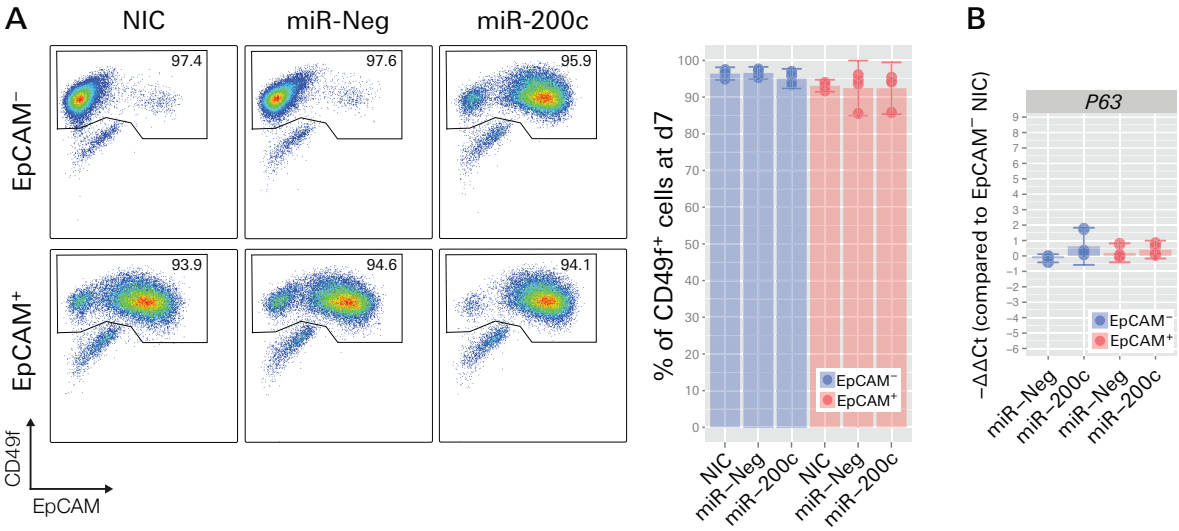

Figure 4.17 | Basal epithelial identity of cultured hTECs not affected by miR-200c overexpression
A The proportion of CD49f⁺ was measured by flow cytometry. It was not affected by the overexpression of miR-200c. Error bars: 95% Student t-test confidence interval. Left: flow cytometry plots and gates from one representative experiment. **B** RT-qPCR gene expression analysis of *P63* (n=4). -ΔΔCt: $\log_2$(relative quantity compared to EpCAM⁻ NIC). Error bars: 95% Student t-test confidence interval. NIC: non-infected control.

EMT hallmarks are abrogated upon miR-200c overexpression in EpCAM⁻ hTECs

We analyzed the effect of miR-200c overexpression on the EMT hallmarks displayed by the EpCAM⁻ subpopulation. As expected, miR-200c overexpression led to the downregulation of *ZEB1* (Fig. 4.18c) and to the loss of the nuclear localization of its protein (Fig. 4.18a), while miR-Neg had no such effects (Fig. 4.18a & c). Surprisingly, although it is its direct target, *ZEB1* was not downregulated further in EpCAM⁺ cells that overexpressed miR-200c (Fig. 4.18c). miR-Neg and miR-200c also seemed to have no effect on *ZEB2*,

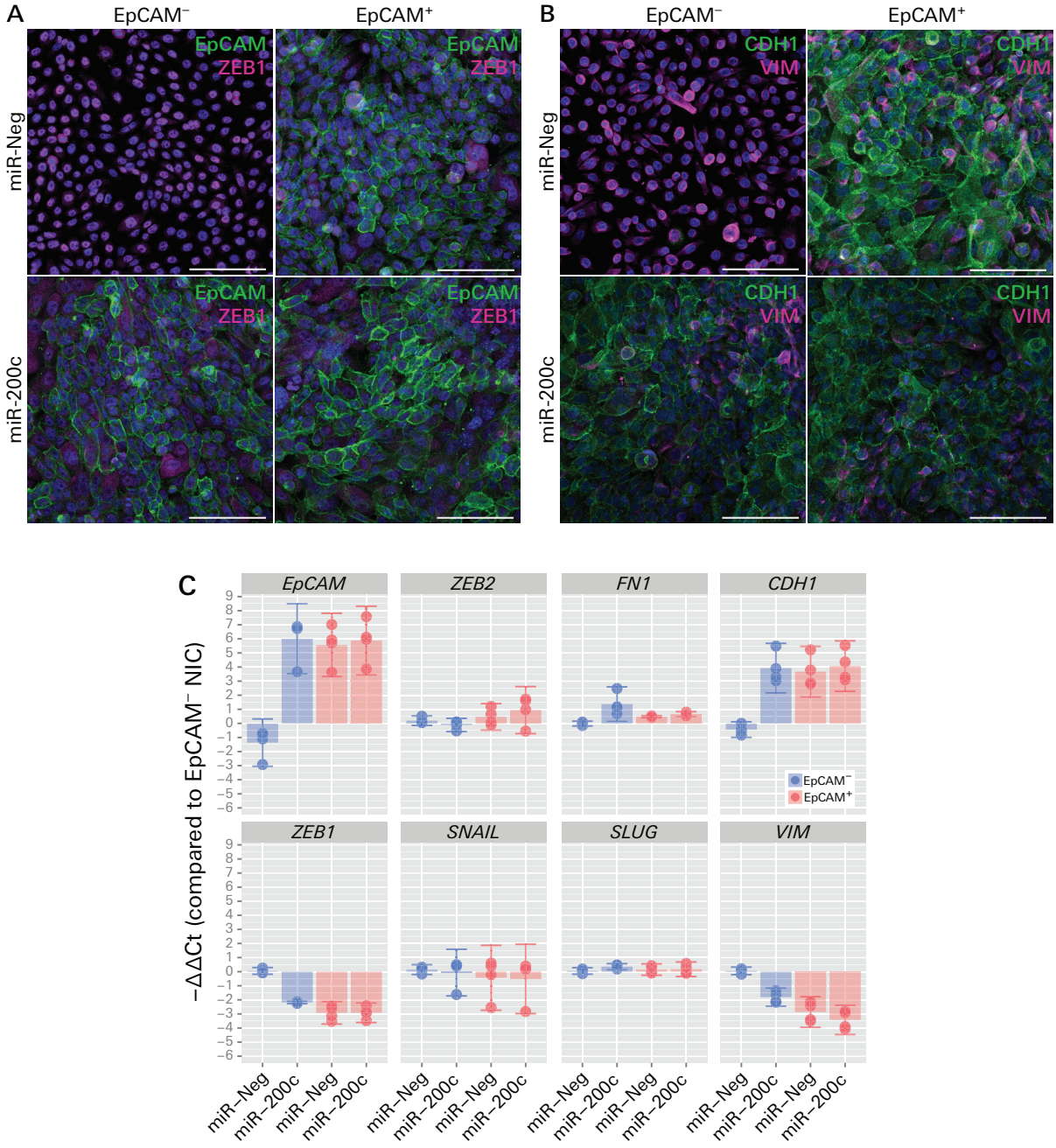

Figure 4.18 | EMT hallmarks displayed by EpCAM⁻ hTECs are abrogated upon miR-200c overexpression

A Immunostaining for EpCAM and ZEB1. miR-200c overexpression in the EpCAM⁻ subpopulation activated EpCAM expression and down-regulated ZEB1. ZEB1 also lost its nuclear localization in the process. Confocal images were acquired as z-stacks and maximum intensity projections from one representative experiment are presented. Scale bar = 100µm. **B** Immunostaining for CDH1 and VIM. CDH1 was upregulated and VIM was downregulated upon miR-200c overexpression in the EpCAM⁻ subpopulation, similarly to what is observed during MET. Confocal images were acquired as z-stacks and maximum intensity projections from one representative experiment are presented. Scale bar = 100µm. **C** RT-qPCR gene expression analysis (n=4). -ΔΔCt: $\log_2$(relative quantity compared to EpCAM⁻ NIC). Error bars: 95% Student t-test confidence interval. NIC: non-infected control.

SNAIL, SLUG and *FN1* as their expression levels were not significantly altered in infected cells from both the EpCAM$^-$ and EpCAM$^+$ subpopulations (Fig. 4.18c). This was expected because these genes were not differentially expressed in non-infected cells.

miR-200c overexpression in the EpCAM$^-$ subpopulation also brought the expression of *CDH1* to a level similar to the one observed in EpCAM$^+$ cells, whereas miR-Neg did not (Fig. 4.18c). Additionally, CDH1 was clearly detectable on the plasma membrane of miR-200c-overexpressing cells from the EpCAM$^-$ subpopulation (Fig. 4.18b). In contrast, VIM was downregulated both at the RNA and protein levels upon miR-200c overexpression compared to the negative controls (Fig. 4.18b & c). Like for all the other genes, miR-200c overexpression had no impact on *CDH1* or *VIM* expression levels in EpCAM$^+$ cells (Fig. 4.18c). Taken together, our results indicate that the partial EMT phenotype observed in EpCAM$^-$ cells is abrogated in favor of a stratified epithelial identity upon miR-200c overexpression. What is more, their basal epithelial identity is maintained, as it is the case in EpCAM$^+$ cells.

In the EpCAM$^-$ subpopulation, miR-200c overexpression alters the expression of other miRNAs, EYA1 and SIX1

In order to characterize the extent of the conversion induced by miR-200c overexpression in the EpCAM$^-$ subpopulation, we analyzed its impact on selected miRNAs. In EpCAM$^-$ cells, miR-141 and miR-429 (two other miR-200 family members) and miR-203 were upregulated to levels comparable to EpCAM$^+$ cells upon miR-200c overexpression (Fig 4.19a). This was expected, given that these three miRNAs were expressed at a higher level in the EpCAM$^+$ subpopulation compared to the EpCAM$^-$ one. On the other hand, the expression of miRNAs that were not differentially expressed between EpCAM$^-$ and EpCAM$^+$ cells, such as miR-205, miR-196a and miR-487b, remained unaltered by the overexpression of miR-200c (Fig. 4.19a).

In the EpCAM$^-$ subpopulation, miR-200c also brought down the expression of two genes essential for thymic development, *EYA1* and *SIX1,* to the same levels observed in EpCAM$^+$ cells (Fig. 4.19b). However, as previously observed in non-infected cells, the difference in gene expression between the miR-200c- and miR-Neg-infected cells was statistically significant only for *EYA1.* Again, the expression of these two genes was unaffected in the miR-Neg control and in EpCAM$^+$ cells. The fact that miR-200c overexpression even alters the expression level of genes essential for thymic development in the EpCAM$^-$ subpopulation suggests that miR-200c is probably not only inducing stratification but a conversion that goes all the way towards the EpCAM$^+$ phenotype.

Overall, we were able to demonstrate that miR-200c overexpression is sufficient to convert EpCAM$^-$ hTECs into stratifying EpCAM$^+$ ones, through the activation of a MET-like process. These cells had lost their partial EMT hallmarks and expressed epidermal differentiation markers and miRNAs at levels comparable to non-infected EpCAM$^+$ cells. Thus, this work emphasizes a central role for the ZEB/miR-200 double-negative feedback loop in the control of hTEC stratification.

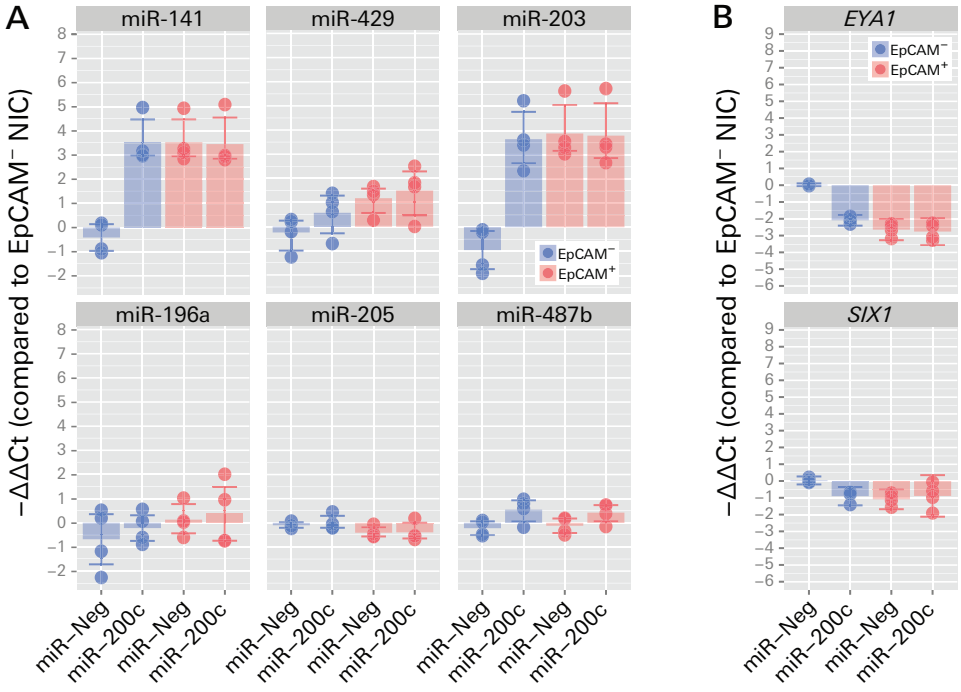

Figure 4.19 | In the EpCAM$^-$ subpopulation, miR-200c overexpression alters the expression of other miRNAs, *EYA1* and *SIX1*

A & B RT-qPCR gene expression analysis (n=4). -ΔΔCt: $\log_2$(relative quantity compared to EpCAM$^-$ NIC). Error bars: 95% Student t-test confidence interval. NIC: non-infected control.

5. Discussion

Epithelia are defined as two-dimensional sheets of cells that rest on a basement membrane and define borders between or within organs. In this respect, the thymic epithelium is unique as it forms a characteristic, sponge-like 3D meshwork. Within this structure, TECs are only loosely attached to each other through cell junctions compared to other epithelial cells, with the exception of the subcapsular zone, where TECs are anchored to a basement membrane that lines the surface of the mesenchymal capsula (Frank *et al.*, 1984; Virtanen *et al.*, 1996).

In previous work, Melissa Maggioni was able to show that hTECs can be extensively expanded *in vitro* and that they form four morphologically distinct colony types in culture (Maggioni, 2012). Each of these subpopulations is present in variable proportions in independent experiments, most likely due to patient-to-patient variability and to the amount of time the cells are kept in culture. However, other unknown factors, such as small differences in temperature, pH or in the state of the feeder cell layer, also have a major influence on the phenotype of cultured hTECs.

Although two cell populations can be clearly distinguished within the thymic epithelium *in vivo*, cTECs and mTECs, whether cultured hTECs belong either one of them remains unclear to this date. As a matter of fact, extracellular markers generally used to discriminate between these two populations, such as Ly51 and CD205 for cTECs and CD80 for mTECs, are not expressed in cultured hTECs. Interestingly, when freshly isolated from the thymus, all clonogenic hTECs were found to express the mTEC marker EpCAM, whereas only thymic fibroblasts grew from the freshly isolated $EpCAM^-$ population (Maggioni *et al.*, in preparation). In addition, all the TECs that grow in our culture system express K5, while K8 expression is only observed in a few cells during the first few days in culture. As a reminder, in the thymus, cTECs mainly express K8/K18 and mTECs preferentially express K5/K14. Thus, these results seem to suggest that we are mostly expanding a population of mTECs. However, EpCAM and K5 are also expressed by TECs of the cortico-medullary junction *in vivo* and freshly isolated $EpCAM^+$ cells

rapidly give rise to an EpCAM$^-$ subpopulation in culture, indicating that cultured hTECs do not possess a strictly medullary identity. This idea is also supported by the fact that cultured hTECs do not express the functional mTEC markers AIRE and MHC class II. In addition, the expression of K5 by all cultured hTECs could result from the phenotype close to the one of the basal cells of the epidermis that is favored by our culture system, as indicated by the expression of CD49f, P63 and SLUG. In summary, although the population that we are able to capture appears to be enriched for mTECs, whether these cells display a cortical or medullary identity in culture remains an unanswered question. In fact, the phenotype of cultured hTECs is different from the one displayed by either of the *in vivo* hTEC populations.

In this work, we first focused on finding an extracellular marker that could distinguish between different hTEC subpopulations in our culture system. Luckily, we were able to demonstrate that EpCAM identifies stratifying cultured hTECs. EpCAM$^+$ cells only gave rise to stratified colonies, whereas EpCAM$^-$ cells mostly yielded non-stratified colonies. We also showed that EpCAM$^-$ cells have the capacity to generate some EpCAM$^+$ cells and stratified colonies, in agreement with the previously established hierarchical organization between clones of different morphologies (Maggioni, 2012). Moreover, as it was shown by mRNA microarray analysis, miRNA microarray analysis confirmed that EpCAM$^+$ hTECs have a gene expression profile closer to hEKs than to EpCAM$^-$ hTECs. These results suggest that, as it is the case *in vivo*, there is a population of hTECs that displays striking similarities with hEKs *in vitro*.

Our laboratory previously demonstrated that a skin inductive microenvironment is sufficient to reprogram cultured rTECs into hair follicle multipotent stem cells (Bonfanti *et al.*, 2010). Unfortunately, our attempts to see hTECs integrate into a regenerating epidermis have all been unsuccessful so far. While this was expected with unsorted or EpCAM$^-$ hTECs, it was surprising to see that EpCAM$^+$ cells were also unable to do so, as they are strikingly similar to hEKs. This inability to contribute to the formation of an epidermis could result from the expression of genes involved in thymic development by both hTEC subpopulations, such as *EYA1, SIX1* and *FOXG1*, as these genes are not expressed in hEKs (Maggioni, 2012). Conversely, miR-196a and miR-196b are expressed by hEKs but not by hTECs, and thus might also be part of the problem. However, we believe that our failure to reproduce the results that were obtained with rTECs, with hTECs, is mostly due to the fact that the assay used with rTECs cannot be used with human cells. Indeed, there is currently no working hair follicle morphogenetic assay available for the latter. Furthermore, the strong morphogenic signals present in the hair follicle morphogenetic assay used to reprogram rTECs into hair follicle multipotent stem cells are absent from the epidermis regeneration assay that we used for hTECs as a replacement. These morphogenic signals have yet to be identified and their absence could explain the incapacity of hTECs to differentiate into epidermal stem cells in our experimental setup.

In our opinion, cultured hTECs represent an insightful system to study the mechanisms governing EMT and stratification in epithelial cells, as a single starting hTEC population yields both cells that have partially undergone EMT and cells that form stratified colonies. Here, we were able to show that the EpCAM$^-$ and EpCAM$^+$ subpopulations display opposite ZEB/miR-200 double-negative feedback loop activity; while EpCAM$^-$ cells

express ZEB1 at a higher level, miR-200 family members are upregulated in EpCAM^{+} cells. We also demonstrated that this feedback loop plays a crucial role in regulating the balance between EMT and stratification in cultured hTECs. Indeed, miR-200c overexpression was sufficient to convert EpCAM^{-} cells into EpCAM^{+} ones, switching from their partial EMT phenotype to a stratified epithelial identity in a process reminiscent of MET. Importantly, the fact that a single miRNA was sufficient to induce this conversion and that AIRE is not expressed in these cells indicates that the intrinsic stratification program observed in hTECs is not likely to be due to promiscuous gene expression. This supports the idea that stratification is an integral part of the TEC differentiation program *in vivo* and that Hassall bodies represent terminally differentiated mTECs, as it has been suggested by other research groups (Hale & Markert, 2004; Yano *et al.*, 2008; Wang *et al.*, 2012).

Despite the fact that miR-141 and miR-200c both belong to the miR-200 family, the overexpression of miR-141 failed to convert most EpCAM^{-} cells into EpCAM^{+} ones like miR-200c did. Instead, the EpCAM^{-} subpopulation acquired an intermediary phenotype upon miR-141 overexpression. Interestingly, similar differences in the capacity of these two miRNAs to induce MET had already been observed in cancer cell lines (Burk *et al.*, 2008). We propose two hypotheses to explain the differences observed between the results obtained with miR-141 and miR-200c. First, as mentioned in the introduction, the seed region of these two miRNAs differs by one nucleotide. Thus, miR-141 and miR-200c suppress largely non-overlapping groups of targets (Kim *et al.*, 2013; Wong *et al.*, 2015). This could explain why, on top of driving the conversion of some EpCAM^{-} cells into EpCAM^{+} ones, miR-141 overexpression appeared to increase the proliferation rate of the infected cells. On the other hand, it is possible that the concentration of these miRNAs in the cytoplasm must reach a certain threshold in order to trigger the dramatic changes observed upon miR-200c overexpression. In fact, RT-qPCR analysis indicated that miR-141 was expressed at a lower level than miR-200c, both before and after their overexpression (Fig. 5.1). This expression pattern is peculiar, given that both of these miRNAs are transcribed from the same chromosomal locus (Brabletz & Brabletz, 2010) but we have yet to find a potential explanation for this discrepancy.

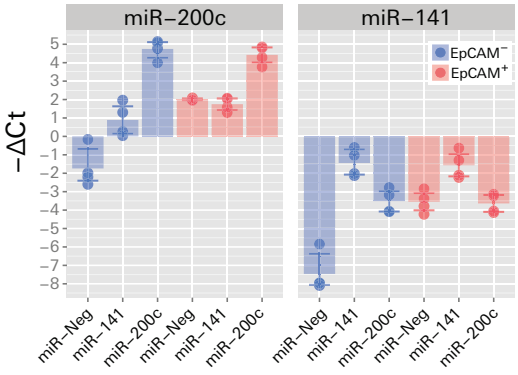

Figure 5.1 | miR-200c and miR-141 are expressed at different levels

RT-qPCR gene expression analysis of miR-200c and miR-141 (n=4). miR-141 is expressed at a lower level than miR-200c, before and after their overexpression. -ΔCt: $\log_2$(relative quantity compared to reference genes). Error bars: 95% Student t-test confidence interval.

Although we were able to demonstrate that hTECs balance between EMT and stratification *in vitro* and that this process is regulated by the ZEB/miR-200 double-negative feedback loop, the relevance of these findings *in vivo* remains to be elucidated. In the thymus, ZEB1 is expressed in developing thymocytes. Nevertheless, it also appears to colocalize with P63 in the nuclei of TECs (our unpublished results). Thus, there is a pos-

sibility that the poorly developed thymi observed in *Zeb1*-null mice might not only result from the thymocyte deficiency that these mice suffer from (Higashi *et al.*, 1997) but also from an intrinsic defect in TEC development (which could worsen the T-cell defect). Histologically, the thymus of these mice is very similar to the medulla of the wild-type organ, but they appear to lack the denser cortex. Interestingly, the TEC-specific deletion of another factor implicated in the activation of EMT, TGFβ receptor II *(Tgfbr2)*, also leads to an enlarged medulla, caused by an increased number of mTECs (Hauri-Hohl *et al.*, 2014). These observations suggest that inhibiting EMT is key to the regulation of the medullary compartment's size and differentiation. miRNAs are indispensable for TEC maintenance and function, possibly because of their crucial role in the regulation of EMT. Indeed, Imran Khan and colleagues have shown recently that miR-34a, miR-205, miR-203 and the five members of the miR-200 family, which all silence key EMT-inducing transcription factors, are upregulated in TECs compared to $CD45^+$ cells, and in mTECs compared to cTECs (Khan *et al.*, 2015). In the same study, the authors showed that the deletion of miR-205 does not affect TEC function. In addition, the fact that miR-29a deletion fails to fully reproduce the effects on mTEC lineage progression and terminal differentiation observed upon TEC-specific *Dicer* or *DGCR8* ablation suggests that other miRNA play a role in these processes (Papdopoulou *et al.*, 2011; Ucar *et al.*, 2013; Ucar & Rattay, 2015). Thus, it is likely that the miR-200 family members play an important role in the differentiation and maintenance of mTECs.

We believe that the data presented in this work supports a role for the ZEB/miR-200 double-negative feedback loop in the building and maintenance of the thymus. Although this is only speculation, it is easy to imagine that TECs need a fine balance between EMT and stratification to maintain the unique tridimensional architecture of the thymic epithelium. In the future, it will be interesting to see whether the overexpression of ZEB1 or of its 3'UTR (that could act as a miRNA sponge for miR-200 family members) can convert cultured $EpCAM^+$ hTECs into $EpCAM^-$ ones. Additionally, to investigate the role of the ZEB/miR-200 double-negative feedback loop in the development and function of the thymic epithelium *in vivo*, we plan on crossing *FOXN1-Cre* and *Zeb1*$^{flox/flox}$ mice to study the effects of a TEC-specific deletion of ZEB1. In parallel, it will be important to see how the downregulation of the whole miR-200 family in the TEC compartment, through the overexpression of the *ZEB1* 3'UTR, impacts thymic maintenance and functionality. Interestingly, in the epidermis, Ovol1 and Ovol2, two zinc finger transcription factors, have been identified as gatekeepers of epithelial adhesion and differentiation. Moreover, these genes promote the differentiation of epidermal progenitor cells in part through the inhibition of components of the EMT pathway such as Zeb1 (Lee *et al.*, 2014; Hong *et al*., 2015). In our culture system, Ovol1 and Ovol2 are upregulated in stratified clones compared to refringent ones (Maggioni, 2012), suggesting a potential regulatory role for these genes on the activity of the Zeb1/miR-200 double-negative feedback loop, which could be worth investigating.

6. Appendix

6.1 miR-141 overexpression fails to convert all EpCAM⁻ hTECs into EpCAM⁺ ones

miR-141 overexpression induces stratification only in a fraction of the EpCAM⁻ hTEC subpopulation

In order to test whether the ZEB/miR-200 double-negative feedback loop could act as a molecular switch in the control of stratification in cultured hTECs, we decided to overexpress miR-200 family members in these cells. Although miR-141 and miR-200c differ only by a few nucleotides (78.3% identity) (Fig. 6.1a), the effects of miR-141 overexpression were far from being as convincing as the ones achieved with miR-200c. For reason of clarity, the results obtained with miR-141 are presented here in the appendix.

The effects of miR-141 and miR-200c overexpression in hTEC subpopulations were analyzed in parallel and were compared to the same miR-Neg and NIC negative controls (Fig. 6.2a). The lentiviral miRNA overexpression vectors that were used were exactly identical, with the exception of the miRNA insert (Fig. 6.1a & b). After one week in

Figure 6.1 | Lentiviral miRNA overexpression vectors

A Mature miR-141, miR-200c and miR-Neg (non-targeting negative control) sequences. miR-141 and miR-200c are 78.3% identical. The seed sequences are highlighted in green and the one nucleotide difference between them, in pink. **B** Schematic representation of the lentiviral miRNA overexpression vectors that were used. The pre-miRNA sequence was inserted in the 1st intron of EF1a, under the control of the SFFV promoter and followed by tRFP.

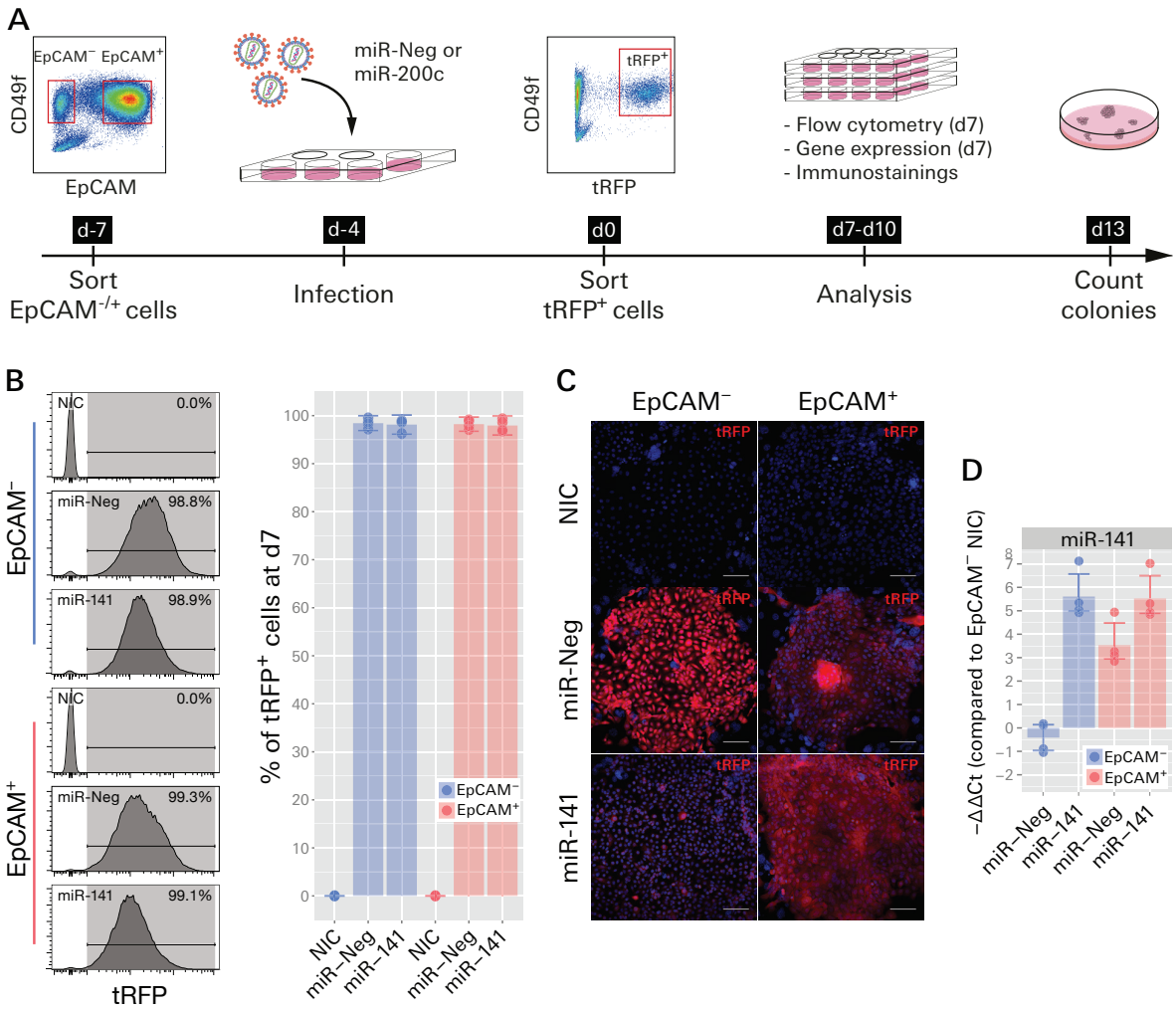

Figure 6.2 | miR-141 overexpression in the EpCAM⁻ and EpCAM⁺ hTEC subpopulations

A Schematic representation of the experimental design used to analyze the effects of miR-141 overexpression in the EpCAM⁻ and EpCAM⁺ hTEC subpopulations. EpCAM⁻ and EpCAM⁺ hTECs were isolated by FACS. 3 days later, they were transduced with miR-141 or miR-Neg lentiviral overexpression vectors. tRFP⁺ infected cells were isolated by FACS 4 days after infection using the gate depicted in red and re-cultured in the appropriate vessels for subsequent analyses. **B** The proportion of tRFP⁺ infected cells within the CD49f⁺ population was measured one week after the sort by flow cytometry (n=4). Error bars: 95% Student t-test confidence interval. Left: proportion of tRFP⁺ cells for one representative experiment. **C** Confocal fluorescence images of tRFP expression obtained from one representative experiment. Images were acquired as z-stacks and maximum intensity projections from one representative experiment are presented. Scale bar = 100µm. **D** RT-qPCR gene expression analysis of miR-141 (n=4). -ΔΔCt: $\log_2$(relative quantity compared to EpCAM⁻ NIC). Error bars: 95% Student t-test confidence interval. NIC: non-infected control.

culture, the cell populations transduced with miR-141 were still more than 95% pure, as marked by the expression of tRFP, whereas no tRFP signal could be detected in the non-infected controls (Fig. 6.2b & c). Moreover, the cells infected with the miR-141 lentiviral vector did overexpress miR-141 (64.9x for EpCAM⁻ and 4x for EpCAM⁺, compared to their respective miR-Neg controls) (Fig. 6.2d). Importantly, as mentioned previously, no noticeable difference was observed between the non-infected and miR-Neg controls in any of the following experiments.

After 13 days, the colonies in the colony-forming efficiency assay dishes from all tested conditions were counted. Although it was not statistically significant, miR-141 overexpression appeared to induce a variable increase in the proportion of stratified colonies

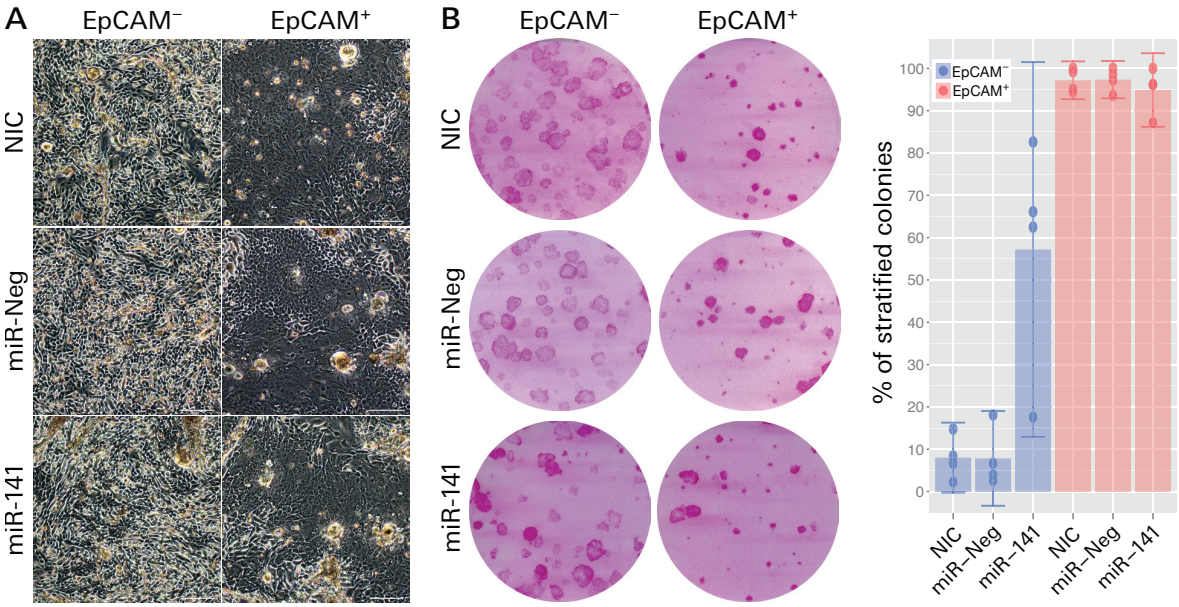

Figure 6.3 | miR-141 overexpression induces stratification only in a fraction of the EpCAM⁻ hTECs

A Phase contrast images from one representative experiment. Scale bar = 100µm. **B** The proportion of stratified colonies was measured by counting the colonies in the colony-forming efficiency assays. miR-141, but not miR-Neg, induced stratification in a variable fraction of the EpCAM⁻ hTEC subpopulation (n=4). Left: colony-forming efficiency assay dishes stained with Rhodamine B, from one representative experiment. Right: Colony-forming efficiency assays were always made in duplicate; each dot represents the average of the two dishes. Error bars: 95% Student t-test confidence interval.

present in the EpCAM⁻ dishes (from 7.8% to 57% on average), while the non-targeting control did not (Fig. 6.3a & b). On the other hand, the EpCAM⁺ cells remained relatively unaffected by miR-141 overexpression (Fig. 6.3a & b). Strangely, miR-141 overexpression also seemed to increase the proliferation rate of infected EpCAM⁻ cells. Indeed, most of the time, colonies were larger in the dishes containing miR-141-overexpress-

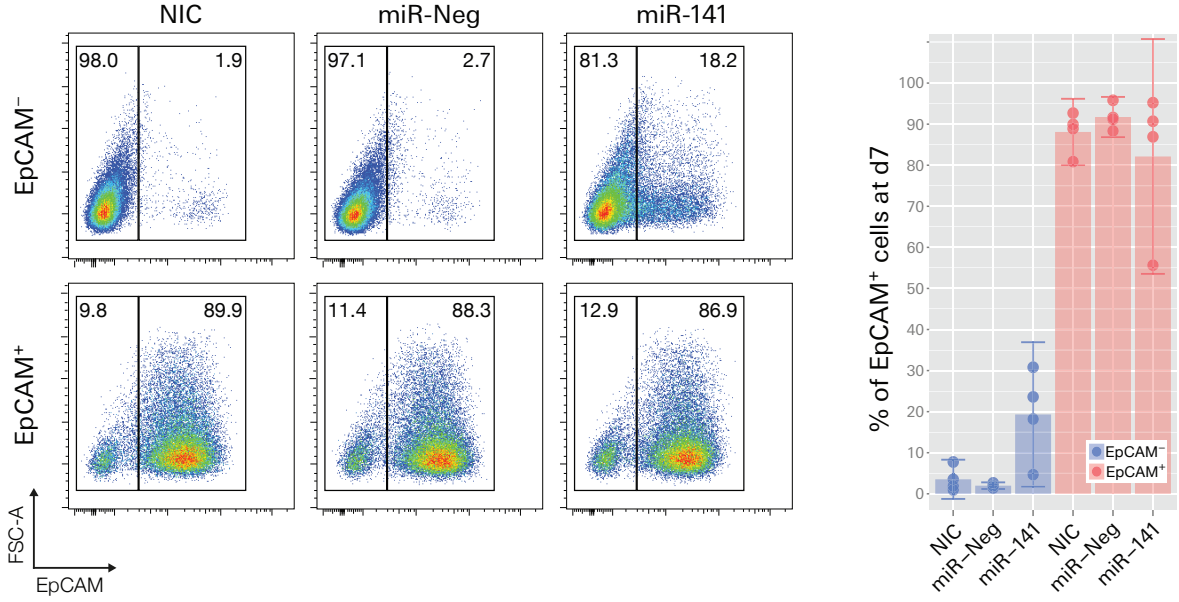

Figure 6.4 | miR-141 overexpression did not dramatically activate EpCAM expression

The proportion of EpCAM⁺ infected cells in the CD49f⁺ population was measured by flow cytometry (n=4). Left: flow cytometry plots and gates from one representative experiment. Error bars: 95% Student t-test confidence interval.

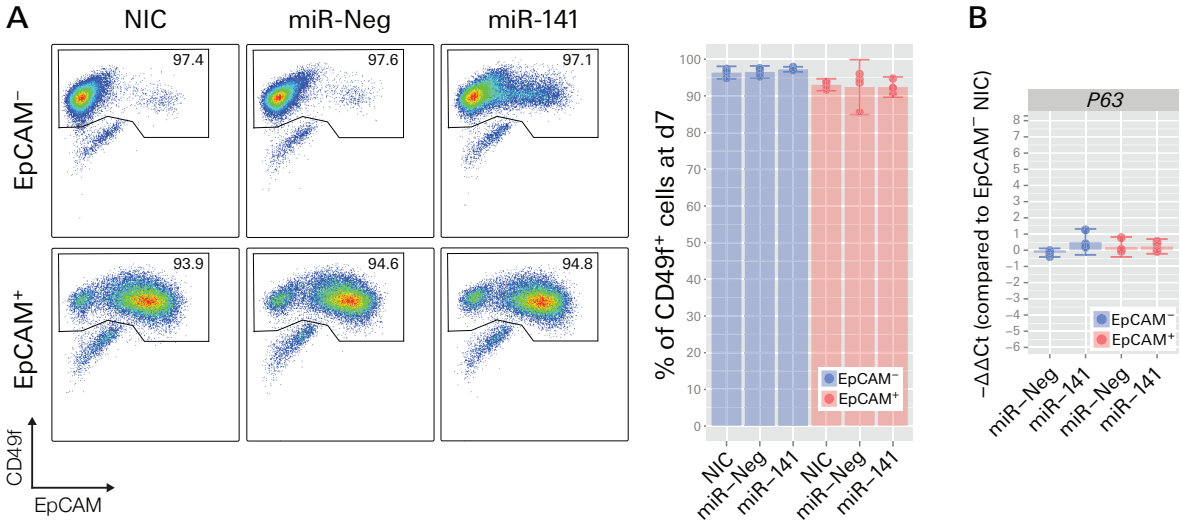

Figure 6.5 | The basal epithelial identity of cultured hTECs is not affected by miR-141 overexpression
A The proportion of CD49f⁺ was measured by flow cytometry. It was not affected by the overexpression of miR-141. Error bars: 95% Student t-test confidence interval. Left: flow cytometry plots and gates from one representative experiment. **B** RT-qPCR gene expression analysis of *P63* (n=4). -ΔΔCt: $\log_2$(relative quantity compared to EpCAM⁻ NIC). Error bars: 95% Student t-test confidence interval. NIC: non-infected control.

ing cells than in the negative controls and, when expanded, these cells were generally faster to reach confluency (data not shown). Thus, it is likely that, on top of favoring stratification, miR-141 also boosts the proliferative capacity of the infected cells through an unknown mechanism.

Surprisingly, given the results obtained with miR-200c, miR-141 overexpression in the EpCAM⁻ subpopulation only induced a small increase in the proportion of EpCAM⁺ cells from 2% to 19.3% (Fig. 6.4). In one case, miR-141 overexpression even appeared to significantly lower the proportion of EpCAM⁺ cells in the EpCAM⁺ subpopulation (Fig. 6.4). miR-141 overexpression also upregulated *EpCAM* at the RNA level in the EpCAM⁻ subpopulation (Fig. 6.6), although not as far as reaching the levels observed in EpCAM⁺ cells. On the other hand, miR-141 overexpression appeared not to affect the basal epithelial identity of the infected cells, as shown by the proportion of CD49f⁺ cells (Fig. 6.5a) and by the expression level of *P63* (Fig.6.5b). This is similar to what was observed with miR-200c. Taken together, these results suggest that miR-141 overexpression is sufficient to convert only a minor fraction of the EpCAM⁻ hTEC subpopulation into stratifying EpCAM⁺ cells.

miR-141 fails to convert all the EpCAM⁻ hTEC subpopulation into EpCAM⁺ cells

We analyzed the effect of miR-141 overexpression on the expression of epidermal differentiation markers. As it was observed for *EpCAM*, it led to a slight upregulation of *K1, IVL, HOPX*, *FOXN1* and miR-203, but their expression systematically failed to reach the levels observed in the EpCAM⁺ subpopulation (Fig. 6.6). In this subpopulation, miR-141 overexpression did not have any effect on the expression of these genes (Fig. 6.6; Fig. 6.7a). The same is true for the markers of epithelial cell identity *CDH1* and miR-200c (Fig. 6.6; Fig. 6.7a). On the other hand, unlike what was observed with miR-200c, miR-141 overexpression failed to alter the expression of *VIM*, *ZEB1* and miR-429 (Fig. 6.6;

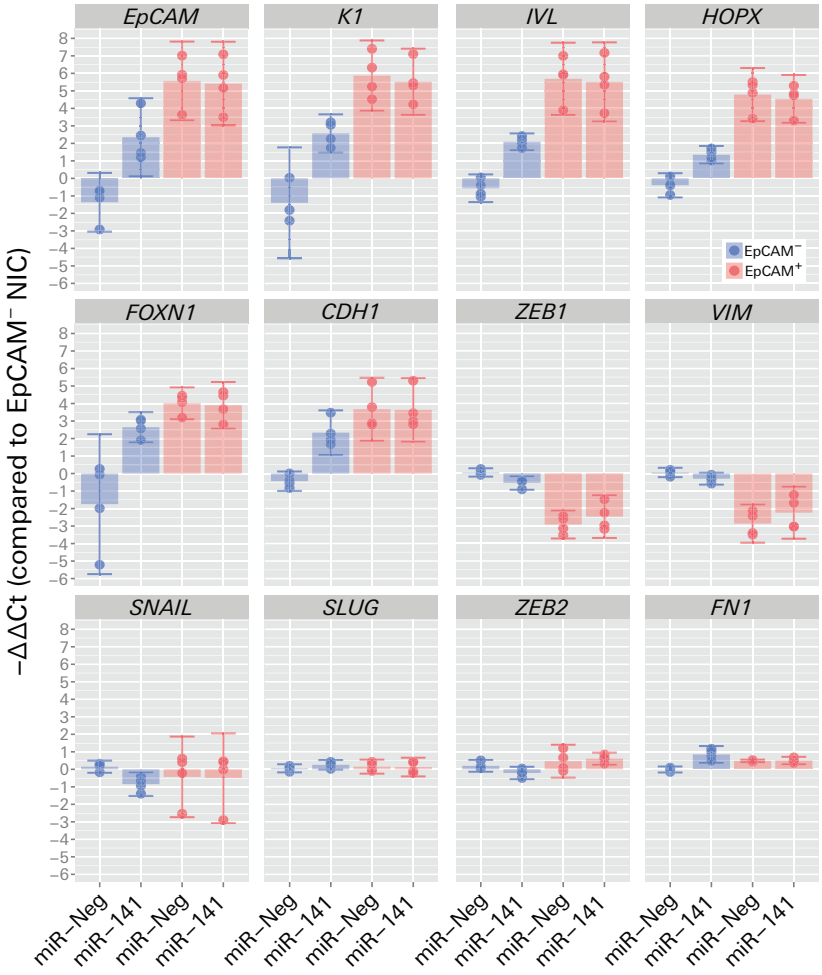

Figure 6.6 | miR-141 overexpression leads to an intermediate phenotype at the population level (I)

RT-qPCR gene expression analysis (n=4). -ΔΔCt: $\log_2$(relative quantity compared to EpCAM$^-$ NIC). Error bars: 95% Student t-test confidence interval. NIC: non-infected control.

Fig. 6.7a). Similarly, it appeared to have no effect on *EYA1* and *SIX1* expression both in the EpCAM$^-$ and EpCAM$^+$ subpopulations. In addition, as expected, miR-141 overexpression did not affect the expression of genes that were not differentially expressed between these two subpopulations, such as *ZEB2*, *SNAIL, SLUG, FN1,* miR-196a, miR-205 and miR-487b (Fig. 6.6; Fig. 6.7a). Overall, we believe that the intermediate phenotype displayed by the infected EpCAM$^-$ subpopulation can be easily explained by the fact that miR-141 overexpression converts only part of these cells into EpCAM$^+$ stratifying ones. This was observed at the protein level through immunostaining for EpCAM, K1, IVL, HOPX, CDH1, ZEB1 and VIM (data not shown). Upon miR-141 overexpression, although some colonies were of a mixed morphology containing both stratified and non-stratified cells, most colonies were of either one or the other group and were not distinguishable from the ones observed in the negative control EpCAM$^-$ or EpCAM$^+$ subpopulations. Then, at the population level, the small increase in the proportion of stratified colonies translates into a gene expression pattern found in-between the ones displayed by the EpCAM$^-$ and EpCAM$^+$ subpopulations.

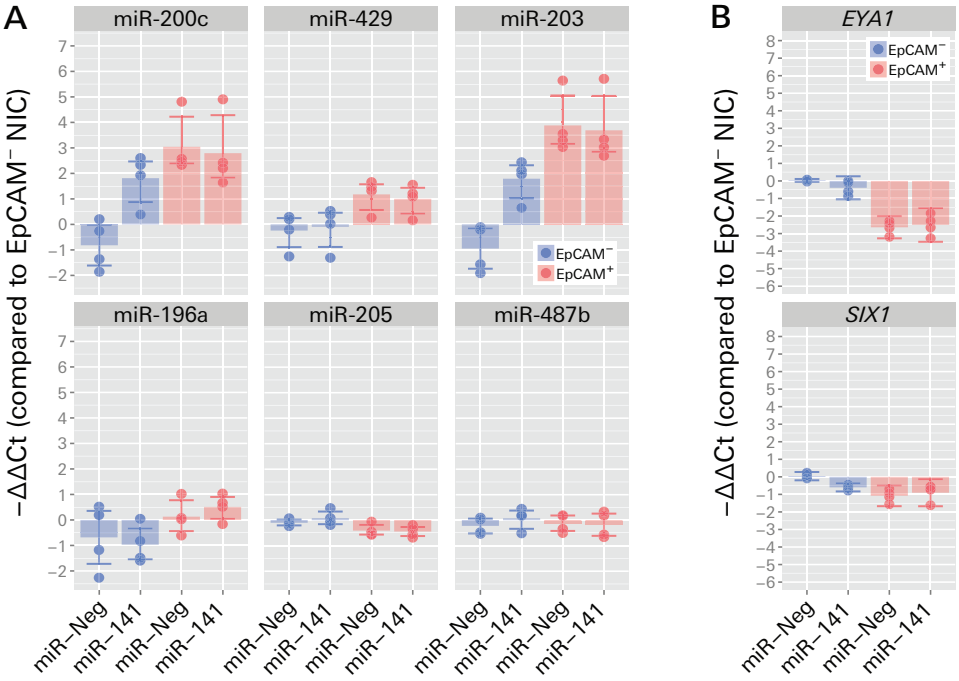

Figure 6.6 | miR-141 overexpression leads to an intermediate phenotype at the population level (II)

RT-qPCR gene expression analysis (n=4). -ΔΔCt: $\log_2$(relative quantity compared to EpCAM$^-$ NIC). Error bars: 95% Student t-test confidence interval. NIC: non-infected control.

7. Bibliography

Abramson, J., Giraud, M., Benoist, C. & Mathis, D. Aire's Partners in the Molecular Control of Immunological Tolerance. *Cell* **140,** 123–135 (2010).

Adam, R. C. *et al.* Pioneer factors govern super-enhancer dynamics in stem cell plasticity and lineage choice. *Nature* **521,** 366–370 (2015).

Anderson, G., Lane, P. J. L. & Jenkinson, E. J. Generating intrathymic microenvironments to establish T-cell tolerance. *Nat. Rev. Immunol.* **7,** 954–963 (2007).

Anderson, G. & Takahama, Y. Thymic epithelial cells: working class heroes for T cell development and repertoire selection. *Trends Immunol.* **33,** 256–263 (2012).

Anderson, M. S. *et al.* Projection of an immunological self shadow within the thymus by the aire protein. *Science* **298,** 1395–401 (2002).

Ansieau, S. *et al.* Induction of EMT by Twist Proteins as a Collateral Effect of Tumor-Promoting Inactivation of Premature Senescence. *Cancer Cell* **14,** 79–89 (2008).

Baik, S., Jenkinson, E. J., Lane, P. J. L., Anderson, G. & Jenkinson, W. E. Generation of both cortical and Aire + medullary thymic epithelial compartments from CD205 + progenitors. *Eur. J. Immunol.* **43,** 589–594 (2013).

Balciunaite, G. *et al.* Wnt glycoproteins regulate the expression of FoxN1, the gene defective in nude mice. *Nat. Immunol.* **3,** 1102–1108 (2002).

Barde, I. *et al.* A KRAB/KAP1-miRNA cascade regulates erythropoiesis through stage-specific control of mitophagy. *Science (80-.).* **340,** 350–3 (2013).

Barde, I., Salmon, P. & Trono, D. in *Current Protocols in Neuroscience* **Chapter 4,** Unit 4.21 (John Wiley & Sons, Inc., 2010).

Barrandon, Y. *et al.* Capturing epidermal stemness for regenerative medicine. *Semin. Cell Dev. Biol.* **23,** 937–944 (2012).

Barrandon, Y. & Green, H. Cell size as a determinant of the clone-forming ability of human keratinocytes. *Proc. Natl. Acad. Sci.* **82,** 5390–4 (1985).

Bartel, D. P. MicroRNAs: genomics, biogenesis, mechanism, and function. *Cell* **116,** 281–97 (2004).

Bartel, D. P. MicroRNAs: target recognition and regulatory functions. *Cell* **136,** 215–33 (2009).

Bennett, A. R. *et al.* Identification and characterization of thymic epithelial progenitor cells. *Immunity* **16,** 803–14 (2002).

Björses, P., Aaltonen, J., Horelli-Kuitunen, N., Yaspo, M. L. & Peltonen, L. Gene defect behind APECED: a new clue to autoimmunity. *Hum. Mol. Genet.* **7,** 1547–53 (1998).

Blackburn, C. C. *et al.* The nu gene acts cell-autonomously and is required for differentiation of thymic

epithelial progenitors. *Proc. Natl. Acad. Sci. U. S. A.* **93,** 5742–6 (1996).

Blackburn, C. C. & Manley, N. R. Developing a new paradigm for thymus organogenesis. *Nat. Rev. Immunol.* **4,** 278–289 (2004).

Blackburn, C. C. *et al.* One for all and all for one: thymic epithelial stem cells and regeneration. *Trends Immunol.* **23,** 391–5 (2002).

Blanpain, C., Lowry, W. E., Geoghegan, A., Polak, L. & Fuchs, E. Self-Renewal, Multipotency, and the Existence of Two Cell Populations within an Epithelial Stem Cell Niche. *Cell* **118,** 635–648 (2004).

Blechschmidt, K. *et al.* The mouse Aire gene: comparative genomic sequencing, gene organization, and expression. *Genome Res.* **9,** 158–66 (1999).

Bleul, C. C. & Boehm, T. BMP signaling is required for normal thymus development. *J. Immunol.* **175,** 5213–21 (2005).

Bleul, C. C. *et al.* Formation of a functional thymus initiated by a postnatal epithelial progenitor cell. *Nature* **441,** 992–996 (2006).

Bockman, D.E. & Kirby, M.L. Dependence of thymus development on derivatives of the neural crest. *Science* 498-500 (1984).

Bonfanti, P. *et al.* Microenvironmental reprogramming of thymic epithelial cells to skin multipotent stem cells. *Nature* **466,** 978–982 (2010).

Brabletz, S. & Brabletz, T. The ZEB/miR-200 feedback loop—a motor of cellular plasticity in development and cancer? *EMBO Rep.* **11,** 670–677 (2010).

Bracken, C. P. *et al.* A Double-Negative Feedback Loop between ZEB1-SIP1 and the microRNA-200 Family Regulates Epithelial-Mesenchymal Transition. *Cancer Res.* **68,** 7846–7854 (2008).

Bredenkamp, N., Nowell, C. S. & Blackburn, C. C. Regeneration of the aged thymus by a single transcription factor. *Development* **141,** 1627–1637 (2014).

Bullock, M. D., Sayan, A. E., Packham, G. K. & Mirnezami, A. H. MicroRNAs: critical regulators of epithelial to mesenchymal (EMT) and mesenchymal to epithelial transition (MET) in cancer progression. *Biol. Cell* **104,** 3–12 (2012).

Burk, U. *et al.* A reciprocal repression between ZEB1 and members of the miR-200 family promotes EMT and invasion in cancer cells. *EMBO Rep.* **9,** 582–9 (2008).

Byrne, C., Tainsky, M. & Fuchs, E. Programming gene expression in developing epidermis. *Development* **120,** 2369–83 (1994).

Cai, X., Hagedorn, C. H. & Cullen, B. R. Human microRNAs are processed from capped, polyadenylated transcripts that can also function as mRNAs. *RNA* **10,** 1957–66 (2004).

Candi, E., Amelio, I., Agostini, M. & Melino, G. MicroRNAs and p63 in epithelial stemness. *Cell Death Differ.* **22,** 12–21 (2015).

Carthew, R. W. & Sontheimer, E. J. Origins and Mechanisms of miRNAs and siRNAs. *Cell* **136,** 642–655 (2009).

Chang, C.-J. *et al.* p53 regulates epithelial–mesenchymal transition and stem cell properties through modulating miRNAs. *Nat. Cell Biol.* **13,** 1467–1467 (2011).

Chen, C., Zhang, Y., Zhang, L., Weakley, S. M. & Yao, Q. MicroRNA-196: critical roles and clinical applications in development and cancer. *J. Cell. Mol. Med.* **15,** 14–23 (2011).

Chen, L., Xiao, S. & Manley, N. R. Foxn1 is required to maintain the postnatal thymic microenvironment in a dosage-sensitive manner. *Blood* **113,** 567–574 (2009).

Chidgey, A., Dudakov, J., Seach, N. & Boyd, R. Impact of niche aging on thymic regeneration and immune reconstitution. *Semin. Immunol.* **19,** 331–340 (2007).

Claudinot, S., Nicolas, M., Oshima, H., Rochat, A. & Barrandon, Y. Long-term renewal of hair follicles from clonogenic multipotent stem cells. *Proc. Natl. Acad. Sci.* **102,** 14677–14682 (2005).

Cunningham, D.J. Textbook of Anatomy. *William Wood and Co.* (1903).

de Maagd, R. a *et al.* The human thymus microenvironment: heterogeneity detected by monoclonal anti-epithelial cell antibodies. *Immunology* **54,** 745–54 (1985).

Derbinski, J., Schulte, A., Kyewski, B. & Klein, L. Promiscuous gene expression in medullary thymic epithelial cells mirrors the peripheral self. *Nat. Immunol.* **2,** 1032–9 (2001).

Dong, C., Martinez, G. J. & T, C. T cells : the usual subsets. *Nat. Rev. Immunol.* **54,** 77030–77030 (2010).

Douek, D. C. *et al.* Changes in thymic function with age and during the treatment of HIV infection. *Nature* **396,** 690–5 (1998).

Droz-Georget Lathion, S. *et al.* A single epidermal stem cell strategy for safe ex vivo gene therapy. *EMBO Mol. Med.* **7,** 380–393 (2015).

Ebert, M. S. & Sharp, P. A. Roles for MicroRNAs in Conferring Robustness to Biological Processes. *Cell* **149,** 515–524 (2012).

Farley, a. M. *et al.* Dynamics of thymus organogenesis and colonization in early human development. *Development* **140,** 2015–2026 (2013).

Filipowicz, W., Bhattacharyya, S. N. & Sonenberg, N. Mechanisms of post-transcriptional regulation by microRNAs: are the answers in sight? *Nat. Rev. Genet.* **2008,** 102–114 (2008).

Fontemaggi, G. *et al.* The Transcriptional Repressor ZEB Regulates p73 Expression at the Crossroad between Proliferation and Differentiation. *Mol. Cell. Biol.* **21,** 8461–8470 (2001).

Fontemaggi, G. *et al.* δEF1 repressor controls selectively p53 family members during differentiation. *Oncogene* **24,** 7273–7280 (2005).

Frank, D. U. *et al.* An Fgf8 mouse mutant phenocopies human 22q11 deletion syndrome. *Development* **129,** 4591–603 (2002).

Friedman, R. C., Farh, K. K.-H., Burge, C. B. & Bartel, D. P. Most mammalian mRNAs are conserved targets of microRNAs. *Genome Res.* **19,** 92–105 (2008).

Fuchs, E. Skin stem cells: rising to the surface. *J. Cell Biol.* **180,** 273–284 (2008).

Fuchs, E. & Green, H. Changes in keratin gene expression during terminal differentiation of the keratinocyte. *Cell* **19,** 1033–1042 (1980).

Fuchs, E. & Raghavan, S. Getting under the skin of epidermal morphogenesis. *Nat. Rev. Genet.* **3,** 199–209 (2002).

Gallico, G. G., O'Connor, N. E., Compton, C. C., Kehinde, O. & Green, H. Permanent Coverage of Large Burn Wounds with Autologous Cultured Human Epithelium. *N. Engl. J. Med.* **311,** 448–451 (1984).

Gheldof, A., Hulpiau, P., van Roy, F., De Craene, B. & Berx, G. Evolutionary functional analysis and molecular regulation of the ZEB transcription factors. *Cell. Mol. Life Sci.* **69,** 2527–2541 (2012).

Gill, J., Malin, M., Holländer, G. A. & Boyd, R. Generation of a complete thymic microenvironment by MTS24+ thymic epithelial cells. *Nat. Immunol.* **3,** 635–642 (2002).

Gonzalez, D. M. & Medici, D. Signaling mechanisms of the epithelial-mesenchymal transition. *Sci. Signal.* **7,** re8–re8 (2014).

Gordon, J., Bennett, a R., Blackburn, C. C. & Manley, N. R. Gcm2 and Foxn1 mark early parathyroid- and thymus-specific domains in the developing third pharyngeal pouch. *Mech. Dev.* **103,** 141–3 (2001).

Gordon, J. & Manley, N. R. Mechanisms of thymus organogenesis and morphogenesis. *Development* **138,** 3865–3878 (2011).

Gordon, J. *et al.* Functional evidence for a single endodermal origin for the thymic epithelium. *Nat. Immunol.* **5,** 546–553 (2004).

Gray, D. H. D., Chidgey, a P. & Boyd, R. L. Analysis of thymic stromal cell populations using flow cytometry. *J. Immunol. Methods* **260,** 15–28 (2002).

Gray, D. H. D. *et al.* Developmental kinetics, turnover, and stimulatory capacity of thymic epithelial cells. *Blood* **108,** 3777–3785 (2006).

Gregory, P. a *et al.* The miR-200 family and miR-205 regulate epithelial to mesenchymal transition by targeting ZEB1 and SIP1. *Nat. Cell Biol.* **10,** 593–601 (2008a).

Gregory, P. a *et al.* An autocrine TGF- /ZEB/miR-200 signaling network regulates establishment and maintenance of epithelial-mesenchymal transition. *Mol. Biol. Cell* **22,** 1686–1698 (2011).

Gregory, P. A., Bracken, C. P., Bert, A. G. & Goodall, G. J. MicroRNAs as regulators of epithelial-mesenchymal transition. *Cell Cycle* **7,** 3112–3117 (2008b).

Gurtan, A. M. & Sharp, P. a. The Role of miRNAs in Regulating Gene Expression Networks. *J. Mol. Biol.* **425,** 3582–3600 (2013).

Ha, M. & Kim, V. N. Regulation of microRNA biogenesis. *Nat. Rev. Mol. Cell Biol.* **15,** 509–524 (2014).

Hale, L. P. & Markert, M. L. Corticosteroids regulate epithelial cell differentiation and Hassall body formation in the human thymus. *J. Immunol.* **172,** 617–24 (2004).

Hamazaki, Y. *et al.* Medullary thymic epithelial cells expressing Aire represent a unique lineage derived from cells expressing claudin. *Nat. Immunol.* **8,** 304–311 (2007).

Hauri-Hohl, M., Zuklys, S., Holländer, G. a & Ziegler, S. F. A regulatory role for TGF-β signaling in the establishment and function of the thymic medulla. *Nat. Immunol.* **15,** 554–61 (2014).

Hay, E.D. Organization and fine structure of epithelium and mesenchyme in the developing chick embryos. *Epithelial-Mesenchymal Interactions: 18th Hahnemann Symposium.* 31–35 (1968).

Haynes, B. F., Markert, M. L., Sempowski, G. D., Patel, D. D. & Hale, L. P. The Role of the Thymus in Immune Reconstitution in Aging, Bone Marrow Transplantation, and HIV-1 Infection. *Annu. Rev. Immunol.* **18,** 529–560 (2000).

Heinzel, K., Benz, C., Martins, V. C., Haidl, I. D. & Bleul, C. C. Bone Marrow-Derived Hemopoietic Precursors Commit to the T Cell Lineage Only after Arrival in the Thymic Microenvironment. *J. Immunol.* **178,** 858–868 (2007).

Hetzer-Egger, C. *et al.* Thymopoiesis requires Pax9 function in thymic epithelial cells. *Eur. J. Immunol.* **32,** 1175–81 (2002).

Higashi, Y. *et al.* Impairment of T cell development in deltaEF1 mutant mice. *J. Exp. Med.* **185,** 1467–79 (1997).

Hogquist, K. a, Baldwin, T. a & Jameson, S. C. Central tolerance: learning self-control in the thymus. *Nat. Rev. Immunol.* **5,** 772–782 (2005).

Hong, T. *et al.* An Ovol2-Zeb1 Mutual Inhibitory Circuit Governs Bidirectional and Multi-step Transition between Epithelial and Mesenchymal States. *PLOS Comput. Biol.* **11,** e1004569 (2015).

Huntzinger, E. & Izaurralde, E. Gene silencing by microRNAs: contributions of translational repression and mRNA decay. *Nat. Rev. Genet.* **12,** 99–110 (2011).

Hurteau, G. J., Carlson, J. A., Spivack, S. D. & Brock, G. J. Overexpression of the MicroRNA hsa-miR-200c Leads to Reduced Expression of Transcription Factor 8 and Increased Expression of E-Cadherin. *Cancer Res.* **67,** 7972–7976 (2007).

Itoi, M., Tsukamoto, N., Yoshida, H. & Amagai, T. Mesenchymal cells are required for functional development of thymic epithelial cells. *Int. Immunol.* **19,** 953–964 (2007).

Janes, S. M., Ofstad, T. a, Campbell, D. H., Watt, F. M. & Prowse, D. M. Transient activation of FOXN1 in keratinocytes induces a transcriptional programme that promotes terminal differentiation: contrasting roles of FOXN1 and Akt. *J. Cell Sci.* **117,** 4157–68 (2004).

Jenkinson, W. E., Jenkinson, E. J. & Anderson, G. Differential Requirement for Mesenchyme in the Proliferation and Maturation of Thymic Epithelial Progenitors. *J. Exp. Med.* **198,** 325–332 (2003).

Jerome, L. a & Papaioannou, V. E. DiGeorge syndrome phenotype in mice mutant for the T-box gene, Tbx1. *Nat. Genet.* **27,** 286–91 (2001).

Jonas, S. & Izaurralde, E. Towards a molecular understanding of microRNA-mediated gene silencing. *Nat. Rev. Genet.* **16,** 421–433 (2015).

Kalluri, R. & Weinberg, R. A. The basics of epithelial-mesenchymal transition. *J. Clin. Invest.* **119,** 1420–1428 (2009).

Khan, I. S., Taniguchi, R. T., Fasano, K. J., Anderson, M. S. & Jeker, L. T. Canonical microRNAs in thymic epithelial cells promote central tolerance. *Eur. J. Immunol.* **44,** 1313–9 (2014).

Khan, I. S. *et al.* Identification of MiR-205 As a MicroRNA That Is Highly Expressed in Medullary Thymic Epithelial Cells. *PLoS One* **10,** e0135440 (2015).

Kim, T. *et al.* p53 regulates epithelial-mesenchymal transition through microRNAs targeting ZEB1 and ZEB2. *J. Exp. Med.* **208,** 875–883 (2011).

Kim, V. N., Han, J. & Siomi, M. C. Biogenesis of small RNAs in animals. *Nat. Rev. Mol. Cell Biol.* **10,** 126–139 (2009).

Kitamura, K. *et al.* MiR-134/487b/655 Cluster Regulates TGF- -Induced Epithelial-Mesenchymal Transition and Drug Resistance to Gefitinib by Targeting MAGI2 in Lung Adenocarcinoma Cells. *Mol. Cancer Ther.* **13,** 444–453 (2014).

Klein, L., Hinterberger, M., Wirnsberger, G. & Kyewski, B. Antigen presentation in the thymus for positive selection and central tolerance induction. *Nat. Rev. Immunol.* **9,** 833–844 (2009).

Klein, L., Kyewski, B., Allen, P. M. & Hogquist, K. a. Positive and negative selection of the T cell repertoire: what thymocytes see (and don't see). *Nat. Rev. Immunol.* 1–15 (2014). doi:10.1038/nri3667

Klug, D. B. *et al.* Interdependence of cortical thymic epithelial cell differentiation and T-lineage commitment. *Proc. Natl. Acad. Sci.* **95,** 11822–7 (1998).

Klug, D. B., Carter, C., Gimenez-Conti, I. B. & Richie, E. R. Thymocyte-Independent and Thymocyte-Dependent Phases of Epithelial Patterning in the Fetal Thymus. *J. Immunol.* **169,** 2842–2845 (2002).

Knouf, E. C. *et al.* An integrative genomic approach identifies p73 and p63 as activators of miR-200 microRNA family transcription. *Nucleic Acids Res.* **40,** 499–510 (2012).

Koch, U. & Radtke, F. Mechanisms of T Cell Development and Transformation. *Annu. Rev. Cell Dev. Biol.* **27,** 539–562 (2011).

Kolesnikoff, N. *et al.* Specificity Protein 1 (Sp1) Maintains Basal Epithelial Expression of the miR-200 Family: implications for epithelial-mesenchymal transition. *J. Biol. Chem.* **289,** 11194–11205 (2014).

Korpal, M., Lee, E. S., Hu, G. & Kang, Y. The miR-200 Family Inhibits Epithelial-Mesenchymal Transition and Cancer Cell Migration by Direct Targeting of E-cadherin Transcriptional Repressors ZEB1 and ZEB2. *J. Biol. Chem.* **283,** 14910–14914 (2008).

Krol, J., Loedige, I. & Filipowicz, W. The widespread regulation of microRNA biogenesis, function and decay. *Nat. Rev. Genet.* **11,** 597–610 (2010).

Kudo-Saito, C., Shirako, H., Takeuchi, T. & Kawakami, Y. Cancer Metastasis Is Accelerated through Immunosuppression during Snail-Induced EMT of Cancer Cells. *Cancer Cell* **15,** 195–206 (2009).

Lamouille, S., Xu, J. & Derynck, R. Molecular mechanisms of epithelial–mesenchymal transition. *Nat. Rev. Mol. Cell Biol.* **15,** 178–196 (2014).

Langbein, L. *et al.* Tight junction-related structures in the absence of a lumen: occludin, claudins and tight junction plaque proteins in densely packed cell formations of stratified epithelia and squamous cell carcinomas. *Eur. J. Cell Biol.* **82,** 385–400 (2003).

Le Douarin, N. M. & Jotereau, F. V. Tracing of cells of the avian thymus through embryonic life in interspecific chimeras. *J. Exp. Med.* **142,** 17–40 (1975).

Lee, B. *et al.* Transcriptional mechanisms link epithelial plasticity to adhesion and differentiation of epidermal progenitor cells. *Dev. Cell* **29,** 47–58 (2014).

Lee, R. C., Feinbaum, R. L. & Ambros, V. The C. elegans heterochronic gene lin-4 encodes small RNAs with antisense complementarity to lin-14. *Cell* **75,** 843–54 (1993).

Lee, Y., Jeon, K., Lee, J.-T., Kim, S. & Kim, V. N. MicroRNA maturation: stepwise processing and subcellular localization. *EMBO J.* **21,** 4663–70 (2002).

Lee, Y. *et al.* MicroRNA genes are transcribed by RNA polymerase II. *EMBO J.* **23,** 4051–4060 (2004).

Lena, a M. *et al.* miR-203 represses 'stemness' by repressing DeltaNp63. *Cell Death Differ.* **15,** 1187–95 (2008).

Lim, J. & Thiery, J. P. Epithelial-mesenchymal transitions: insights from development. *Development* **139,** 3471–3486 (2012).

Liston, A., Lesage, S., Wilson, J., Peltonen, L. & Goodnow, C. C. Aire regulates negative selection of organ-specific T cells. *Nat. Immunol.* **4,** 350–354 (2003).

Liu, Y., El-Naggar, S., Darling, D. S., Higashi, Y. & Dean, D. C. Zeb1 links epithelial-mesenchymal transition and cellular senescence. *Development* **135,** 579–588 (2008).

Lobach, D. F. & Haynes, B. F. Ontogeny of the human thymus during fetal development. *J. Clin. Immunol.* **7,** 81–97 (1987).

Lynch, H. E. *et al.* Thymic involution and immune reconstitution. *Trends Immunol.* **30,** 366–373 (2009).

Maggioni, M. Molecular and functional characterization of clonogenic human thymic epithelial cells. *EPFL PhD thesis* (2012).

Mani, S. a. *et al.* The Epithelial-Mesenchymal Transition Generates Cells with Properties of Stem Cells. *Cell* **133,** 704–715 (2008).

Manley, N. R. & Capecchi, M. R. The role of Hoxa-3 in mouse thymus and thyroid development. *Development* **121,** 1989–2003 (1995).

Manley, N. R. & Blackburn, C. C. A developmental look at thymus organogenesis: where do the non-hematopoietic cells in the thymus come from? *Curr. Opin. Immunol.* **15,** 225–232 (2003).

Manley, N. R. & Condie, B. G. in *Progress in Molecular Biology and Translational Science* **92,** 103–120 (Elsevier, 2010).

Markert, M. L. *et al.* Transplantation of Thymus Tissue in Complete DiGeorge Syndrome. *N. Engl. J. Med.* **341,** 1180–1189 (1999).

Mascré, G. *et al.* Distinct contribution of stem and progenitor cells to epidermal maintenance. *Nature* **489,** 257–262 (2012).

Mathis, D. & Benoist, C. Aire. *Annu. Rev. Immunol.* **27,** 287–312 (2009).

Miller, J. Immunological function of the thymus. *Lancet* 748–749 (1961).

Miller, J. F. A. P. The discovery of thymus function and of thymus-derived lymphocytes. *Immunol. Rev.* **185,** 7–14 (2002).

Miller, J. F. A. P. Immunological function of the thymus. *Lancet* **278,** 748–749 (1961).

Miller, J. F. A. P. Immunological Significance of the Thymus of the Adult Mouse. *Nature* **195,** 1318–1319 (1962).

Miller, J. F. A. P. Effect of Neonatal Thymectomy on the Immunological Responsiveness of the Mouse. *Proc. R. Soc. B Biol. Sci.* **156,** 415–428 (1962).

Mills, A. a *et al.* p63 is a p53 homologue required for limb and epidermal morphogenesis. *Nature* **398,** 708–13 (1999).

Miyoshi, T. *et al.* Complementary expression pattern ofZfhx1 genesSip1 andδEF1 in the mouse embryo and their genetic interaction revealed by compound mutants. *Dev. Dyn.* **235,** 1941–1952 (2006).

Moes, M. *et al.* A Novel Network Integrating a miRNA-203/SNAI1 Feedback Loop which Regulates Epithelial to Mesenchymal Transition. *PLoS One* **7,** e35440 (2012).

Moore-Scott, B. a & Manley, N. R. Differential expression of Sonic hedgehog along the anterior–posterior axis regulates patterning of pharyngeal pouch endoderm and pharyngeal endoderm-derived organs. *Dev. Biol.* **278,** 323–335 (2005).

Moreno-Bueno, G. *et al.* The morphological and molecular features of the epithelial-to-mesenchymal transition. *Nat. Protoc.* **4,** 1591–1613 (2009).

Mukherji, S. *et al.* MicroRNAs can generate thresholds in target gene expression. *Nat. Genet.* **43,** 854–859 (2011).

Murata, S. *et al.* Regulation of CD8+ T Cell Development by Thymus-Specific Proteasomes. *Science.* **316,** 1349–1353 (2007).

Nehls, M., Pfeifer, D., Schorpp, M., Hedrich, H. & Boehm, T. New member of the winged-helix protein family disrupted in mouse and rat nude mutations. *Nature* **372,** 103–107 (1994).

Nelson, A. J., Dunn, R. J., Peach, R., Aruffo, A. & Farr, A. G. The murine homolog of human Ep-CAM, a homotypic adhesion molecule, is expressed by thymocytes and thymic epithelial cells. *Eur. J. Immunol.* **26,** 401–408 (1996).

Nieto, M. A. The Ins and Outs of the Epithelial to Mesenchymal Transition in Health and Disease. *Annu. Rev. Cell Dev. Biol.* **27,** 347–376 (2011).

Nieto, M. A. & Cano, A. The epithelial–mesenchymal transition under control: Global programs to regulate epithelial plasticity. *Semin. Cancer Biol.* **22,** 361–368 (2012).

Nitta, T. *et al.* Thymoproteasome Shapes Immunocompetent Repertoire of CD8+ T Cells. *Immunity* **32,** 29–40 (2010).

Nitta, T., Ohigashi, I., Nakagawa, Y. & Takahama, Y. Cytokine crosstalk for thymic medulla formation. *Curr. Opin. Immunol.* **23,** 190–197 (2011).

O'Connor, N., Mulliken, J., Banks-Schlegel, S., Kehinde, O. & Green, H. Grafting of burns with cultured epithelium prepared from autologous epidermal cells. *Lancet* **317,** 75–78 (1981).

Ohigashi, I. *et al.* Aire-expressing thymic medullary epithelial cells originate from 5t-expressing progenitor cells. *Proc. Natl. Acad. Sci.* **110,** 9885–9890 (2013).

Org, T. *et al.* The autoimmune regulator PHD finger binds to non-methylated histone H3K4 to activate gene expression. *EMBO Rep.* **9,** 370–376 (2008).

Papadopoulou, A. S. *et al.* The thymic epithelial microRNA network elevates the threshold for infection-associated thymic involution via miR-29a mediated suppression of the IFN-α receptor. *Nat. Immunol.* **13,** 181–187 (2011).

Pasquinelli, A. E. MicroRNAs and their targets: recognition, regulation and an emerging reciprocal relationship. *Nat. Rev. Genet.* **13,** 271–282 (2012).

Patel, D. D., Whichard, L. P., Radcliff, G., Denning, S. M. & Haynes, B. F. Characterization of human thymic epithelial cell surface antigens: Phenotypic similarity of thymic epithelial cells to epidermal keratinocytes. *J. Clin. Immunol.* **15,** 80–92 (1995).

Peinado, H., Olmeda, D. & Cano, A. Snail, Zeb and bHLH factors in tumour progression: an alliance against the epithelial phenotype? *Nat. Rev. Cancer* **7,** 415–428 (2007).

Pellegrini, G. *et al.* p63 identifies keratinocyte stem cells. *Proc. Natl. Acad. Sci.* **98,** 3156–3161 (2001).

Peterson, P., Org, T. & Rebane, A. Transcriptional regulation by AIRE: molecular mechanisms of central tolerance. *Nat. Rev. Immunol.* **8,** 948–957 (2008).

Piersol, G.A. Human Anatomy. *J. B. Lippincott Company* (1908).

Popa, I. *et al.* Regeneration of the adult thymus is preceded by the expansion of K5+K8+ epithelial cell progenitors and by increased expression of Trp63, cMyc and Tcf3 transcription factors in the thymic stroma. *Int. Immunol.* **19,** 1249–1260 (2007).

Postigo, A. A., Depp, J. L., Taylor, J. J. & Kroll, K. L. Regulation of Smad signaling through a differential recruitment of coactivators and corepressors by ZEB proteins. *EMBO J.* **22,** 2453–62 (2003).

Puisieux, A., Brabletz, T. & Caramel, J. Oncogenic roles of EMT-inducing transcription factors. *Nat. Cell Biol.* **16,** 488–494 (2014).

Purnama, C., Camous, X. & Larbi, A. An Overview of T Cell Subsets and Their Potential Use as Markers of Immunological Ageing. *Int. Trends Immun.* **1,** 21–32 (2013).

R Core Team. R: A language and environment for statistical computing. *R Foundation for Statistical Computing, Vienna, Austria. URL* https://www.R-project.org/ (2015).

Revest, J.-M., Suniara, R. K., Kerr, K., Owen, J. J. T. & Dickson, C. Development of the Thymus Requires Signaling Through the Fibroblast Growth Factor Receptor R2-IIIb. *J. Immunol.* **167,** 1954–1961 (2001).

Rheinwald, J. G. & Green, H. Serial Cultivation of Human Epidermal Keratinocytes: the Formation of Keratinizing Colonies from Single Cells. *Cell* **6,** 331–344 (1975).

Ritter, M. a & Palmer, D. B. The human thymic microenvironment: new approaches to functional analysis. *Semin. Immunol.* **11,** 13–21 (1999).

Roberts, N. & Horsley, V. Developing stratified epithelia: lessons from the epidermis and thymus. *Wiley Interdiscip. Rev. Dev. Biol.* **3,** 389–402 (2014).

Rochat, A., Kobayashi, K. & Barrandon, Y. Location of stem cells of human hair follicles by clonal analysis. *Cell* **76,** 1063–73 (1994).

Rochat, A., Grasset, N., Gorostidi, F., Lathion, S. & Barrandon, Y. in *Handbook of Stem Cells* 767–780 (Elsevier, 2013). doi:10.1016/B978-0-12-385942-6.00065-2

Rode, I. & Boehm, T. Regenerative capacity of adult cortical thymic epithelial cells. *Proc. Natl. Acad. Sci.* **109,** 3463–3468 (2012).

Rodewald, H.-R. Thymus organogenesis. *Annu. Rev. Immunol.* **26,** 355–88 (2008).

Rodewald, H.-R., Paul, S., Haller, C., Bluethmann, H. & Blum, C. Thymus medulla consisting of epithelial islets each derived from a single progenitor. *Nature* **414,** 763–768 (2001).

Rossi, S. W., Jenkinson, W. E., Anderson, G. & Jenkinson, E. J. Clonal analysis reveals a common progenitor for thymic cortical and medullary epithelium. *Nature* **441,** 988–991 (2006).

Rossi, S. W. *et al.* RANK signals from CD4+3 inducer cells regulate development of Aire-expressing epithelial cells in the thymic medulla. *J. Exp. Med.* **204,** 1267–1272 (2007a).

Rossi, S. W. *et al.* Redefining epithelial progenitor potential in the developing thymus. *Eur. J. Immunol.* **37,** 2411–2418 (2007c).

Rossi, S. W. *et al.* Keratinocyte growth factor (KGF) enhances postnatal T-cell development via enhancements in proliferation and function of thymic epithelial cells. *Blood* **109,** 3803–3811 (2007b).

Rothenberg, E. V. T Cell Lineage Commitment: Identity and Renunciation. *J. Immunol.* **186,** 6649–6655 (2011).

Sayed, D. & Abdellatif, M. MicroRNAs in Development and Disease. *Physiol. Rev.* **91,** 827–887 (2011).

Schindelin, J. *et al.* Fiji: an open-source platform for biological-image analysis. *Nat. Methods* **9,** 676–682 (2012).

Sekai, M., Hamazaki, Y. & Minato, N. Medullary Thymic Epithelial Stem Cells Maintain a Functional Thymus to Ensure Lifelong Central T Cell Tolerance. *Immunity* **41,** 753–761 (2014).

Senoo, M., Pinto, F., Crum, C. P. & McKeon, F. p63 Is Essential for the Proliferative Potential of Stem Cells in Stratified Epithelia. *Cell* **129,** 523–536 (2007).

Serwold, T., Richie Ehrlich, L. I. & Weissman, I. L. Reductive isolation from bone marrow and blood implicates common lymphoid progenitors as the major source of thymopoiesis. *Blood* **113,** 807–815 (2009).

Shakib, S. *et al.* Checkpoints in the Development of Thymic Cortical Epithelial Cells. *J. Immunol.* **182,** 130–137 (2009).

Shirley, S. H., Hudson, L. G., He, J. & Kusewitt, D. F. The skinny on slug. *Mol. Carcinog.* **49,** 851–861 (2010).

Smith, A. A glossary for stem-cell biology. *Nature* **441,** 1060–1060 (2006).

Spaderna, S. *et al.* The Transcriptional Repressor ZEB1 Promotes Metastasis and Loss of Cell Polarity in Cancer. *Cancer Res.* **68,** 537–544 (2008).

Stark, K., Vainio, S., Vassileva, G. & McMahon, A. P. Epithelial transformation of metanephric mesenchyme in the developing kidney regulated by Wnt-4. *Nature* **372**, 679–683 (1994).

Su, D., Navarre, S., Oh, W., Condie, B. G. & Manley, N. R. A domain of Foxn1 required for crosstalk-dependent thymic epithelial cell differentiation. *Nat. Immunol.* **4,** 1128–1135 (2003).

Sutherland, J. S. *et al.* Activation of thymic regeneration in mice and humans following androgen blockade. *J. Immunol.* **175,** 2741–53 (2005).

Takagi, T., Moribe, H., Kondoh, H. & Higashi, Y. DeltaEF1, a zinc finger and homeodomain transcription factor, is required for skeleton patterning in multiple lineages. *Development* **125,** 21–31 (1998).

Takahama, Y. Journey through the thymus: stromal guides for T-cell development and selection. *Nat. Rev. Immunol.* **6,** 127–35 (2006).

Teta, M. *et al.* Inducible deletion of epidermal Dicer and Drosha reveals multiple functions for miRNAs in postnatal skin. *Development* **139,** 1405–1416 (2012).

Thiery, J. P., Acloque, H., Huang, R. Y. J. & Nieto, M. A. Epithelial-Mesenchymal Transitions in Development and Disease. *Cell* **139,** 871–890 (2009).

Turner, F. E. *et al.* Slug Regulates Integrin Expression and Cell Proliferation in Human Epidermal Keratinocytes. *J. Biol. Chem.* **281,** 21321–21331 (2006).

Ucar, O. & Rattay, K. Promiscuous Gene Expression in the Thymus: A Matter of Epigenetics, miRNA, and More? *Front. Immunol.* **6,** 1–7 (2015).

Ucar, O., Tykocinski, L.-O., Dooley, J., Liston, A. & Kyewski, B. An evolutionarily conserved mutual interdependence between Aire and microRNAs in promiscuous gene expression. *Eur. J. Immunol.* **43,** 1769–78 (2013).

Van de Putte, T. *et al.* Mice Lacking Zfhx1b, the Gene That Codes for Smad-Interacting Protein-1, Reveal a Role for Multiple Neural Crest Cell Defects in the Etiology of Hirschsprung Disease–Mental Retardation Syndrome. *Am. J. Hum. Genet.* **72,** 465–470 (2003).

van de Wijngaert, F. P., Kendall, M. D., Schuurman, H. J., Rademakers, L. H. & Kater, L. Heterogeneity of epithelial cells in the human thymus. An ultrastructural study. *Cell Tissue Res.* **237,** 227–37 (1984).

van Ewijk, W., Holländer, G., Terhorst, C. & Wang, B. Stepwise development of thymic microenvironments in vivo is regulated by thymocyte subsets. *Development* **127,** 1583–91 (2000).

van Ewijk, W. *et al.* Thymic microenvironments, 3-D versus 2-D? *Semin. Immunol.* **11,** 57–64 (1999).

Vandewalle, C., Van Roy, F. & Berx, G. The role of the ZEB family of transcription factors in development and disease. *Cell. Mol. Life Sci.* **66,** 773–787 (2009).

Vega, S. *et al.* Snail blocks the cell cycle and confers resistance to cell death. *Genes Dev.* **18,** 1131–43 (2004).

Virtanen, I. *et al.* Laminin chains in the basement membranes of human thymus. *Histochem. J.* **28,** 643–650 (1996).

Vrisekoop, N., Monteiro, J. P., Mandl, J. N. & Germain, R. N. Revisiting Thymic Positive Selection and the Mature T Cell Repertoire for Antigen. *Immunity* **41,** 181–190 (2014).

Wallin, J. *et al.* Pax1 is expressed during development of the thymus epithelium and is required for normal T-cell maturation. *Development* **122,** 23–30 (1996).

Wang, X. *et al.* Post-Aire maturation of thymic medullary epithelial cells involves selective expression of keratinocyte-specific autoantigens. *Front. Immunol.* **3,** 19 (2012).

Wickham, H. ggplot2: elegant graphics for data analysis. *Springer New York* (2009).

Wightman, B., Ha, I. & Ruvkun, G. Posttranscriptional regulation of the heterochronic gene lin-14 by lin-4 mediates temporal pattern formation in C. elegans. *Cell* **75,** 855–62 (1993).

Wong, C. *et al.* MiR-200b/200c/429 subfamily negatively regulates Rho/ROCK signaling pathway to suppress hepatocellular carcinoma metastasis. *Oncotarget* (2015).

Wong, K. *et al.* Multilineage Potential and Self-Renewal Define an Epithelial Progenitor Cell Population in the Adult Thymus. *Cell Rep.* **8,** 1198–1209 (2014).

Xu, P.-X. *et al.* Eya1 is required for the morphogenesis of mammalian thymus, parathyroid and thyroid. *Development* **129,** 3033–44 (2002).

Yang, A. *et al.* p63 is essential for regenerative proliferation in limb, craniofacial and epithelial development. *Nature* **398,** 714–717 (1999).

Yang, J.-M., Sim, S. M., Kim, H.-Y. & Park, G. T. Expression of the homeobox gene, HOPX, is modulated by cell differentiation in human keratinocytes and is involved in the expression of differentiation markers. *Eur. J. Cell Biol.* **89,** 537–46 (2010).

Yano, M. *et al.* Aire controls the differentiation program of thymic epithelial cells in the medulla for the establishment of self-tolerance. *J. Exp. Med.* **205,** 2827–2838 (2008).

Yi, R. *et al.* Morphogenesis in skin is governed by discrete sets of differentially expressed microRNAs. *Nat. Genet.* **38,** 356–362 (2006).

Yi, R. *et al.* DGCR8-dependent microRNA biogenesis is essential for skin development. *Proc. Natl. Acad. Sci.* **106,** 498–502 (2009).

Yi, R., Poy, M. N., Stoffel, M. & Fuchs, E. A skin microRNA promotes differentiation by repressing 'stemness'. *Nature* **452,** 225–9 (2008).

Yui, M. a. & Rothenberg, E. V. Developmental gene networks: a triathlon on the course to T cell identity. *Nat. Rev. Immunol.* **14,** 529–545 (2014).

Zaravinos, A. The Regulatory Role of MicroRNAs in EMT and Cancer. *J. Oncol.* **2015,** 1–13 (2015).

Zeisberg, M. & Neilson, E. G. Biomarkers for epithelial-mesenchymal transitions. *J. Clin. Invest.* **119,** 1429–1437 (2009).

Zheng, H. & Kang, Y. Multilayer control of the EMT master regulators. *Oncogene* **33,** 1755–1763 (2014).

Zou, D. *et al.* Patterning of the third pharyngeal pouch into thymus/parathyroid by Six and Eya1. *Dev. Biol.* **293,** 499–512 (2006).

Zuklys, S. *et al.* MicroRNAs Control the Maintenance of Thymic Epithelia and Their Competence for T Lineage Commitment and Thymocyte Selection. *J. Immunol.* **189,** 3894–3904 (2012).

Abbreviations

Abbreviation	Meaning
3′-UTR	3′ untranslated region
αSMA	Alpha-smooth muscle actin
Ago	Argonaute
AIRE	Autoimmune regulator
bHLH	Basic helix-loop-helix
BMP	Bone morphogenetic protein
BS	Bovine serum
CBP	CREB-binding protein
CD	Cluster of differentiation
CDH1	E-cadherin
cFAD	Complete FAD medium
Chr	Chromosome
cTEC	Cortical TEC
DGCR8	DiGeorge Syndrome Critical Region 8
DMEM	Dulbecco-Vogt modification of Eagle's Medium
DN	Double-negative
DP	Double-positive
ECM	Extracellular matrix
EMT	Epithelial-mesenchymal transition

EpCAM	Epithelial cell adhesion molecule
FACS	Fluorescence-activated cell sorting
FBS	Fetal bovine serum
FGF	Fibroblast growth factor
Fgfr	Fgf receptor
FLG	Filaggrin
FN1	Fibronectin
Fox	Forkhead/winged-helix
Gcm	Glial cells missing
HBSS	Hank's Balanced Salt Solution
HOPX	Homeodomain only protein X
Hox	Homeobox
hEK	Human epidermal keratinocyte
hTEC	Human TEC
IVL	Involucrin
K	Keratin
MET	Mesenchymal-eptihelial transition
MHC	Major histocompatibility complex
miRNA	microRNA
MMP	Matrix metalloproteinase
mTEC	Medullary TEC
NIC	Non-infected control
Nt	Nucleotide
PanK	Pan-Keratin
Pax	Paired box
PBS	Phosphate buffered saline
PCR	Polymerase chain reaction
pp	Pharyngeal pouch
Pre-miRNA	Precursor miRNA
Pri-miRNA	miRNA primary transcript
RISC	RNA-induced silencing complex
RNA pol II	Type II RNA polymerase
RT	Room temperature

RT	Reverse transcription
RT-qPCR	Reverse-transcription quantitative PCR
rTEC	Rat TEC
RTK	Receptor tyrosine kinase
Shh	Sonic hedgehog
Six	Sine oculis-related homeobox
SP	Single-positive
Tbx	T-box transcription factor
TCR	T Cell Receptor
TEC	Thymic epithelial cell
TGFβ	Transforming growth factor-beta
TRA	Tissue-restricted antigen
TRBP	TAR RNA-binding protein
tRFP	Turbo red fluorescent protein
VIM	Vimentin
ZEB	zinc finger E-box–binding homeobox
ZO-1	Zona occludens 1

Matteo Pluchinotta

5, rue de la Faucille | 1201 Genève | Switzerland | +41 (0) 76 615 59 53 | matteo.pluchinotta@gmail.com

Objective

To share my enthusiasm, my creativity and my strong interest for life science research, while teaching young students the basics of biological research and its importance in the understanding of our world.

Education

PhD in Sciences **12/2011 – 01/2016**

Lausanne federal institute of technology (EPFL), Lausanne, Switzerland

Doctoral program in Molecular Life Sciences (EDMS)

Thesis: "A balancing act between stratification & EMT in cultured human epithelial cells"

Under the supervision of Prof. Yann Barrandon, Laboratory for Stem Cells Dynamics

Master of Science MSc in Life Sciences and Technology **09/2009 – 07/2011**

Lausanne federal institute of technology (EPFL), Lausanne, Switzerland

Specialization in Oncology and Molecular medicine

Master's thesis: "Expansion of a VE-Cadherin^{+}CD45^{+} population in the yolk sac upon Etv2 overexpression in the mouse embryo - Effects of BMP and Wnt signaling inhibition on the differentiation of a Flk1^{+} extra-embryonic mesoderm *in vitro* model"

Under the supervision of Prof. Shin-Ichi Nishikawa, Laboratory for Stem Cell Biology, RIKEN Center for developmental biology (CDB), Kôbe, Japan

Bachelor of Science BSc in Life Sciences and Technology **10/2005 - 07/2008**

Lausanne federal institute of technology (EPFL), Lausanne, Switzerland

High School Diploma **08/2001 - 07/2005**

Voltaire High School (Collège Voltaire), Geneva

Denise Lecoultre award for best plastic arts diploma project

Publications and presentations

Short talk and poster presentation **10/2015**

Joint CSH Asia / ISSCR Conference – Stem cells: basic biology to disease therapy, Suzhou, China

Co-first author **06/2012**

M. Hayashi, M. Pluchinotta, A. Momiyama, Y. Tanaka, S.-I. Nishikawa, H. Kataoka, Endothelialization and altered hematopoiesis by persistent Etv2 expression in mice. *Experimental hematology* (2012)

Fellowships

Exciting Biologies: Biology at the Interface Travel Fellowship
09/2011
Travel Fellowship

Swiss-Japan Association grant **09/2010 – 06/2011**
Travel fellowship

Experience

Brain And Mind Institute – Laboratory of Neural Microcircuitry- EPFL **02/2007 – 07/2008**

Computer neuronal reconstructions with Neurolucida ***part time***

Swiss Ski and Snowboard School – Villars **12/2005 - present**

Ski and snowboard teacher ***winter holidays and weekends***

Snowsports professor with federal certificate of higher VET (highest possible qualification in Switzerland)

Training children and adults, individually or in groups

Café "Buvette des Bains des Pâquis" **07/2005 – 09/2011**

Waiter and cook's assistant *(up to a thousand meals per day)* ***summer holidays and weekends***

Skills

Bilingual in French and Italian, fluent in English and Spanish, scholar notions in German and Japanese.
Proficient user of MS-Office, Adobe Photoshop, Illustrator and InDesign. Strong basis in R.

Standard laboratory techniques (PCR, qRT-PCR, cell culture, immunostaining, production of lentiviral vectors, single molecule RNA FISH, Western blot, …).

Familiar with flow cytometry (machines: FACS Aria II and LSR II, software: FACS Diva and FlowJo)

Design and manual screen printing of limited edition t-shirts.

References

Shin-Ichi Nishikawa, RiKEN Center for developmental biology (CDB), Kôbe, Japan (nishikawa@aasj.jp)

Yann Barrandon, Lausanne federal institute of technology, Switzerland (yann.barrandon@epfl.ch)

Marc-Henri Duc, Swiss ski and snowboard school, Villars-sur-Ollon (director@ess-villars.ch)